

A New Bayesian Huberised Regularisation and Beyond

Sanna Soomro¹, Keming Yu ^{*1}, Yan Yu²

¹Brunel University London

²University of Cincinnati

Abstract

Robust regression has attracted a great amount of attention in the literature recently, particularly for taking asymmetry into account simultaneously and for high-dimensional analysis. However, the majority of research on the topics falls in frequentist approaches, which are not capable of full probabilistic uncertainty quantification. This paper first proposes a new Huberised-type of asymmetric loss function and its corresponding probability distribution which is shown to have the scale-mixture of normals. Then we introduce a new Bayesian Huberised regularisation for robust regression. A by-product of the research is that a new Bayesian Huberised regularised quantile regression is also derived. We further present their theoretical posterior properties. The robustness and effectiveness of the proposed models are demonstrated in the simulation studies and the real data analysis.

Keywords: Asymmetric Huber loss function, Bayesian elastic net, Bayesian lasso, Quantile regression, Robustness

1 Introduction

Robust regression methods have a wide range of applications and attracted a great amount of attention in the literature recently, particularly for taking asymmetry into account simultaneously and for high-dimensional analysis, such as the adaptive Huber regression (Sun et al. (2020)) and asymmetric Huber loss and asymmetric Tukey's biweight loss functions for robust regression (Fu and Wang (2021)). The Lasso (Tibshirani (1996)) and the Elastic Net (Zou and Hastie (2005)) are some popular choices for regularising regression coefficients. The former has the ability to automatically set irrelevant coefficients to zero. The latter retains this property and the effectiveness of the ridge penalty, and it deals with highly correlated variables more effectively. Robust regularisation methods for quantile regression provide a promising technique for variable selection and model estimation in presence of outliers or heavy-tailed errors (Li and Zhu (2008); Wu and Liu (2009); Belloni and Chernozhukov (2011); Su and Wang (2021)). However, the majority of research on the topics falls in frequentist approaches, which are not capable of full probabilistic uncertainty quantification. Quantile regression, particularly Bayesian quantile regression enjoys some of robustness such as median more robust than mean, but has different modelling aims from robust regression.

*keming.yu@brunel.ac.uk

Exploring unconditional Bayesian regularisation prior, such as the Bayesian lasso (Park and Casella (2008)) and the Bayesian elastic net (Li and Lin (2010)), for robust regression is not straightforward. Several issues may arise. The joint posterior may be multimodal, which slows down the convergence of the Gibbs sampler and the point estimates may be computed through multiple modes, which lead to the inaccurate estimators (Kyung et al. (2010); Park and Casella (2008)). The choices of the hyperparameters in gamma priors of regularisation parameters may also have strong influences on the posterior estimates. For the former, it was firstly observed by Park and Casella (2008) in the Bayesian lasso. For the latter, it is common to employ invariant prior on scale parameter (Berger (1985)). Cai and Sun (2021) address these two issues by introducing the scale parameter to the Bayesian lasso and its generalisation for quantile regression. Moreover, Kawakami and Hashimoto (2023) use the scale parameter of the hyperbolic loss function (Park and Casella (2008)) to propose the Bayesian Huberised lasso, which is the robust version of Bayesian lasso. Along this line, we will propose Bayesian Huberised regularisation in this paper.

Quantile regression introduced by Koenker and Bassett (1978) is a useful supplement to ordinary mean regression in statistical analysis, owing to its robustness property and its ability to offer unique insights into the relation between the response variables and the predictors that are not available in doing mean regression. Recently, the Bayesian approaches for variable selection in quantile regression have also attracted much attention in research area (Li et al. (2010); Alhamzawi et al. (2012); Alhamzawi and Yu (2012); Alhamzawi and Yu (2013); Chen et al. (2013); Reich and Smith (2013); Alhamzawi (2016); Alshaybawee et al. (2017); Adlouni et al. (2018); Alhamzawi et al. (2019)). In Bayesian quantile regression, the error distribution would usually be assumed to follow asymmetric Laplace distribution proposed by Yu and Moyeed (2001) that guaranteed posterior consistency of Bayesian estimators (Sriram et al. (2013)) and robustness (Yu and Moyeed (2001)). Furthermore, Alhamzawi et al. (2012) adopt the inverse gamma prior density to the penalty parameters and treated its hyperparameters as unknown and estimated them along with other parameters. This allows the different regression coefficients to have different penalisation parameters, which improves the predictive accuracy. Quantile regression, particularly Bayesian quantile regression enjoys some of robustness such as median more robust than mean, but has different modelling aims from robust regression.

Therefore, this paper first proposes a new Huberised-type of asymmetric loss function and its corresponding probability distribution, which is shown to have the scale-mixture of normals. Then we introduce a new Bayesian Huberised regularisation for robust regression. Furthermore, by taking advantage of the good quantile property of this probability distribution, we develop Bayesian Huberised lasso quantile regression and Bayesian Huberised elastic net quantile regression. This results in the proposed models covering both Bayesian robust regularisation and Bayesian quantile regularisation. Besides, Cai and Sun (2021) emphasise that the posterior impropriety does exist in Bayesian lasso quantile regression and its generalisation when the prior on regression coefficients is independent of the scale parameter. Thus, we will discuss some properties of the Bayesian Huberised regularised quantile regression, including posterior propriety and posterior unimodality. The approximate Gibbs sampler of Kawakami and Hashimoto (2023) is adopted to enable the data-dependent estimation of the tuning robustness parameter in the fully Bayesian hierarchical model. The advantage of this sampling step is that it does not

require cross validation evaluation of tuning parameters (see Alhamzawi (2016) for example) nor the rejection steps, such as the inversion method and adaptive rejection sampling algorithm (see Alhamzawi et al. (2019) for example). We demonstrate the effectiveness and robustness of the Bayesian Huberised regularised quantile regression model through simulation studies following by real data analysis.

The remainder of this paper is as follows. In Section 2, we define a Huberised asymmetric loss function with its corresponding probability density function and derive a scale mixture of normal representation for Bayesian inference. Section 3 presents the Bayesian Huberised regularisation including the Bayesian Huberised lasso (Kawakami and Hashimoto (2023)) and the Bayesian Huberised elastic net. This results in a new robust Bayesian regularised quantile regression. In Section 4 and 5, a wide range of simulation studies and three real data examples were conducted. In Section 6, we draw the conclusions.

2 Huberised Asymmetric Loss Function

The lasso and elastic net estimates are all regularised estimates and the differences among them are only at their penalty terms. Specifically, they are all solutions to the following form of minimization problem for regularised quantile regression

$$\min_{\boldsymbol{\beta}} \sum_{i=1}^n \rho_{\tau}(y_i - \mathbf{x}_i \boldsymbol{\beta}) + \lambda_1 g_1(\boldsymbol{\beta}) + \lambda_2 g_2(\boldsymbol{\beta}), \quad (1)$$

for some $\lambda_1, \lambda_2 \geq 0$, penalty functions $g_1(\cdot)$ and $g_2(\cdot)$, $\rho_{\tau}(x) = x(\tau - I(X < 0))$ is the check loss function and $I(\cdot)$ is the indicator function. The lasso corresponds to $\lambda_1 > 0$, $\lambda_2 = 0$, $g_1(\boldsymbol{\beta}) = \|\boldsymbol{\beta}\|$ and $g_2(\boldsymbol{\beta}) = 0$. The elastic net corresponds to $\lambda_1 = \lambda_3, \lambda_2 = \lambda_4 > 0$, $g_1(\boldsymbol{\beta}) = \|\boldsymbol{\beta}\|$ and $g_2(\boldsymbol{\beta}) = \|\boldsymbol{\beta}\|_2^2$.

Letting $\tau = 0.5$, the first term of Equation (1) reduces to $\sum_{i=1}^n |y_i - \mathbf{x}_i \boldsymbol{\beta}|$ and the corresponding method is called the least absolute deviation (LAD) regression, which is known to be robust against outliers in response variables. However, the LAD regression might underestimate regression coefficients for non-outlying observations. To remedy this problem, the Huber loss function is used and it is defined as

$$L_{\delta}^{Huber}(x) = \begin{cases} \frac{1}{2}x^2, & |x| \leq \delta, \\ \delta(|x| - \delta/2), & |x| > \delta, \end{cases} \quad (2)$$

where $\delta > 0$ is a robustness parameter and it is practically set as $\delta = 1.345$ (Huber (1964)). The behaviour of this loss function is such that it is quadratic for small values of x and becomes linear when ϵ exceeds δ in magnitude.

Clearly, the Huber loss function has non-differentiable points and it has limited scope in applications. Li et al. (2020) propose two generalised Huber loss functions, which are Soft Huber and Nonconvex Huber. They are attractive alternatives to the Huber loss function because they are analogous to the pseudo Huber loss function and they have a normal scale mixture property resulting in a broader range of

Bayesian applications. The Soft Huber loss function can be defined as

$$L_{\zeta_1, \zeta_2}^{SH}(x) = \sqrt{\zeta_1 \zeta_2} \left(\sqrt{1 + \frac{x^2}{\zeta_2}} - 1 \right), \quad (3)$$

and the Nonconvex Huber loss function as

$$L_{\zeta_1, \zeta_2}^{NH}(x) = \sqrt{\zeta_1 \zeta_2} \left(\sqrt{1 + \frac{|x|}{\zeta_2}} - 1 \right), \quad (4)$$

where $\zeta_1, \zeta_2 > 0$ are non-negative hyperparameters. Here, the Soft Huber loss bridges the ℓ_1 (absolute) loss and the ℓ_2 (squared) loss. On the other hand, the Nonconvex Huber loss bridges the $\ell_{1/2}$ loss and the ℓ_1 loss. By letting $\eta = \sqrt{\zeta_1 \zeta_2}$ and $\rho^2 = \sqrt{\frac{\zeta_2}{\zeta_1}}$, the Soft Huber loss function becomes the hyperbolic loss function, that is,

$$L_{\eta, \rho^2}^{Hyp}(x) = \sqrt{\eta \left(\eta + \frac{x^2}{\rho^2} \right)} - \eta, \quad (5)$$

where $\eta > 0$ is the robustness parameter and $\rho^2 > 0$ is a scale parameter. Park and Casella (2008) used this hyperbolic loss function to formulate the Bayesian Huberised lasso, which has proven to be robust to outliers.

When the error distribution is asymmetric or contaminated by asymmetric outliers, the estimators obtained from Equations (2), (3), (4) and (5) may result in inconsistency of predictions of a conditional mean given the regressors (Fu and Wang (2021)).

Therefore, we propose the Huberised-type asymmetric loss function by letting $\eta = \sqrt{\zeta_1 \zeta_2}$ and $\rho^2 = \sqrt{\frac{\zeta_2}{\zeta_1}}$ in Equation (4) and it is given by

$$L_{\eta, \rho^2, \tau}^{Asy}(x) = \sqrt{\eta \left(\eta + \frac{x}{\rho^2} (\tau - I(x < 0)) \right)} - \eta.$$

The corresponding density function is

$$f(x|\mu, \eta, \rho^2, \tau) = \frac{\eta \tau (1 - \tau) e^\eta}{2 \rho^2 (\eta + 1)} \exp \left\{ -\sqrt{\eta \left(\eta + \frac{x - \mu}{\rho^2} (\tau - I(x < 0)) \right)} \right\}, \quad (6)$$

where $\mu \in \mathbb{R}$ is a location parameter. Here, ρ^2 acts as a scale parameter and η acts as a shape parameter of this density function.

The following proposition states that the parameters μ and τ in (6) satisfy: μ is the τ th quantile of the distribution.

Proposition 2.1 *If a random variable X follows the density function in (6) then we have $P(X \leq \mu) = \tau$ and $P(X > \mu) = 1 - \tau$.*

Proof: The proof can be found in Appendix A.1. □

To observe the behaviour of the proposed loss function, we set $\eta = \sqrt{\zeta_2} (\sqrt{\zeta_2} + \sqrt{\zeta_2 + 1})$ and $\rho^2 = \frac{\sqrt{\zeta_2}}{\sqrt{\zeta_2} + \sqrt{\zeta_2 + 1}}$ then we have the following limits,

$$\lim_{\zeta_2 \rightarrow 0} L_{\eta, \rho^2, \tau}^{Asy}(x) = \sqrt{x(\tau - I(x < 0))} \quad \text{and} \quad \lim_{\zeta_2 \rightarrow \infty} L_{\eta, \rho^2, \tau}^{Asy}(x) = x(\tau - I(x < 0)),$$

which suggests that the proposed loss bridges the quantile loss function. Daouia et al. (2018) use the quantile loss function for tail expectiles to estimate alternative measures to the value at risk and marginal expected shortfall, which are two instruments of risk protection of utmost importance in actuarial science and statistical finance. Ehm et al. (2016) show that any scoring function that is consistent for a quantile or an expectile functional can be represented as a mixture of elementary or extremal scoring functions that form a linearly parameterised family. However, in this paper, we show a totally new way to achieve it, and our proposed loss is a novel representative of asymmetric least squares (Daouia et al. (2019)). Figure 1 illustrates the asymmetric shape behaviour for five different values of τ (0.1, 0.25, 0.5, 0.75, 0.9). From the figure, $L_{\eta, \rho^2, \tau}^{Asy}(x)$ approaches the square root of the quantile loss function, as $\eta \rightarrow 0$, and $L_{\eta, \rho^2, \tau}^{Asy}(x)$ approaches the quantile loss function, as $\eta \rightarrow \infty$.

Kawakami and Hashimoto (2023) discussed that it is essential to choose the right value of hyperparameters of η and ρ^2 where ρ^2 can easily be estimated by a Gibbs sampler in a Bayesian model whereas the estimation of η is difficult. They proposed the approximate Gibbs sampler to enable the data-dependent estimation of η . This paper will also adopt their approximate Gibbs sampler.

To fully enable the Gibbs sampling algorithm for Bayesian modelling, the density function in (6) has a scale mixture of normal representation with exponential and generalised inverse Gaussian densities. Suppose that a random variable X has a probability density function $f(x|\theta)$ and unknown parameter θ that satisfies

$$f(x|\theta) = \int \phi(x|\mu, \sigma) \pi(\sigma|\theta) d\sigma, \quad (7)$$

where $\phi(\cdot)$ is the mixing distribution and $\pi(\cdot)$ is some density function that is defined on $(0, \infty)$, then X or its $f(x|\theta)$ is a scale mixture of a normal distribution. It has many applications in statistics, finance and, particularly in Bayesian inference. Probability distribution with a scale mixture of normal expression could be grouped into two groups: symmetric probability distributions (Andrews and Mallows (1974); West (1987)) and asymmetric probability distributions (Reed and Yu (2009); da Silva Ferreira et al. (2011); Kozumi and Kobayashi (2011)). Therefore, the following proposition provides an alternative stochastic representation, which is a normal scale-mixture.

Theorem 2.1 *If the model error $\epsilon_i = y_i - \mathbf{x}_i\boldsymbol{\beta}$ follows the density function (6), then we can represent ϵ_i as scale mixture of normals given by*

$$\begin{aligned} & f(\epsilon_i; \tau, \eta, \rho^2) \\ & \propto \iint N(\epsilon_i; (1 - 2\tau)v_i, 4v_i\sigma_i) E\left(v_i; \frac{\tau(1 - \tau)}{2\sigma_i}\right) GIG\left(\sigma_i; 1, \frac{\eta}{\rho^2}, \eta\rho^2\right) dv_i d\sigma_i, \\ & i = 1, \dots, n, \end{aligned} \quad (8)$$

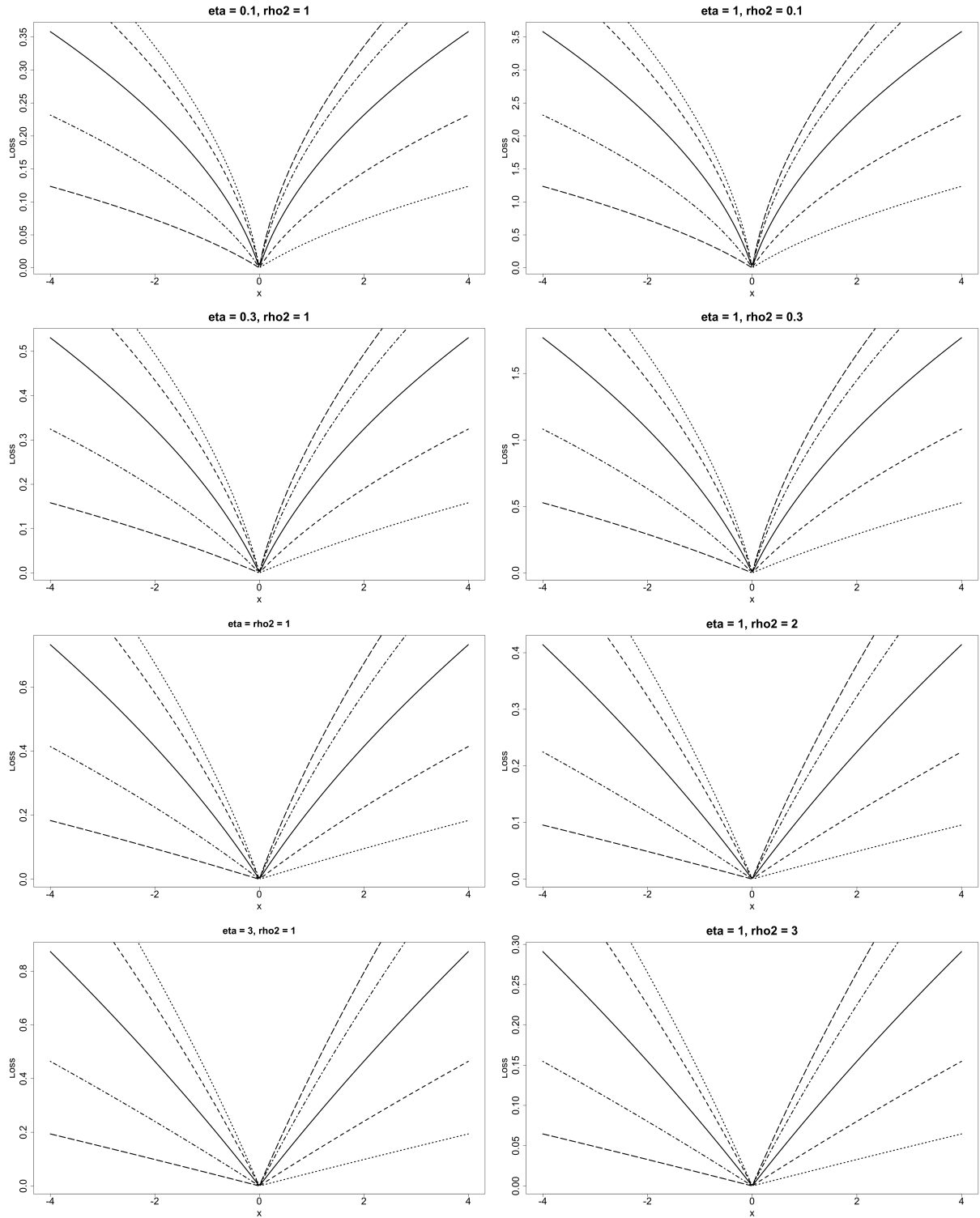


Figure 1: The asymmetrical behaviour of the proposed loss function for $\tau=0.1$ (short dashed), 0.25 (normal dashed), 0.5 (solid), 0.75 (short-normal dashed), and 0.9 (long dashed) for different values of η and ρ^2 .

where $GIG(x|\nu, c, d)$ denotes the GIG distribution and its density is specified by

$$f_{GIG}(x) = \frac{(c/d)^\nu}{2K_1(cd)} x^{\nu-1} \exp\left(-\frac{1}{2}(c^2x + d^2x^{-1})\right), \quad \nu > 0, \quad (9)$$

and $K_\nu(\cdot)$ is the modified Bessel function of the second kind at index ν (Barndorff-Nielsen and Shephard (2001)).

Proof: The proof can be found in Appendix A.2. □

3 Bayesian Huberised Regularised Quantile Regression Model

3.1 Bayesian Huberised Lasso Quantile Regression

In this paper, we consider a Bayesian analogous of Huberised regularised quantile regression model. Kawakami and Hashimoto (2023) showed that the unconditional Laplace prior of $\boldsymbol{\beta}$ (Park and Casella (2008)) would lead to multimodality of a posterior density and resolved this issue by introducing ρ^2 as a scale parameter to formulate the Bayesian Huberised lasso, that is,

$$\pi(\boldsymbol{\beta}|\rho^2, \lambda_1) = \prod_{j=1}^k \frac{\lambda_1}{2\sqrt{\rho^2}} \exp\left\{-\frac{\lambda_1|\beta_j|}{\sqrt{\rho^2}}\right\}. \quad (10)$$

By using the scale mixture of normal representation of Laplace distribution Andrews and Mallows (1974), the Bayesian Huberised lasso can be expressed as

$$\boldsymbol{\beta}|\mathbf{s}, \rho^2 \sim N(\mathbf{0}, \rho^2 \boldsymbol{\Lambda}), \quad s_j|\lambda_1 \sim \text{Exp}\left(\frac{\lambda_1^2}{2}\right), \quad j = 1, \dots, k,$$

where $\mathbf{s} = (s_1, \dots, s_k)^T$ and $\boldsymbol{\Lambda} = \text{diag}(s_1, \dots, s_k)$.

Therefore, with the Bayesian Huberised lasso, we present the following hierarchical model using the scale mixture of normal representation in Theorem 2.1:

$$\begin{aligned} \mathbf{y}|\mathbf{X}, \boldsymbol{\beta}, \boldsymbol{\sigma}, \mathbf{v} &\sim N(\mathbf{X}\boldsymbol{\beta} + (1 - 2\tau)\mathbf{v}, \mathbf{V}), \\ \sigma_i|\rho^2, \eta &\sim GIG\left(1, \frac{\eta}{\rho^2}, \eta\rho^2\right), \quad i = 1, \dots, n, \\ v_i|\sigma_i &\sim \text{Exp}\left(\frac{\tau(1 - \tau)}{2\sigma_i}\right), \quad i = 1, \dots, n, \\ \beta_j|s_j, \rho^2 &\sim N(0, \rho^2 s_j), \quad j = 1, \dots, k, \\ s_j|\lambda_1^2 &\sim \text{Exp}\left(\frac{\lambda_1^2}{2}\right), \quad j = 1, \dots, k, \\ \rho^2 &\sim \pi(\rho^2) \propto \frac{1}{\rho^2}, \\ \eta, \lambda_1^2 &\sim \text{Gamma}(\lambda_1^2; a, b)\text{Gamma}(\eta; c, d), \end{aligned}$$

where $\mathbf{V} = \text{diag}(4\sigma_1 v_1, \dots, 4\sigma_n v_n)$. As a prior of ρ^2 , we assume the improper scale invariant prior, that is proportional to $\frac{1}{\rho^2}$, but a proper inverse gamma prior can also be employed, for example. Similar to Kawakami and Hashimoto (2023) and Cai and Sun (2021), Proposition 3.1 shows that using the improper prior on ρ^2 will lead to a proper posterior density. Based on this proposition, Subsection 4.1 will show that the unconditional prior on $\boldsymbol{\beta}$ can result in multimodality of the joint posterior. We further impose

a gamma prior on λ_1^2 and η . We set hyperparameters $a = b = c = d = 1$ for simulation studies and real data analysis. The sensitivity analysis of hyperparameters is detailed in Subsection 4.2.

As for the Gibbs sampler, the full conditional distribution of $\boldsymbol{\beta}$ is a multivariate normal distribution and those of $\boldsymbol{\sigma}$, \mathbf{v} , \mathbf{s} and ρ^2 are generalised inverse Gaussian distributions. The full conditional distribution of λ_1^2 is a Gamma distribution. The approximate Gibbs sampler is used for η . Appendix B.1 gives the details of the full conditional posterior distributions for the Gibbs sampling algorithm.

Proposition 3.1 *Let $\rho^2 \sim \pi(\rho^2) \propto \frac{1}{\rho^2}$ (improper scale invariant prior). For fixed $\lambda_1 > 0$ and $\eta > 0$, the posterior distribution is proper for all n .*

Proof: The proof can be found in Appendix A.3. □

Proposition 3.2 *Under the conditional prior for $\boldsymbol{\beta}$ given ρ^2 and fixed $\lambda_1 > 0$ and $\eta > 0$, the joint posterior $(\boldsymbol{\beta}, \rho^2 | \mathbf{y})$ is unimodal with respect to $(\boldsymbol{\beta}, \rho^2)$.*

Proof: The proof can be found in Appendix A.4. □

3.2 Bayesian Huberised Elastic Net Quantile Regression

We also present the Bayesian Huberised elastic net, that is,

$$\pi(\boldsymbol{\beta} | \rho^2, \lambda_3, \lambda_4) = \prod_{j=1}^k C(\tilde{\lambda}_3, \lambda_4) \frac{\lambda_3}{2\sqrt{\rho^2}} \exp \left\{ -\frac{\lambda_3 |\beta_j|}{\sqrt{\rho^2}} - \frac{\lambda_4 \beta_j^2}{\rho^2} \right\}, \quad (11)$$

where $C(\tilde{\lambda}_3, \lambda_4) = \Gamma^{-1}\left(\frac{1}{2}, \tilde{\lambda}_3\right) (\tilde{\lambda}_3)^{-1/2} \exp\{-\tilde{\lambda}_3\}$ is the normalising constant and $\tilde{\lambda}_3 = \frac{\lambda_3^2}{4\lambda_4}$. The computations of the normalising constant is detailed in Appendix B of Li et al. (2010). Note that by letting $\rho^2 = 1$, Equation (11) reduces to the original Bayesian elastic net (Li and Lin (2010)).

By using the scale mixture property (Andrews and Mallows (1974)), the Bayesian Huberised elastic net can be expressed as a scale mixture of normal with truncated gamma density:

$$\begin{aligned} \pi(\boldsymbol{\beta} | \rho^2, \lambda_3, \lambda_4) &= \prod_{j=1}^k \int_0^\infty \Gamma^{-1}\left(\frac{1}{2}, \tilde{\lambda}_3\right) \sqrt{\frac{2\lambda_4 t_j}{2\pi\rho^2(t_j - 1)}} \sqrt{\frac{\tilde{\lambda}_3}{t_j}} \\ &\quad \times N\left(\beta_j; 0, \frac{\rho^2(t_j - 1)}{2\lambda_4 t_j}\right) \exp\{-\tilde{\lambda}_3 t_j\} I(t_j > 1) dt. \end{aligned}$$

With the Bayesian Huberised elastic net, we have the following hierarchical model:

$$\begin{aligned}
\mathbf{y}|\mathbf{X}, \boldsymbol{\beta}, \boldsymbol{\sigma}, \mathbf{v} &\sim N(\mathbf{X}\boldsymbol{\beta} + (1 - 2\tau)\mathbf{v}, \mathbf{V}), \\
\sigma_i|\rho^2, \eta &\sim GIG\left(1, \frac{\eta}{\rho^2}, \eta\rho^2\right), \quad i = 1, \dots, n, \\
v_i|\sigma_i &\sim \text{Exp}\left(\frac{\tau(1 - \tau)}{2\sigma_i}\right), \quad i = 1, \dots, n, \\
\beta_j|t_j, \lambda_4, \rho^2 &\sim N\left(0, \frac{2\rho^2(t_j - 1)}{\lambda_4 t_j}\right), \quad j = 1, \dots, k, \\
t_j|\tilde{\lambda}_3 &\sim \Gamma^{-1}\left(\frac{1}{2}, \tilde{\lambda}_3\right) \sqrt{\frac{\tilde{\lambda}_3}{t_j}} \exp\{-\tilde{\lambda}_3 t_j\} I(t_j > 1), \quad j = 1, \dots, k, \\
\rho^2 &\sim \pi(\rho^2) \propto \frac{1}{\rho^2}, \\
\tilde{\lambda}_3, \lambda_4, \eta &\sim \text{Gamma}(\tilde{\lambda}_3; a_1, b_1) \text{Gamma}(\lambda_4; a_2, b_2) \text{Gamma}(\eta; a_3, b_3),
\end{aligned}$$

where $a_1, a_2, a_3, b_1, b_2, b_3 \geq 0$ are hyperparameters, they are set to 1 for simulation studies and real data analysis and $\Gamma(\cdot, \cdot)$ is the upper incomplete gamma function.

Appendix B.2 gives the details of the full conditional posterior distributions for the Gibbs sampling algorithm. The full conditional distributions are all well-known distributions except the full conditional distributions of $\tilde{\lambda}_3$ and η and the Metropolis-Hasting algorithm is employed on $\tilde{\lambda}_3$. We also present Proposition 3.4 for the use of improper prior on ρ^2 and provide demonstration of the unconditional prior on $\boldsymbol{\beta}$ in Subsection 4.1.

Proposition 3.3 *Let $\rho^2 \sim \pi(\rho^2) \propto \frac{1}{\rho^2}$ (improper scale invariant prior). For fixed $\lambda_3 > 0$, $\lambda_4 > 0$ and $\eta > 0$, the posterior distribution is proper for all n .*

Proof: The proof can be found in Appendix A.5. □

Proposition 3.4 *Under the conditional prior for $\boldsymbol{\beta}$ given ρ^2 and fixed $\lambda_3 > 0$, $\lambda_4 > 0$ and $\eta > 0$, the joint posterior $(\boldsymbol{\beta}, \rho^2|\mathbf{y})$ is unimodal with respect to $(\boldsymbol{\beta}, \rho^2)$.*

Proof: The proof can be found in Appendix A.6. □

3.3 Approximate Gibbs Sampler for Estimation of η

In this subsection, we will briefly discuss the approximate Gibbs sampler for the data-dependent estimation of η that is proposed by Kawakami and Hashimoto (2023). Notice that in a Bayesian Huberised regularised quantile regression model, the full conditional distribution of η is

$$\pi(\eta|\boldsymbol{\sigma}, \rho^2) \propto \frac{1}{K_1(\eta)^n} \eta^{a-1} \exp\left\{-\eta \left(\frac{1}{2} \sum_{i=1}^n \left(\frac{\sigma_i}{\rho^2} + \frac{\rho^2}{\sigma_i}\right) + b\right)\right\}, \quad (12)$$

where $a = c$ and $b = d$ in case of Bayesian Huberised lasso quantile regression and $a = a_3$ and $b = b_3$ in case of Bayesian Huberised elastic net quantile regression. Since the right side of Equation (12) contains

the modified Bessel function of the second kind, the full conditional distribution of η does not have a conjugacy property. However, it is possible to approximate (12) by a common probability distribution.

For the selection of an initial value of the approximate Gibbs sampling algorithm, we need to approximate the modified Bessel function of the second kind. According to Abramowitz and Stegun (1965), we have $K_\nu(x) \sim \left(\frac{1}{2}\right) \Gamma(\nu) \left(\frac{x}{2}\right)^{-\nu}$ as $x \rightarrow 0$ for $\nu > 0$ and $K_\nu(x) \sim \sqrt{\frac{x}{2\pi}} e^{-x}$ as $x \rightarrow \infty$. Kawakami and Hashimoto (2023) stated that in either case, it would not make much difference in estimating η . So, we will focus on the latter case only for this paper. As $\eta \rightarrow \infty$, we have

$$\pi(\eta|\boldsymbol{\sigma}, \rho^2) \approx \eta^{a+n/2-1} \exp \left\{ -\eta \left(\frac{1}{2} \sum_{i=1}^n \left(\frac{\sigma_i}{\rho^2} + \frac{\rho^2}{\sigma_i} \right) + b - n \right) \right\},$$

which holds the approximation $\pi(\eta|\boldsymbol{\sigma}, \rho^2) \approx \text{Gamma} \left(\eta; a + \frac{n}{2}, \frac{1}{2} \sum_{i=1}^n \left(\frac{\sigma_i}{\rho^2} + \frac{\rho^2}{\sigma_i} \right) + b - n \right)$ for large η .

The algorithm of the approximate Gibbs sampler is as follows.

Given the current Markov chain states $(\boldsymbol{\sigma}, \rho^2)$, we set the initial value as $A = a + n/2$ and $B = \frac{1}{2} \sum_{i=1}^n \left(\frac{\sigma_i}{\rho^2} + \frac{\rho^2}{\sigma_i} \right) + b - n$. For $m = 1, \dots, M$, do the following steps

- $\eta \leftarrow \frac{A}{B}$;
- $A \leftarrow a + n\eta^2 \frac{\partial^2}{\partial \eta^2} \log K_1(\eta)$;
- $B \leftarrow b + \frac{A-a}{\eta} + n \frac{\partial}{\partial \eta} \log K_1(\eta) + \frac{1}{2} \sum_{i=1}^n \left(\frac{\sigma_i}{\rho^2} + \frac{\rho^2}{\sigma_i} \right)$.

until $|\eta/(A/B) - 1| < \varepsilon$ or in other words, the convergence of η is met. The full derivation of the algorithm is detailed in Kawakami and Hashimoto (2023) and they also illustrated that in their simulation results, the approximation is close to the true full conditional distribution and the approximation accuracy increases as the sample size increase. For simulation studies and real data analysis, we set $M = 10$ and a tolerance $\varepsilon = 10^{-8}$.

4 Simulations

4.1 Multimodality of Joint Posteriors

As related to Propositions 3.2 and 3.4, we present a simple simulation to demonstrate that the unconditional prior for $\boldsymbol{\beta}$ can result in multimodality of the joint posterior. Instead of Equations (10) and (11), we specify the unconditional lasso prior

$$\pi(\boldsymbol{\beta}|\lambda_1) = \prod_{j=1}^k \frac{\lambda_1}{2} \exp \{-\lambda_1 |\beta_j|\},$$

and the unconditional elastic net prior

$$\pi(\boldsymbol{\beta}|\lambda_3, \lambda_4) = \prod_{j=1}^k C(\lambda_3, \lambda_4) \frac{\lambda_3}{2} \exp \{-\lambda_3 |\beta_j| - \lambda_4 \beta_j^2\},$$

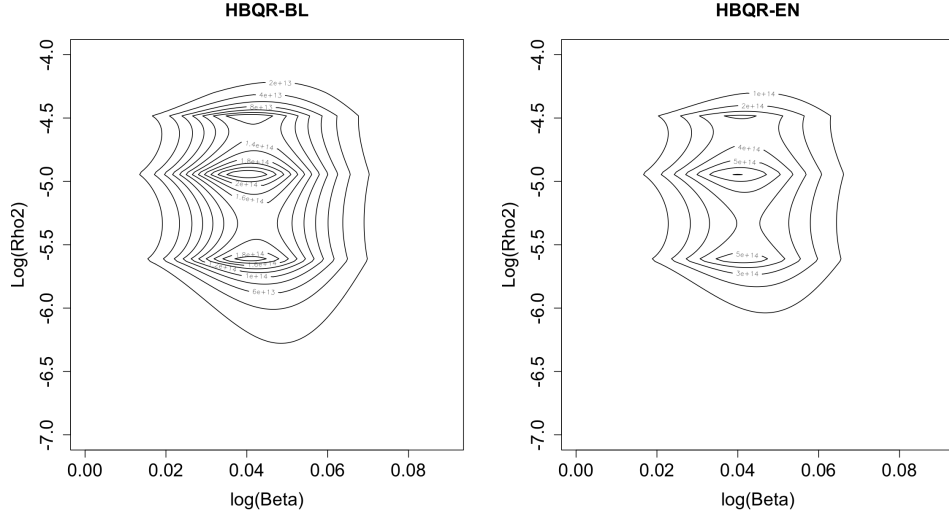


Figure 2: Contour plot of an artificially generated posterior density of $(\log(\beta), \log(\rho^2))$ of the joint posterior density (13) and (14) for Bayesian Huberised lasso quantile regression and Bayesian Huberised elastic net quantile regression, respectively. The logarithm of β and ρ^2 is used for a better visibility.

with same improper prior $\pi(\rho^2) \propto \frac{1}{\rho^2}$. Then the joint posterior distribution of β and ρ^2 for Bayesian Huberised lasso quantile regression is proportional to

$$\pi(\beta, \rho^2 | \mathbf{y}) \propto (\rho^2)^{-n-1} \exp \left\{ -\lambda_1 \sum_{j=1}^k |\beta_j| \right\} \times \prod_{i=1}^n K_0 \left(\sqrt{\frac{\eta}{\rho^2} \left(\frac{|y_i - \mathbf{x}_i \beta| + (1 - 2\tau)(y_i - \mathbf{x}_i \beta)}{2} \right)} \right), \quad (13)$$

and that for Bayesian Huberised elastic net quantile regression is proportional to

$$\pi(\beta, \rho^2 | \mathbf{y}) \propto (\rho^2)^{-n-1} \exp \left\{ -\lambda_3 \sum_{j=1}^k |\beta_j| - \lambda_4 \sum_{j=1}^k \beta_j^2 \right\} \times \prod_{i=1}^n K_0 \left(\sqrt{\frac{\eta}{\rho^2} \left(\frac{|y_i - \mathbf{x}_i \beta| + (1 - 2\tau)(y_i - \mathbf{x}_i \beta)}{2} \right)} \right), \quad (14)$$

In Appendices A.4 and A.6, it is shown that using the conditional prior (10) and (11), respectively, lead to a unimodal posterior for any choice of $\lambda_1, \lambda_3, \lambda_4 \geq 0$ and $\eta > 0$ with an improper prior $\pi(\rho^2)$. On the other hand, the joint posteriors (13) and (14) can have more than one mode. For example, Figure 2 showed the contour plots of a multimodal joint density of $\log(\beta)$ and $\log(\rho^2)$. This particular example results from considering the following data generated model,

$$y_i = x_i \beta + \epsilon_i, \quad \epsilon_i \sim ALD(0, \sigma = 0.03, \tau = 0.5),$$

where $\beta = 1$ and $x_i \sim N(0, 1)$ for $i = 1, \dots, 10$, which is similar to Cai and Sun (2021). Due to multimodality in the joint posterior with unconditional prior for β , we use the prior for β conditioning

on the scale parameter ρ^2 .

4.2 Sensitivity analysis of hyper-parameters

In this subsection, we test the sensitivity of hyperparameters of Gamma prior of η , λ_1 , λ_3 and λ_4 on the posterior estimates for the proposed methods. We equally divide $x \in [-2, 2]$ into 50 pieces and the data are generated from

$$y_i = \mathbf{x}_i \boldsymbol{\beta} + \epsilon_i, \quad \epsilon_i \sim ALD(0, \sigma = 0.03, \tau = 0.5), \quad i = 1, \dots, 50,$$

with $\mathbf{x}_i = \left((1 + e^{-4(x_i - 0.3)})^{-1}, (1 + e^{3(x_i - 0.2)})^{-1}, (1 + e^{-4(x_i - 0.7)})^{-1}, (1 + e^{5(x_i - 0.8)})^{-1} \right)^T$ and $\boldsymbol{\beta} = (1, 1, 1, 1)^T$. It indicates that the true curve is

$$f(x) = \left(1 + e^{-4(x-0.3)}\right)^{-1} + \left(1 + e^{3(x-0.2)}\right)^{-1} + \left(1 + e^{-4(x-0.7)}\right)^{-1} + \left(1 + e^{5(x-0.8)}\right)^{-1}.$$

In fact, this function was utilised in Jullion and Lambert (2007) to test the sensitivity of hyperparameters of the Gamma prior on the scale component in Bayesian P-spline.

We consider the proposed models to estimate $\boldsymbol{\beta}$. Note that there are four prior hyperparameters a , b , c and d in the Bayesian Huberised lasso quantile regression and six prior hyperparameters a_1 , b_1 , a_2 , b_2 , a_3 and b_3 in the Bayesian Huberised elastic net quantile regression. We mainly set $a = b = c = d = a_1 = a_2 = a_3 = b_1 = b_2 = b_3 = 1$ in both simulation studies and data analysis. We generate 3000 posterior samples after discarding the first 1000 posterior samples as burn-in. Then we plot $y_i = \mathbf{x}_i \boldsymbol{\beta}$ for $i = 1, \dots, 50$ in Figures 3 and 4 for both proposed Bayesian models, where $\boldsymbol{\beta}$ is the posterior mean for the corresponding proposed model. In Figure 3, we fixed $a = 1$ with b varied for the top-left plot and $b = 1$ with a varied for the top-right plot. In both cases, we keep $c = d = 1$ fixed. Both bottom plots of Figure 3 follows in a similar manner. As for Figure 4, we also fixed $a_1 = 1$ with b_1 varied for the top-left plot while keeping $a_2 = b_2 = a_3 = b_3 = 1$. The rest of Figure 4 also follows in a similar manner. From the figures, we observe that the estimation results do not change very much for a variety selection of hyperparameters.

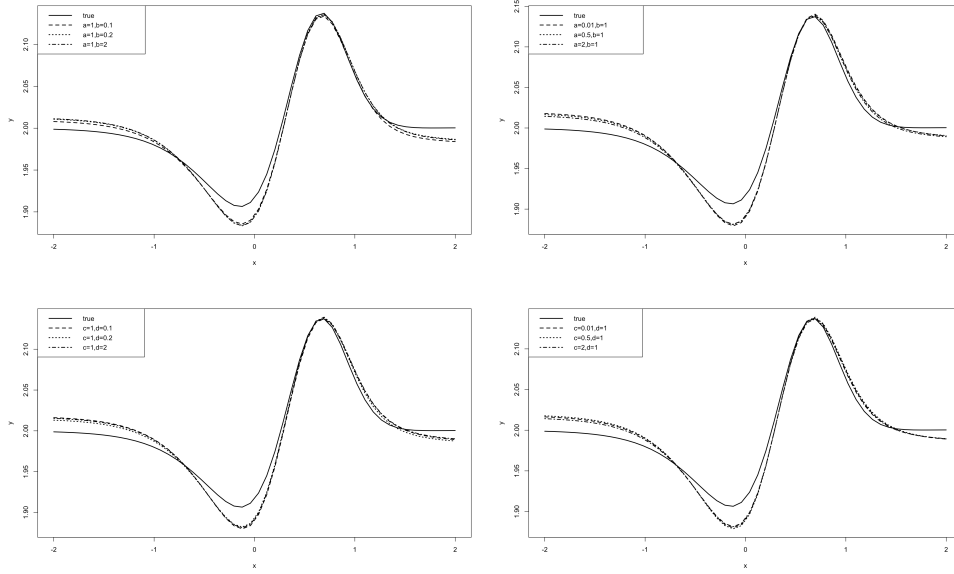


Figure 3: Sensitivity analysis of hyper-parameters for the Bayesian Huberised lasso quantile regression.

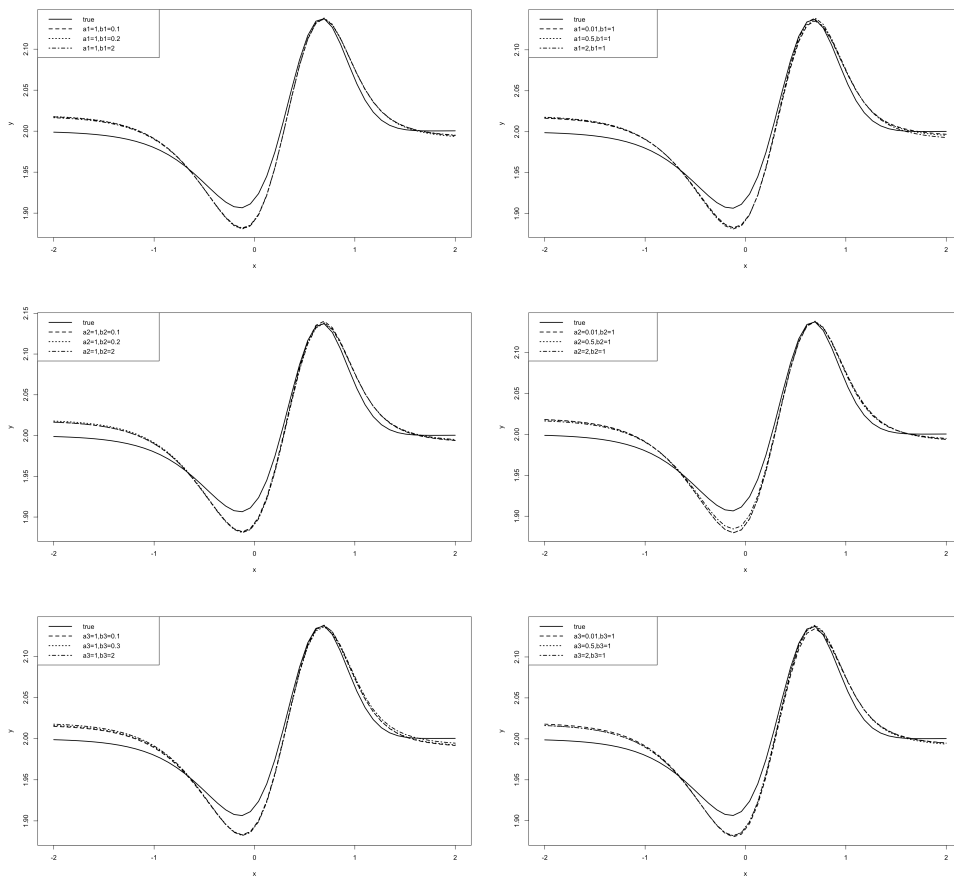


Figure 4: Sensitivity analysis of hyper-parameters for the Bayesian Huberised elastic net quantile regression.

4.3 Simulation Studies

In simulation studies, we illustrate performance of the proposed methods. We compare the point and interval estimation performance of the proposed methods with those of some existing methods. To this end, we consider the following regression model with $n \in \{100, 200\}$, $k = 20$ and $\tau \in \{0.25, 0.5, 0.75\}$:

$$y_i = \beta_0 + \beta_1 x_{i1} + \dots + \beta_k x_{ik} + \sigma \epsilon_i, \quad i = 1, \dots, n,$$

where $\beta_0 = 1$, $\beta_1 = 3$, $\beta_2 = 0.5$, $\beta_4 = \beta_{11} = 1$, $\beta_7 = 1.5$ and the other β_j 's were set to 0. We assume $\mathbf{y} = (y_1, \dots, y_n)^T$ is the response vector. The predictors $\mathbf{x}_i = (x_{i1}, \dots, x_{ik})^T$ were generated from a multivariate normal distribution $N_k(\mathbf{0}, \Sigma)$ with $\Sigma = (r^{|i-j|})_{1 \leq i, j \leq k}$ for $|r| < 1$. Similar to Kawakami and Hashimoto (2023) and Lambert-Lacroix and Zwald (2011), we consider the six scenarios.

- Simulation 1: Low correlation and Gaussian noise. $\epsilon \sim N_n(0, I_n)$, $\sigma = 2$ and $r = 0.5$.
- Simulation 2: Low correlation and large outliers. $\epsilon = W/\sqrt{\text{var}(W)}$, $\sigma = 9.67$ and $r = 0.5$. W is a random variable according to the contaminated density defined by $0.9 \times N(0, 1) + 0.1 \times N(0, 15^2)$, where $\sqrt{\text{var}(W)} = 4.83$.
- Simulation 3: High correlation and large outliers. $\epsilon = W/\sqrt{\text{var}(W)}$, $\sigma = 9.67$ and $r = 0.95$.
- Simulation 4: Large outliers and skew Student-t noise. $\epsilon_i \sim 0.9 \times \text{Skew-}t_3(\gamma = 3) + 0.1 \times N(0, 20^2)$, $\sigma = 1$ and $r = 0.5$.
- Simulation 5: Heavy-tailed noise. $\epsilon_i \sim \text{Cauchy}(0, 1)$, $\sigma = 2$ and $r = 0.5$.
- Simulation 6: Multiple outliers. $\epsilon_i \sim 0.8 \times \text{Skew-}t_3(\gamma = 3) + 0.1 \times N(0, 10^2) + 0.1 \times \text{Cauchy}(0, 1)$, $\sigma = 1$ and $r = 0.5$.

For the simulated dataset, we applied the proposed robust methods denoted by HBQR-BL and HBQR-EN where they were employed with Bayesian Huberised Lasso and Bayesian Huberised elastic net, respectively. We also applied the existing robust methods, including Bayesian linear regression with Bayesian Huberised lasso (Kawakami and Hashimoto (2023)), and Bayesian quantile regression with original Bayesian lasso and Bayesian elastic net (Li et al. (2010)) denoted by HBL, BQR-BL and BQR-EN, respectively. For HBL and BQR-BL, we assume $\lambda_1 \sim \text{Gamma}(a = 1, b = 1)$ and for BQR-EN, we assume $\lambda_1 \sim \text{Gamma}(a_1 = 1, b_1 = 1)$ and $\lambda_2 \sim \text{Gamma}(a_2 = 1, b_2 = 1)$. For the HBQR-BL and HBQR-EN, We implement both Gibbs and Metropolis-within-Gibbs algorithms, respectively and set all the hyperparameters to 1.

When applying the above methods, we generated 2000 posterior samples after discarding the first 500 samples as burn-in. We computed posterior median of each element of β_j 's for point estimates of β_j 's, and the performance is evaluated via root of mean squared error (RMSE) defined as $\left[(k+1)^{-1} \sum_{j=0}^k (\hat{\beta}_j - \beta_j^{\text{true}})^2 \right]^{1/2}$, and median of mean absolute error (MMAD) defined as $\text{median} \left[(k+1)^{-1} \sum_{j=0}^k \left| \hat{\beta}_j - \beta_j^{\text{true}} \right| \right]$. We also computed 95% credible intervals of β_j 's, and calculated average lengths (AL) and coverage probability (CP) defined as $(k+1)^{-1} \sum_{j=0}^k |CI_j|$ and $(k+$

$1)^{-1} \sum_{j=0}^k I(\beta_j \in CI_j)$, respectively. These values were averaged over 300 replications of simulating datasets.

We report simulation results in Tables 1-6 and Figures 5-8. In Simulation 1, there is no outliers in simulated datasets. In the median case ($\tau = 0.5$), both HBL and BQR-BL have the smallest RMSE and MMAD for both $n = 100$ and $n = 200$. In the upper and lower quantile cases ($\tau = 0.25, 0.75$), HBQR-BL and HBQR-EN outperformed BQR-BL and BQR-EN even though they are comparable. In the presence of large outliers (Simulations 2 and 3) for $\tau = 0.5$, HBQR-BL and HBL perform better for $n = 100$ for Simulation 2. As the sample size increases to $n = 200$, BQR-BL and HBL outperform the proposed methods. Similarly, HBL and BQR-EN have the smallest RMSE and MMAD for Simulation 3. However, for both simulations, the proposed methods perform significantly better in case of upper and lower quantiles. Particularly, in Simulations 4-6 where there are skewed & heavy-tailed noise with large outliers, heavy-tailed noise (Cauchy distribution) and multiple outliers, respectively, the proposed methods perform significantly better than the existing robust methods in all cases of τ . Observing the performance of BQR-EN, the boxplots of Simulation 5 in Figures 5-7 were wider compared to other methods, which suggest that this method may not produce as efficient estimates as the proposed HBQR-EN did. All the boxplots for $\tau = 0.25$ and $\tau = 0.75$ can be found in Appendix C. Looking at the CP, they are reasonable in all simulations. For AL, it is evident that the proposed methods have the lowest AL in all cases while the BQR-BL has the largest AL. To conclude these simulation studies, the proposed methods seem to perform well consistently in all scenarios.

We also present the boxplot of posterior median of η in Figure 8 for $\tau = 0.5$. In the absence of outliers (Simulation 1), the posterior median of η has large values. On the other hand, in the present of large outliers (Simulations 2-4,6) and in a model following a heavy-tailed noise (Simulation 5), small η is chosen. The results for $\tau = 0.25$ and $\tau = 0.75$ are similar (see Appendix C). Therefore, like the HBL method (Kawakami and Hashimoto (2023)), it is evident that η is adaptively chosen for each simulated dataset.

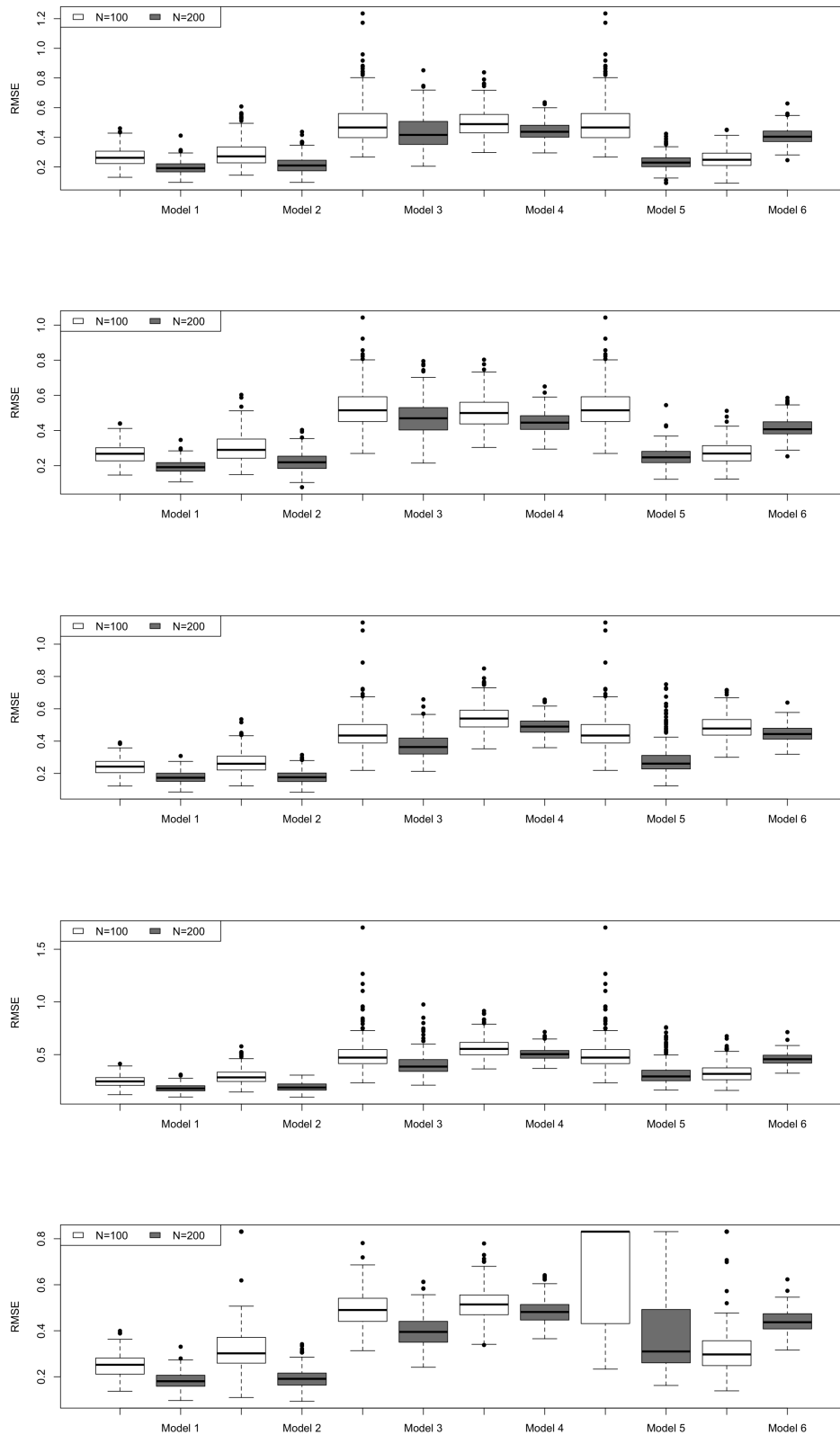


Figure 5: Boxplots of RMSE based on 300 replications in six simulation scenarios for HBQR-BL, HBQR-EN, HBL, BQR-BL and BQR-EN in this order ($\tau = 0.5$).

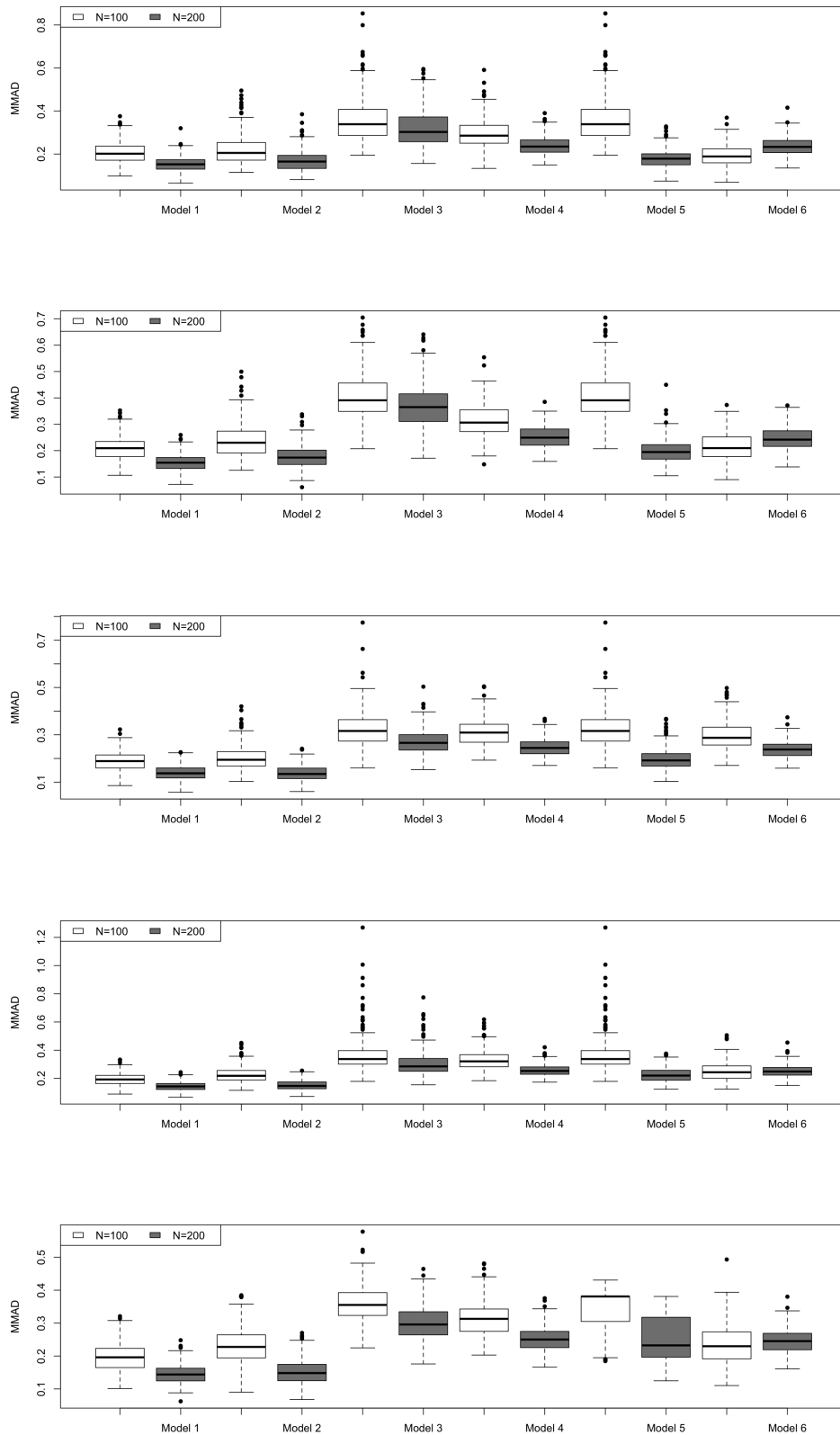


Figure 6: Boxplots of MMAD based on 300 replications in six simulation scenarios for HBQR-BL, HBQR-EN, HBL, BQR-BL and BQR-EN in this order ($\tau = 0.5$).

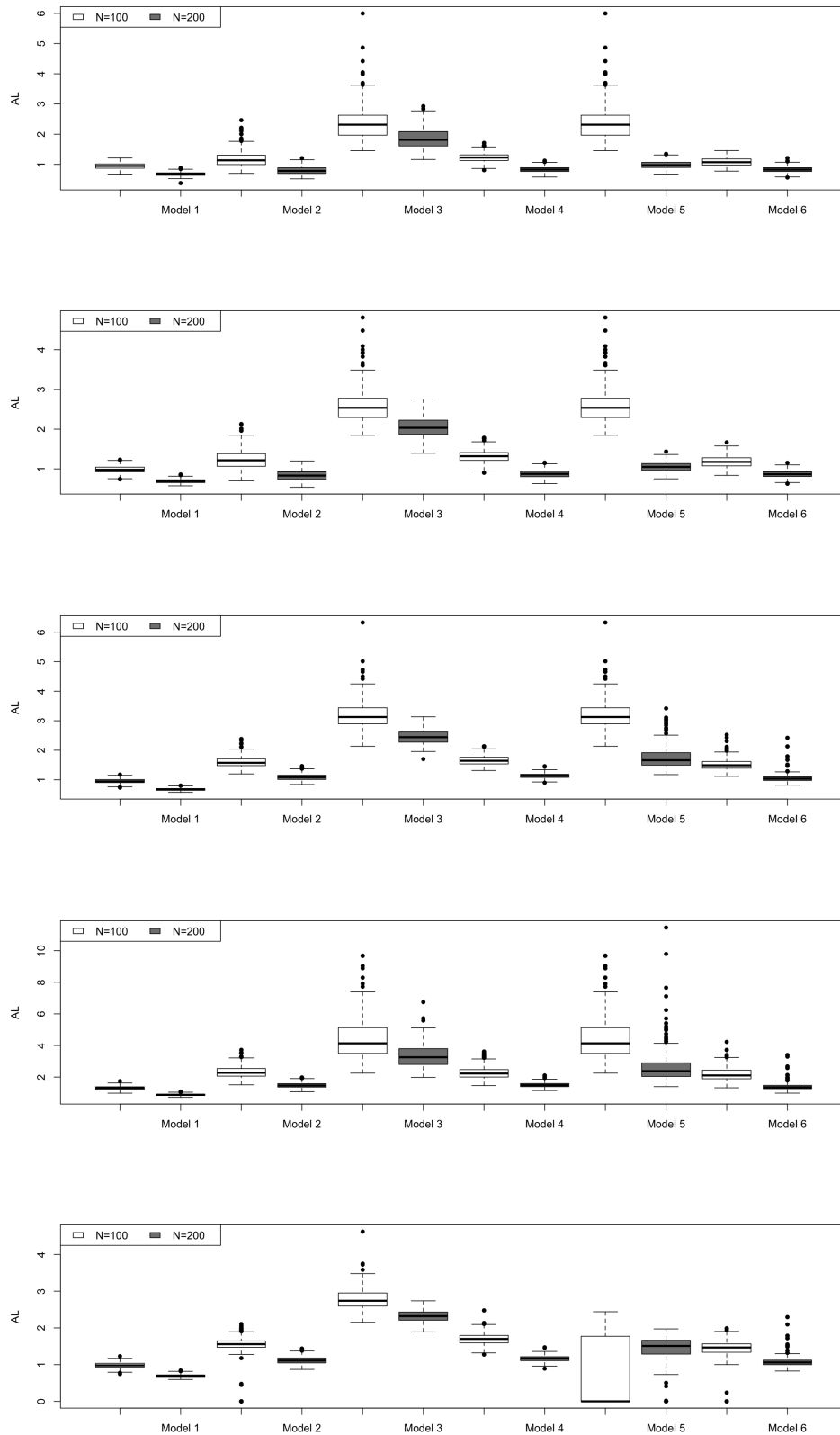


Figure 7: Boxplots of AL based on 300 replications in six simulation scenarios for HBQR-BL, HBQR-EN, HBL, BQR-BL and BQR-EN in this order ($\tau = 0.5$).

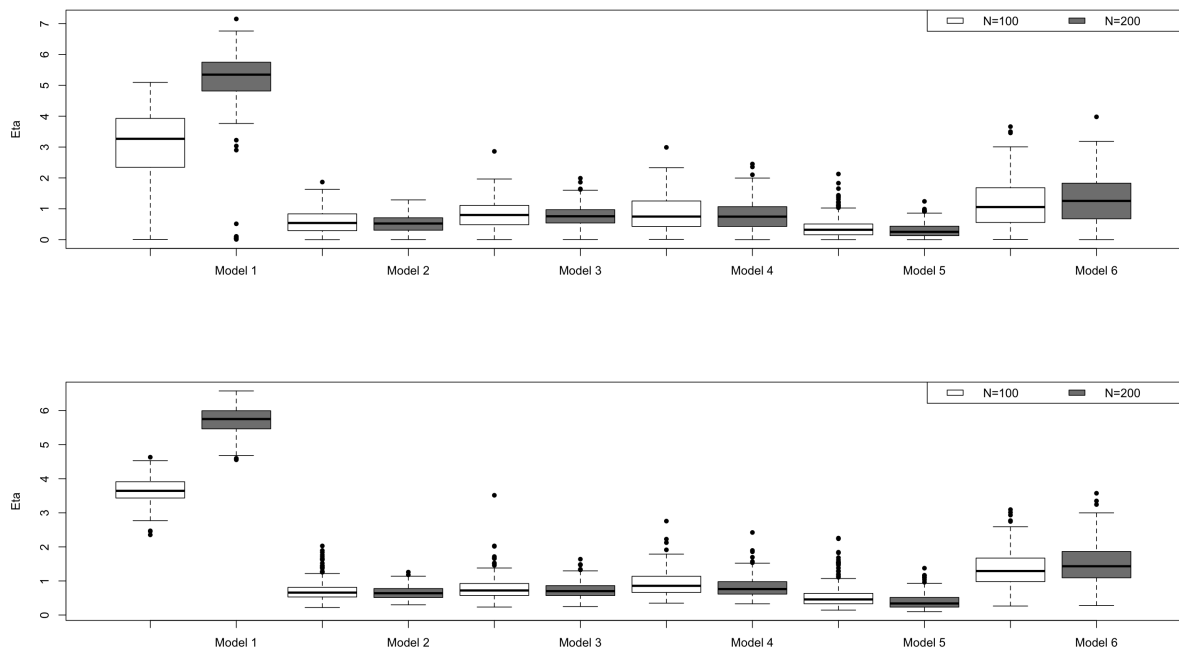


Figure 8: Boxplots of posterior median of η based on 300 replications in six simulation scenarios for HBQR-BL (top) and HBQR-EN (bottom) ($\tau = 0.5$).

	Methods	RMSE	MMAD	AL	CP
$\tau = 0.25$	HBQR-BL100	0.3675	0.2548	0.9238	0.8711
	HBQR-EN100	0.3795	0.2585	0.9673	0.8725
	BQR-BL100	0.3956	0.2627	1.3406	0.9411
	BQR-EN100	0.3859	0.2628	0.9624	0.8821
	HBQR-BL200	0.3328	0.2108	0.6624	0.8483
	HBQR-EN200	0.3380	0.2104	0.6822	0.8576
	BQR-BL200	0.3534	0.2118	0.9076	0.9311
	BQR-EN200	0.3476	0.2123	0.6819	0.8732
$\tau = 0.5$	HBQR-BL100	0.2659	0.2059	0.9465	0.9211
	HBQR-EN100	0.2678	0.2100	0.9834	0.9289
	HBL100	0.2426	0.1891	0.9553	0.9432
	BQR-BL100	0.2468	0.1946	1.2976	0.9848
	BQR-EN100	0.2502	0.1968	0.9838	0.9413
	HBQR-BL200	0.1962	0.1550	0.6810	0.9143
	HBQR-EN200	0.1952	0.1549	0.6927	0.9192
	HBL200	0.1777	0.1404	0.6763	0.9384
	BQR-BL200	0.1825	0.1452	0.8756	0.9778
	BQR-EN200	0.1841	0.1460	0.6900	0.9329
$\tau = 0.75$	HBQR-BL100	0.3635	0.2521	0.9395	0.8756
	HBQR-EN100	0.3662	0.2503	0.9891	0.8722
	BQR-BL100	0.3943	0.2587	1.3484	0.9440
	BQR-EN100	0.3853	0.2664	0.9920	0.8859
	HBQR-BL200	0.3386	0.2141	0.6703	0.8573
	HBQR-EN200	0.3315	0.2105	0.6895	0.8562
	BQR-BL200	0.3571	0.2146	0.9053	0.9340
	BQR-EN200	0.3512	0.2174	0.6890	0.8659

Table 1: Numerical results in Simulation 1.

	Methods	RMSE	MMAD	AL	CP
$\tau = 0.25$	HBQR-BL100	0.3822	0.2579	1.1290	0.9046
	HBQR-EN100	0.4051	0.2767	1.2135	0.9002
	BQR-BL100	0.5643	0.3385	2.6992	0.9506
	BQR-EN100	0.4950	0.3100	1.6428	0.9311
	HBQR-BL200	0.3418	0.2233	0.8011	0.8762
	HBQR-EN200	0.3528	0.2368	0.8484	0.8765
	BQR-BL200	0.4588	0.2540	1.7800	0.9521
	BQR-EN200	0.4221	0.2436	1.2130	0.9394
$\tau = 0.5$	HBQR-BL100	0.2886	0.2203	1.175	0.9533
	HBQR-EN100	0.2945	0.2336	1.2251	0.9522
	HBL100	0.2683	0.2013	1.604	0.9946
	BQR-BL100	0.2954	0.2262	2.333	0.9992
	BQR-EN100	0.3273	0.2340	1.5357	0.9733
	HBQR-BL200	0.2060	0.1591	0.7990	0.9279
	HBQR-EN200	0.2130	0.1679	0.8332	0.9297
	HBL200	0.1793	0.1386	1.0921	0.9943
	BQR-BL200	0.1926	0.1511	1.4813	0.9992
	BQR-EN200	0.1941	0.1522	1.1176	0.9929
$\tau = 0.75$	HBQR-BL100	0.3791	0.2624	1.1734	0.9066
	HBQR-EN100	0.3889	0.2822	1.2615	0.9000
	BQR-BL100	0.5761	0.3468	2.7564	0.9525
	BQR-EN100	0.4697	0.3086	1.8026	0.9433
	HBQR-BL200	0.3324	0.2188	0.8013	0.8792
	HBQR-EN200	0.3352	0.2198	0.8442	0.8705
	BQR-BL200	0.4530	0.2498	1.7595	0.9521
	BQR-EN200	0.4087	0.2416	1.2458	0.9437

Table 2: Numerical results in Simulation 2.

	Methods	RMSE	MMAD	AL	CP
$\tau = 0.25$	HBQR-BL100	0.5676	0.4038	2.3005	0.9259
	HBQR-EN100	0.5805	0.4285	2.5853	0.9268
	BQR-BL100	0.6854	0.4754	5.0697	0.9524
	BQR-EN100	0.6147	0.4293	2.9063	0.9430
	HBQR-BL200	0.5173	0.3732	1.8027	0.9094
	HBQR-EN200	0.5319	0.3825	2.0427	0.9060
	BQR-BL200	0.5836	0.4033	3.7568	0.9519
	BQR-EN200	0.5542	0.3872	2.4114	0.9422
$\tau = 0.5$	HBQR-BL100	0.4949	0.3576	2.370	0.9719
	HBQR-EN100	0.4958	0.3856	2.583	0.9700
	HBL100	0.4525	0.3248	3.199	0.9980
	BQR-BL100	0.5023	0.3671	4.4369	0.9992
	BQR-EN100	0.4910	0.3566	2.7858	0.9871
	HBQR-BL200	0.4317	0.3197	1.8692	0.9611
	HBQR-EN200	0.4317	0.3178	2.0474	0.9624
	HBL200	0.3707	0.2719	2.4534	0.9965
	BQR-BL200	0.4053	0.3041	3.3309	0.9992
	BQR-EN200	0.3975	0.2995	2.3221	0.9921
$\tau = 0.75$	HBQR-BL100	0.5563	0.3993	2.3546	0.9300
	HBQR-EN100	0.5911	0.4240	2.7935	0.9321
	BQR-BL100	0.6650	0.4591	4.9652	0.9531
	BQR-EN100	0.5984	0.4318	3.3417	0.9482
	HBQR-BL200	0.5241	0.3856	1.8819	0.9114
	HBQR-EN200	0.5390	0.3926	2.1538	0.9033
	BQR-BL200	0.5786	0.4008	3.8405	0.9522
	BQR-EN200	0.5455	0.3940	2.6987	0.9479

Table 3: Numerical results in Simulation 3.

	Methods	RMSE	MMAD	AL	CP
$\tau = 0.25$	HBQR-BL100	0.2705	0.1957	1.0598	0.9416
	HBQR-EN100	0.2803	0.2093	1.1574	0.9408
	BQR-BL100	0.3335	0.2542	2.5406	0.9990
	BQR-EN100	0.3300	0.2362	1.5557	0.9769
	HBQR-BL200	0.2265	0.1572	0.6799	0.9038
	HBQR-EN200	0.2287	0.1584	0.7199	0.9004
	BQR-BL200	0.2168	0.1679	1.5867	0.9979
	BQR-EN200	0.2143	0.1636	1.0815	0.9721
$\tau = 0.5$	HBQR-BL100	0.4965	0.2950	1.2265	0.9193
	HBQR-EN100	0.5048	0.3049	1.2383	0.9213
	HBL100	0.5434	0.3111	1.6510	0.9450
	BQR-BL100	0.5609	0.3312	2.2801	0.9503
	BQR-EN100	0.5184	0.3134	1.6965	0.9430
	HBQR-BL200	0.4407	0.2385	0.8315	0.9029
	HBQR-EN200	0.4466	0.2314	0.8457	0.9006
	HBL200	0.4927	0.2461	1.1366	0.9446
	BQR-BL200	0.5061	0.2571	1.4968	0.9506
	BQR-EN200	0.4835	0.2515	1.1630	0.9444
$\tau = 0.75$	HBQR-BL100	0.8388	0.4236	1.4484	0.9070
	HBQR-EN100	0.8417	0.4460	1.5382	0.9005
	BQR-BL100	1.1330	0.5333	2.7729	0.9492
	BQR-EN100	1.0732	0.5514	2.1302	0.9281
	HBQR-BL200	0.7868	0.3716	1.0323	0.8829
	HBQR-EN200	0.7940	0.3874	1.0884	0.8676
	BQR-BL200	1.0651	0.4624	1.9991	0.9462
	BQR-EN200	1.0206	0.4729	1.5216	0.9149

Table 4: Numerical results in Simulation 4.

	Methods	RMSE	MMAD	AL	CP
$\tau = 0.25$	HBQR-BL100	0.4465	0.3012	1.4890	0.9169
	HBQR-EN100	0.4460	0.3193	1.5992	0.9189
	BQR-BL100	0.8163	0.4688	4.3100	0.9522
	BQR-EN100	0.7197	0.3866	1.2336	0.8401
	HBQR-BL200	0.3741	0.2456	1.0247	0.9108
	HBQR-EN200	0.3926	0.2647	1.1039	0.9035
	BQR-BL200	0.7137	0.3841	3.1585	0.9521
	BQR-EN200	0.6376	0.3508	1.5062	0.8983
$\tau = 0.5$	HBQR-BL100	0.3292	0.2257	1.4712	0.9668
	HBQR-EN100	0.2469	0.2002	1.0604	0.9616
	HBL100	0.4151	0.2771	2.3541	0.9909
	BQR-BL100	0.4577	0.3172	3.6592	0.9963
	BQR-EN100	0.6727	0.3435	0.7418	0.8184
	HBQR-BL200	0.2320	0.1780	0.9866	0.9594
	HBQR-EN200	0.2495	0.1861	1.0505	0.9570
	HBL200	0.2861	0.1996	1.7512	0.9951
	BQR-BL200	0.3155	0.2263	2.6611	0.9990
	BQR-EN200	0.4242	0.2551	1.2599	0.9279
$\tau = 0.75$	HBQR-BL100	0.4315	0.2998	1.5445	0.9321
	HBQR-EN100	0.4356	0.3011	1.7046	0.9303
	BQR-BL100	0.7818	0.4538	4.2976	0.9649
	BQR-EN100	0.6703	0.3859	1.7851	0.8868
	HBQR-BL200	0.3732	0.2442	1.0471	0.9089
	HBQR-EN200	0.3913	0.2607	1.1202	0.9008
	BQR-BL200	0.7062	0.3789	3.2171	0.9554
	BQR-EN200	0.5920	0.3386	1.8842	0.9287

Table 5: Numerical results in Simulation 5.

	Methods	RMSE	MMAD	AL	CP
$\tau = 0.25$	HBQR-BL100	0.2669	0.2034	1.0971	0.9503
	HBQR-EN100	0.2734	0.2141	1.1773	0.9546
	BQR-BL100	0.3397	0.2591	2.2468	0.9960
	BQR-EN100	0.3285	0.2438	1.4439	0.9639
	HBQR-BL200	0.1931	0.1454	0.6920	0.9203
	HBQR-EN200	0.1978	0.1466	0.7353	0.9235
	BQR-BL200	0.2025	0.1595	1.4260	0.9984
	BQR-EN200	0.2002	0.1557	0.9916	0.9814
$\tau = 0.5$	HBQR-BL100	0.2550	0.1937	1.0816	0.9516
	HBQR-EN100	0.2634	0.2050	1.1773	0.9546
	HBL100	0.4862	0.2947	1.5152	0.9384
	BQR-BL100	0.3228	0.2480	2.1960	0.9970
	BQR-EN100	0.3200	0.2370	1.4295	0.9698
	HBQR-BL200	0.4094	0.2328	0.8321	0.8971
	HBQR-EN200	0.4147	0.2355	0.8701	0.8959
	HBL200	0.4450	0.2384	1.0562	0.9379
	BQR-BL200	0.4584	0.2502	1.3950	0.9498
	BQR-EN200	0.4392	0.2452	1.0774	0.9363
$\tau = 0.75$	HBQR-BL100	0.8115	0.4248	1.4426	0.8998
	HBQR-EN100	0.8229	0.4399	1.5531	0.8946
	BQR-BL100	1.0427	0.5067	2.5333	0.94682
	BQR-EN100	0.9903	0.5243	1.8811	0.9092
	HBQR-BL200	0.7661	0.3735	1.0210	0.8689
	HBQR-EN200	0.7734	0.3836	1.0743	0.8630
	BQR-BL200	0.9763	0.4381	1.8219	0.9437
	BQR-EN200	0.9407	0.4492	1.3898	0.9019

Table 6: Numerical results in Simulation 6.

5 Real Data Analysis

The robustness and efficiency of the Bayesian Huberised regularised quantile regression models are demonstrated via the analysis of two benchmarking datasets: Crime data and Top Gear data. They have large outliers. For a better interpretation of the parameters and to put the regressors on the common scale, we standardised all the numerical predictors and response variables to have mean 0 and

variance 1. Like in simulation studies, we also consider all the five methods of which we generated 10,000 posterior samples after discarding the first 5,000 posterior samples as a burn-in. Then we report posterior medians of regression coefficients and their 95% credible intervals. For brevity, we drop the names of predictors of the datasets and keep the corresponding number to indicate each predictor. For BQR-BL, BQR-EN, HBQR-BL and HBQR-EN, we set the quantile levels as $\tau \in \{0.1, 0.5, 0.9\}$ for the Crime and Top Gear datasets.

Since datasets may contain outliers, we adopt the following four criteria as measures of predictive accuracy; mean squared prediction error (MSPE), mean absolute prediction error (MAPE), mean Huber prediction error (MHPE) for $\delta = 1.345$ and median of squared prediction error (MedSPE) via 10-fold cross validation. They are defined by $\text{MSPE} = 10^{-1} \sum_{j=1}^{10} (\mathbf{y}_j - \mathbf{X}_j^T \hat{\boldsymbol{\beta}}^{(-j)})^2$, $\text{MAPE} = 10^{-1} \sum_{j=1}^{10} |\mathbf{y}_j - \mathbf{X}_j^T \hat{\boldsymbol{\beta}}^{(-j)}|$, $\text{MHPE} = 10^{-1} \sum_{j=1}^{10} L_{\delta}^{\text{Huber}}(\mathbf{y}_j - \mathbf{X}_j^T \hat{\boldsymbol{\beta}}^{(-j)})$ and $\text{MedSPE} = \text{median}_{1 \leq j \leq 10} (\mathbf{y}_j - \mathbf{X}_j^T \hat{\boldsymbol{\beta}}^{(-j)})^2$, where $L_{\delta}^{\text{Huber}}(\cdot)$ is defined by (2), $\hat{\boldsymbol{\beta}}^{(-j)}$ is the posterior median based on dataset except for j th validation set, and \mathbf{y}_j and \mathbf{X}_j are the response variables and covariate matrix based on the j th validation set, respectively.

	Methods	MSPE	MAPE	MedSPE	MHPE
$\tau = 0.1$	HBQR-BL	0.0226	0.1223	0.0044	0.0113
	HBQR-EN	0.0156	0.1034	0.0071	0.0078
	BQR-BL	0.0157	0.1054	0.0137	0.0078
	BQR-EN	0.0169	0.1285	0.0150	0.0085
$\tau = 0.5$	HBQR-BL	0.0123	0.0946	0.0067	0.0061
	HBQR-EN	0.0121	0.0938	0.0073	0.0061
	HBL	0.0304	0.1534	0.0173	0.0152
	BQR-BL	0.0192	0.1008	0.0081	0.0096
	BQR-EN	0.0250	0.1474	0.0185	0.0125
$\tau = 0.9$	HBQR-BL	0.0400	0.1439	0.0077	0.0200
	HBQR-EN	0.0278	0.1346	0.0079	0.0139
	BQR-BL	0.0453	0.1582	0.0106	0.0226
	BQR-EN	0.0401	0.1629	0.0146	0.0200

Table 7: Mean squared prediction error (MSPE), mean absolute prediction error (MAPE), mean Huber prediction error (MHPE) for $\delta = 1.345$ and median of squared prediction error (MedSPE) for Crime data, computed from 10-fold cross-validation.

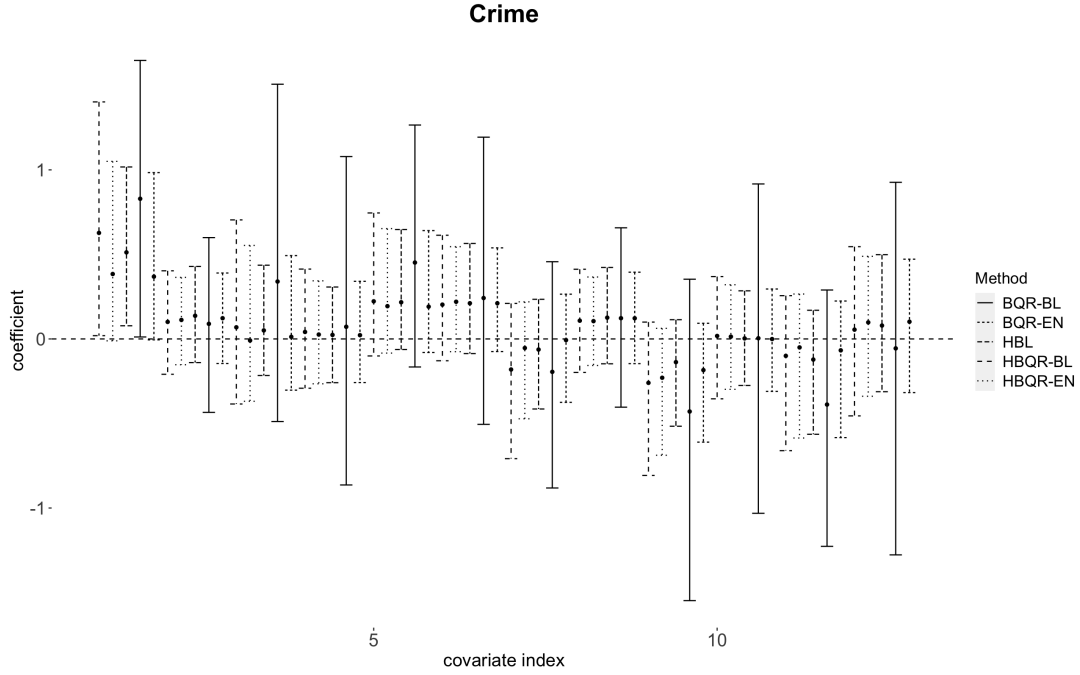


Figure 9: Posterior medians and 95% credible intervals of the regression coefficients at $\tau = 0.5$ in the Bayesian quantile regression with Bayesian lasso (BQR-BL), Bayesian quantile regression with elastic net (BQR-EN), the Huberized Bayesian lasso (HBL) and the proposed Bayesian quantile regression with Bayesian lasso (HBQR-BL) and elastic net (HBQR-EN), applied to the Crime data.

	Methods	MSPE	MAPE	MedSPE	MHPE
$\tau = 0.1$	HBQR-BL	0.0288	0.1500	0.0196	0.0144
	HBQR-EN	0.0296	0.1505	0.0229	0.0148
	BQR-BL	0.0360	0.1736	0.0331	0.0180
	BQR-EN	0.0331	0.1605	0.0267	0.0166
$\tau = 0.5$	HBQR-BL	0.0127	0.0942	0.0064	0.0064
	HBQR-EN	0.0120	0.0905	0.0070	0.0060
	HBL	0.0110	0.0863	0.0055	0.0055
	BQR-BL	0.0183	0.1102	0.0101	0.0092
	BQR-EN	0.0110	0.0864	0.0063	0.0055
$\tau = 0.9$	HBQR-BL	0.0643	0.2309	0.0410	0.0322
	HBQR-EN	0.0843	0.2662	0.0628	0.0421
	BQR-BL	0.6942	0.7652	0.7337	0.3471
	BQR-EN	0.2290	0.4461	0.1790	0.1145

Table 8: Mean squared prediction error (MSPE), mean absolute prediction error (MAPE), mean Huber prediction error (MHPE) for $\delta = 1.345$ and median of squared prediction error (MedSPE) for Top Gear data, computed from 10-fold cross-validation.

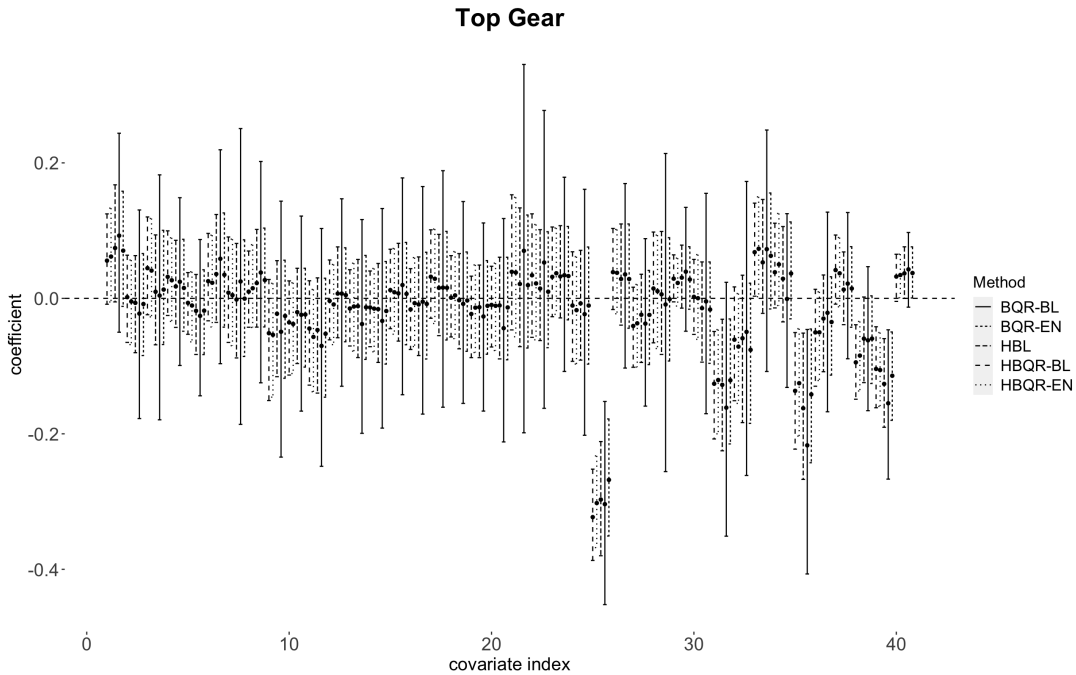


Figure 10: Posterior medians and 95% credible intervals of the regression coefficients at $\tau = 0.5$ in the Bayesian quantile regression with Bayesian lasso (BQR-BL), Bayesian quantile regression with elastic net (BQR-EN), the Huberized Bayesian lasso (HBL) and the proposed Bayesian quantile regression with Bayesian lasso (HBQR-BL) and elastic net (HBQR-EN), applied to the Top Gear data.

5.1 Crime Dataset

The data are collected from Statistical Abstract of the United States for the 50 states and the District of Columbia (U.S. Census Bureau (2006)). This data were analysed in the book of Statistical Methods for the Social Sciences (Agresti and Finlay (1997)). The predictors are the number of murders per 100,000 people in the population, the percentage of the population living in metropolitan areas, the percentage of the population who are white, the percentage of the population who are high school graduates or higher, the percentage of families living below the poverty level, and the percentage of families headed by a single parent (male householders with no wife present and with own children, or female householders with no husband present and with own children). The response of interest is the number of murders, forcible rapes, robberies, and aggravated assaults per 100,000 people in the population. In total, we have 51 observations and included squared variables, which results in 12 predictors in our models.

The posterior medians and 95% credible intervals of the regression coefficients based on the five methods are reported in Figure 9. From the figure, all the methods behave similarly and the estimation are very close. The BQR-BL method produces relatively largest credible intervals, which suggests that this method may be unstable in producing estimates. The similar performances can also be found in $\tau = 0.1$ and $\tau = 0.9$ (see Appendix C). Table 7 also presents the predictive performance of the five methods for $\tau = 0.5$ and the four Bayesian quantile regression based methods for $\tau \in \{0.1, 0.9\}$. The proposed methods perform better than the existing robust methods in both median and upper quantile levels. The HBL method produces relatively large error measures in the median case among the rest

of methods. Looking at the lower quantile level ($\tau = 0.1$), MSPE, MAPE and MHPE suggest that HBQR-EN and BQR-BL perform better while MedSPE suggests that both proposed methods perform better. In this case, they are very comparable.

5.2 Top Gear Dataset

The data uses information on cars featuring on the website of the popular BBC television show Top Gear. It is available in the R package 'robustHD' (Alfons (2021)) and contains 242 observations on 29 numerical and categorical variables after removing the missing values. A description of the variables is provided in Table 3 of the paper (Alfons et al. (2016)). The response of interest is MPG (fuel consumption) and the remaining variables are predictors. For categorical variables, there are 4 binary variables and 12 variables with three levels. These 12 variables are assigned two dummy variables each. The resulting design matrix consists of 12 numerical variables, 4 individual dummy variables, and 12 groups of two dummy variables each, giving a total of 40 predictors.

The posterior medians and 95% credible intervals of the regression coefficients based on the five methods are reported in Figure 10. From the figure, all the methods are comparable. Like for the Crime dataset, the BQR-BL method produces relatively largest credible intervals. The similar performances can also be found in $\tau = 0.1$ and $\tau = 0.9$ (see Appendix C). Table 8 also presents the predictive performance of the five methods for $\tau = 0.5$ and the four Bayesian quantile regression based methods for $\tau \in \{0.1, 0.9\}$. All the methods are comparable in the median case ($\tau = 0.5$) where both HBL and BQR-EN have the lowest error measures. Looking at the extreme quantile levels ($\tau = 0.1, 0.9$), the proposed methods significantly outperform the BQR-BL and BQR-EN methods especially at the upper quantile level where the existing robust methods perform slightly worse than the proposed methods. Furthermore, BQR-BL has the highest error measures in all cases.

6 Conclusion

In this paper, we have presented the Bayesian Huberised regularisation. We proposed the Huberised asymmetric loss function and its corresponding probability density function that leads to a scale mixture of normal distribution with exponential and generalised inverse Gaussian mixing densities. This results in fully Bayesian hierarchical models for quantile regression and its Gibbs sampling algorithm with approximate Gibbs sampler for the data-dependent estimation of the robustness parameter. We have proved theoretically that the proposed Bayesian models yield a good posterior propriety and unimodality in their joint posterior density with conditional prior for the regression coefficients. Simulation studies and real data examples show that the proposed methods are effective in predictive accuracy and their robustness is evident under a wide range of scenarios. In many situations, the proposed methods outperform the existing Bayesian regularised quantile regression methods especially at the extreme quantile levels. Our proposed methods have proven to be robust in obtaining valuable results.

7 Acknowledgments

This work is supported by the UK Engineering and Physical Sciences Research Council (EPSRC) grant 2295266 for the Brunel University London for Doctoral Training.

References

- Abramowitz, M. and Stegun, I. (1965), ‘Handbook of mathematical functions with formulas, graphs, and mathematical table. In US Department of Commerce’, *National Bureau of Standards Applied Mathematics Series* **55**.
- Adlouni, S. E., Salaou, G. and St-Hilaire, A. (2018), ‘Regularized Bayesian quantile regression’, *Communications in Statistics-Simulation and Computation* **47**(1), 277–293.
- Agresti, A. and Finlay, B. (1997), *Statistical Methods for Social Sciences*, third edn, Prentice Hall.
- Alfons, A. (2021), ‘RobustHD: an R package for robust regression with high-dimensional data’, *Journal of Open Source Software* **6**(67). Article ID 3786.
- Alfons, A., Croux, C. and Gelper., S. (2016), ‘Robust groupwise least angle regression’, *Computational Statistics & Data Analysis* **93**, 421–435.
- Alhamzawi, R. (2016), ‘Bayesian elastic net Tobit quantile regression’, *Communications in Statistics-Simulation and Computation* **45**(7), 2409–2427.
- Alhamzawi, R., Alhamzawi, A. and Ali, H. T. M. (2019), ‘New Gibbs sampling methods for Bayesian regularized quantile regression’, *Computers in Biology and Medicine* **110**, 52–65.
- Alhamzawi, R. and Yu, K. (2012), ‘Variable selection in quantile regression via Gibbs sampling’, *Journal of Applied Statistics* **39**(4), 799–813.
- Alhamzawi, R. and Yu, K. (2013), ‘Conjugate priors and variable selection for Bayesian quantile regression’, *Computational Statistics & Data Analysis* **64**, 209–219.
- Alhamzawi, R., Yu, K. and Benoit, D. F. (2012), ‘Bayesian adaptive Lasso quantile regression’, *Statistical Modelling* **12**(3), 279–297.
- Alshaybawee, T., Midi, H. and Alhamzawi, R. (2017), ‘Bayesian elastic net single index quantile regression’, *Journal of Applied Statistics* **44**(5), 853–871.
- Andrews, D. F. and Mallows, C. L. (1974), ‘Scale mixtures of normal distributions’, *Journal of the Royal Statistical Society: Series B (Methodological)* **36**(1), 99–102.
- Baricz, A., Ponnusamy, S. and Vuorinen, M. (2011), ‘Functional inequalities for modified Bessel functions’, *Expositiones Mathematicae* **29**(4), 399–414.

- Barndorff-Nielsen, O. E. and Shephard, N. (2001), ‘Non-Gaussian Ornstein–Uhlenbeck-based models and some of their uses in financial economics’, *Journal of the Royal Statistical Society: Series B (Statistical Methodology)* **63**(2), 167–241.
- Belloni, A. and Chernozhukov, V. (2011), ‘L1-penalized quantile regression in high-dimensional sparse models’, *Annals of Statistics* **39**, 82–130.
- Berger, J. O. (1985), *Statistical Decision Theory and Bayesian Analysis*, second edn, Springer-Verlag Inc.
- Cai, Z. and Sun, D. (2021), ‘Prior conditioned on scale parameter for Bayesian quantile LASSO and its generalizations’, *Statistics and Its Interface* **14**(4), 459–474.
- Chen, C. W., Dunson, D. B., Reed, C. and Yu, K. (2013), ‘Bayesian variable selection in quantile regression’, *Statistics and its Interface* **6**(2), 261–274.
- da Silva Ferreira, C., Bolfarine, H. and Lachos, V. H. (2011), ‘Skew scale mixtures of normal distributions: Properties and estimation’, *Statistical Methodology* **8**(2), 154–171.
- Daouia, A., Gijbels, I. and Stupfler, G. (2019), ‘Extremiles: A new perspective on asymmetric least squares’, *Journal of the American Statistical Association* **114**(527), 1366–1381.
- Daouia, A., Girard, S. and Stupfler, G. (2018), ‘Estimation of tail risk based on extreme expectiles’, *Journal of the Royal Statistical Society: Series B (Statistical Methodology)* **80**(2), 263–292.
- Ehm, W., Gneiting, T., Jordan, A. and Krüger, F. (2016), ‘Of quantiles and expectiles: consistent scoring functions, Choquet representations and forecast rankings’, *Journal of the Royal Statistical Society: Series B: Statistical Methodology* **78**(3), 505–562.
- Fu, L. and Wang, Y.-G. (2021), ‘Robust regression with asymmetric loss functions’, *Statistical Methods in Medical Research* **30**(8), 1800–1815.
- Henderson, H. V. and Searle, S. R. (1981), ‘On deriving the inverse of a sum of matrices’, *SIAM Review* **23**(1), 53–60.
- Huber, P. J. (1964), ‘Robust estimation of a location parameter’, *Annals of Mathematical Statistics* **35**(1), 73–101. doi:10.1214/aoms/1177703732.
- Jullion, A. and Lambert, P. (2007), ‘Robust specification of the roughness penalty prior distribution in spatially adaptive Bayesian P-splines models’, *Computational Statistics and Data Analysis* **51**, 2542–2558.
- Kawakami, J. and Hashimoto, S. (2023), ‘Approximate Gibbs sampler for Bayesian Huberized lasso’, *Journal of Statistical Computation and Simulation* **93**(1), 128–162.
- Koenker, R. and Bassett, G. (1978), ‘Regression Quantiles’, *Econometrica*, **46**(1), 33–50.

- Kozumi, H. and Kobayashi, G. (2011), ‘Gibbs sampling methods for Bayesian quantile regression’, *Journal of Statistical Computation and Simulation* **81**(11), 1565–1578.
- Kyung, M., Gill, J., Ghosh, M. and Casella, G. (2010), ‘Penalized regression, standard errors, and Bayesian lassos’, *Bayesian Analysis* **5**, 369–412.
- Lambert-Lacroix, S. and Zwald, L. (2011), ‘Robust regression through the Huber’s criterion and adaptive lasso penalty’, *Electronic Journal of Statistics* **5**, 1015–1053.
- Li, J., Chen, Q., Leng, J., Zhang, W. and Guo, M. (2020), ‘Probabilistic robust regression with adaptive weights — a case study on face recognition’, *Frontiers of Computer Science* **14**(5), 1–12.
- Li, Q. and Lin, N. (2010), ‘The Bayesian elastic net’, *Bayesian Analysis* pp. 151–170.
- Li, Q., Lin, N. and Xi, R. (2010), ‘Bayesian regularized quantile regression’, *Bayesian Analysis* **5**(3), 533–556.
- Li, Y. and Zhu, J. (2008), ‘L1-norm quantile regression’, *Journal of Computational and Graphical Statistics* **17**(1), 163–185.
- Park, T. and Casella, G. (2008), ‘The Bayesian lasso’, *Journal of the American Statistical Association* **103**, 681–686.
- Reed, C. and Yu, K. (2009), ‘A partially collapsed Gibbs sampler for Bayesian quantile regression’, <https://bura.brunel.ac.uk/bitstream/2438/3593/1/fulltext.pdf>.
- Reich, B. J. and Smith, L. B. (2013), ‘Bayesian quantile regression for censored data’, *Biometrics* **69**(3), 651–660.
- Sriram, K., Ramamoorthi, R. and Ghosh, P. (2013), ‘Posterior consistency of Bayesian quantile regression based on the misspecified asymmetric Laplace density’, *Bayesian Analysis* **8**, 479–504.
- Su, M. and Wang, W. (2021), ‘Elastic net penalized quantile regression model’, *Journal of Computational and Applied Mathematics* **392**.
- Sun, Q., Zhou, W.-X. and Fan, J. (2020), ‘Adaptive Huber Regression’, *Journal of the American Statistical Association* **115**(529), 254–265.
- Tibshirani, R. (1996), ‘Regression shrinkage and selection via the lasso’, *Journal of the Royal Statistical Society: Series B (Methodological)* **58**(1), 267–288.
- U.S. Census Bureau (2006), ‘Statistical Abstract of the United States’. Retrieved from the Library of Congress, <https://www.loc.gov/item/lcwaN0014424/>.
- West, M. (1987), ‘On scale mixtures of normal distributions’, *Biometrika* **74**(3), 646–648.
- Wu, Y. and Liu, Y. (2009), ‘Variable selection in quantile regression’, *Statistica Sinica* pp. 801–817.

Yang, Z.-H. and Chu, Y.-M. (2017), ‘On approximating the modified Bessel function of the second kind’, *Journal of Inequalities and Applications* **2017**(1), 1–8.

Yu, K. and Moyeed, R. A. (2001), ‘Bayesian quantile regression’, *Statistics & Probability Letters* **54**(4), 437–447.

Zou, H. and Hastie, T. (2005), ‘Regularization and variable selection via the elastic net’, *Journal of the Royal Statistical Society: Series B (Statistical Methodology)* **67**(2), 301–320.

A Proofs

A.1 Proposition 2.1

We set $\mu = 0$ and we wish to calculate $P(X \leq 0)$, that is,

$$\begin{aligned} P(X \leq 0) &= \int_{-\infty}^0 f_X(x) dx \\ &= \frac{\eta\tau(1-\tau)e^\eta}{2\rho^2(\eta+1)} \int_{-\infty}^0 \exp\left\{-\sqrt{\eta\left(\eta - \frac{x(1-\tau)}{\rho^2}\right)}\right\} dx \\ &= \frac{\eta\tau(1-\tau)e^\eta}{2\rho^2(\eta+1)} \int_0^\infty \exp\left\{-\sqrt{\eta\left(\eta + \frac{x(1-\tau)}{\rho^2}\right)}\right\} dx. \end{aligned}$$

By letting $u = \sqrt{\eta\left(\eta + \frac{x(1-\tau)}{\rho^2}\right)}$, we have

$$\begin{aligned} P(X \leq 0) &= \frac{\eta\tau(1-\tau)e^\eta}{2\rho^2(\eta+1)} \int_\eta^\infty e^{-u} \times \frac{2u\rho^2}{\eta(1-\tau)} du \\ &= \frac{\tau e^\eta}{(\eta+1)} \int_\eta^\infty u e^{-u} du \\ &= \frac{\tau e^\eta}{(\eta+1)} \left([-ue^{-u}]_\eta^\infty + \int_\eta^\infty e^{-u} du \right) \\ &= \frac{\tau e^\eta}{(\eta+1)} \left(\eta e^{-\eta} + [-e^{-u}]_\eta^\infty \right) \\ &= \frac{\tau e^\eta}{(\eta+1)} (e^{-\eta}(\eta+1)) \\ &= \tau. \end{aligned}$$

On the other hand, it follows that $P(X > 0) = 1 - \tau$. This completes the proof.

A.2 Theorem 2.1

Let a, b be some real constants. By using the equality

$$\exp(-|ab|) = \int_0^\infty \frac{a}{\sqrt{2\pi}\sigma} \exp\left\{-\frac{1}{2}(a^2\sigma + b^2\sigma^{-1})\right\} d\sigma, \quad (\text{A.1})$$

(Andrews and Mallows (1974)) and let $a = \sqrt{\frac{\eta}{\rho^2}}$ and $b = \sqrt{\eta + \frac{\epsilon_i}{\rho^2} (\tau - I(\epsilon_i < 0))}$, $f(\epsilon_i)$ can be expressed as a scale mixture of asymmetric Laplace (AL) and generalised inverse Gaussian (GIG) densities:

$$\begin{aligned} & \frac{\eta\tau(1-\tau)e^\eta}{2\rho^2(\eta+1)} \exp \left\{ -\sqrt{\eta \left(\eta + \frac{\epsilon_i}{\rho^2} (\tau - I(\epsilon_i < 0)) \right)} \right\} \\ & \propto \int_0^\infty \mathcal{ALD}(\epsilon_i; 0, 2\sigma_i, \tau) GIG\left(\sigma_i; 1, \sqrt{\frac{\eta}{\rho^2}}, \sqrt{\eta\rho^2}\right) d\sigma_i, \end{aligned}$$

where $GIG(v|1, c, d)$ denotes the GIG distribution and its density is given by (7) and ALD.

The ALD can be expressed as a scale mixture of normal and exponential densities using the equality (Equation (A.1)) by letting $a = \frac{1}{\sqrt{4\sigma_i}}$, $b = \frac{\epsilon_i}{\sqrt{4\sigma_i}}$ and multiplying a factor of $\exp\left\{-\frac{(2\tau-1)\epsilon}{4\sigma_i}\right\}$ (Kozumi and Kobayashi (2011)). Therefore, $f(\epsilon_i)$ is expressed as a normal scale mixture of exponential and generalised inverse Gaussian (GIG) densities:

$$\begin{aligned} & \frac{\eta\tau(1-\tau)e^\eta}{2\rho^2(\eta+1)} \exp \left\{ -\sqrt{\eta \left(\eta + \frac{\epsilon_i}{\rho^2} (\tau - I(\epsilon_i < 0)) \right)} \right\} \\ & \propto \int_0^\infty \int_0^\infty N(\epsilon_i | (1-2\tau)v_i, 4\sigma_i v_i) \text{Exp}\left(v_i; \frac{\tau(1-\tau)}{2\sigma_i}\right) GIG\left(\sigma_i; 1, \sqrt{\frac{\eta}{\rho^2}}, \sqrt{\eta\rho^2}\right) d\sigma_i dv_i, \end{aligned}$$

where $N(\cdot)$ and $\text{Exp}(\cdot)$ are the normal and exponential densities, respectively.

A.3 Proposition 3.1

The overall posterior distribution is given by

$$\begin{aligned} & \pi(\boldsymbol{\beta}, \rho^2, \mathbf{v}, \boldsymbol{\sigma}, \mathbf{s} | \mathbf{y}) \\ & = \frac{\pi(\mathbf{y} | \mathbf{X}, \boldsymbol{\beta}, \mathbf{v}, \boldsymbol{\sigma}) \pi(\boldsymbol{\beta} | \mathbf{s}, \rho^2) \pi(\mathbf{v} | \boldsymbol{\sigma}) \pi(\boldsymbol{\sigma} | \rho^2) \pi(\rho^2) \pi(\mathbf{s})}{\iiint \pi(\mathbf{y} | \mathbf{X}, \boldsymbol{\beta}, \mathbf{v}, \boldsymbol{\sigma}) \pi(\boldsymbol{\beta} | \mathbf{s}, \rho^2) \pi(\mathbf{v} | \boldsymbol{\sigma}) \pi(\boldsymbol{\sigma} | \rho^2) \pi(\rho^2) \pi(\mathbf{s}) d\boldsymbol{\beta} d\mathbf{v} d\boldsymbol{\sigma} d\rho^2}. \end{aligned}$$

We show that the normalising constant of the posterior distribution is finite, that is,

$$\iiint \pi(\mathbf{y} | \mathbf{X}, \boldsymbol{\beta}, \mathbf{v}, \boldsymbol{\sigma}) \pi(\boldsymbol{\beta} | \mathbf{s}, \rho^2) \pi(\mathbf{v} | \boldsymbol{\sigma}) \pi(\boldsymbol{\sigma} | \rho^2) \pi(\rho^2) \pi(\mathbf{s}) d\boldsymbol{\beta} d\mathbf{v} d\boldsymbol{\sigma} d\rho^2 < \infty.$$

First, we consider the integral with respect to $\boldsymbol{\beta}$. We have

$$\begin{aligned}
& \int \pi(\mathbf{y}|\mathbf{X}, \boldsymbol{\beta}, \mathbf{v}, \boldsymbol{\sigma})\pi(\boldsymbol{\beta}|\mathbf{s}, \rho^2)d\boldsymbol{\beta} \\
&= \int \prod_{i=1}^n \frac{1}{\sqrt{8\pi\sigma_i v_i}} \exp\left\{-\frac{(y_i - \mathbf{x}_i\boldsymbol{\beta} - (1-2\tau)v_i)^2}{8\sigma_i v_i}\right\} \\
&\quad \times \prod_{j=1}^k \frac{1}{\sqrt{2\pi\rho^2 s_j}} \exp\left\{-\frac{\beta_j^2}{2\rho^2 s_j}\right\} d\boldsymbol{\beta} \\
&= \int (8\pi)^{-n/2} (2\pi)^{-k/2} (\rho^2)^{-k/2} \left(\prod_{i=1}^n \sigma_i\right)^{-1/2} \left(\prod_{i=1}^n v_i\right)^{-1/2} \left(\prod_{j=1}^k s_j\right)^{-1/2} \\
&\quad \times \exp\left\{-\frac{1}{2}(\mathbf{y} - \mathbf{X}\boldsymbol{\beta} - (1-2\tau)\mathbf{v})^T \mathbf{V}^{-1}(\mathbf{y} - \mathbf{X}\boldsymbol{\beta} - (1-2\tau)\mathbf{v})\right\} \\
&\quad \times \exp\left\{-\frac{1}{2\rho^2}\boldsymbol{\beta}^T \boldsymbol{\Lambda}^{-1}\boldsymbol{\beta}\right\} d\boldsymbol{\beta},
\end{aligned}$$

where $\mathbf{V} = \text{diag}(4\sigma_1 v_1, \dots, 4\sigma_n v_n)$ and $\boldsymbol{\Lambda} = \text{diag}(s_1, \dots, s_k)$. In particular, we have

$$\begin{aligned}
& \int \exp\left\{-\frac{1}{2}(\mathbf{y} - \mathbf{X}\boldsymbol{\beta} - (1-2\tau)\mathbf{v})^T \mathbf{V}^{-1}(\mathbf{y} - \mathbf{X}\boldsymbol{\beta} - (1-2\tau)\mathbf{v})\right\} \times \exp\left\{-\frac{1}{2\rho^2}\boldsymbol{\beta}^T \boldsymbol{\Lambda}^{-1}\boldsymbol{\beta}\right\} d\boldsymbol{\beta} \\
&= \exp\left\{-\frac{1}{2}(\mathbf{y} - (1-2\tau)\mathbf{v})^T \mathbf{V}^{-1}(\mathbf{y} - (1-2\tau)\mathbf{v})\right\} \\
&\quad \times \int \exp\left\{-\frac{1}{2}\left(\boldsymbol{\beta}^T \left(\mathbf{X}^T \mathbf{V}^{-1} \mathbf{X} + \frac{1}{\rho^2} \boldsymbol{\Lambda}^{-1}\right) \boldsymbol{\beta} - 2\boldsymbol{\beta}^T \mathbf{X}^T \mathbf{V}^{-1}(\mathbf{y} - (1-2\tau)\mathbf{v})\right)\right\} d\boldsymbol{\beta} \\
&= \exp\left\{-\frac{1}{2}(\mathbf{y} - (1-2\tau)\mathbf{v})^T \mathbf{V}^{-1}(\mathbf{y} - (1-2\tau)\mathbf{v})\right\} \\
&\quad \times (2\pi)^{k/2} \left|\left(\mathbf{X}^T \mathbf{V}^{-1} \mathbf{X} + \frac{1}{\rho^2} \boldsymbol{\Lambda}^{-1}\right)^{-1}\right|^{1/2} \\
&= \exp\left\{-\frac{1}{2}(\mathbf{y} - (1-2\tau)\mathbf{v})^T \mathbf{V}^{-1}(\mathbf{y} - (1-2\tau)\mathbf{v})\right\} \\
&\quad \times (2\pi)^{k/2} \left|\frac{1}{\rho^2} \boldsymbol{\Lambda}^{-1}\right|^{-1/2} |\mathbf{V}|^{1/2} |\mathbf{V} + \rho^2 \mathbf{X} \boldsymbol{\Lambda} \mathbf{X}^T|^{-1/2} \tag{A.2} \\
&= \exp\left\{-\frac{1}{2}(\mathbf{y} - (1-2\tau)\mathbf{v})^T \mathbf{V}^{-1}(\mathbf{y} - (1-2\tau)\mathbf{v})\right\} \\
&\quad \times (2\pi)^{k/2} 2^n (\rho^2)^{k/2} \left(\prod_{j=1}^k s_j\right)^{1/2} \left(\prod_{i=1}^n \sigma_i\right)^{1/2} \left(\prod_{i=1}^n v_i\right)^{1/2} |\mathbf{V} + \rho^2 \mathbf{X} \boldsymbol{\Lambda} \mathbf{X}^T|^{-1/2}.
\end{aligned}$$

The expression in (A.2) is due to the identity of $|I + AB| = |I + BA|$ (Henderson and Searle (1981)).

Hence, we have

$$\begin{aligned}
& \int \pi(\mathbf{y}|\mathbf{X}, \boldsymbol{\beta}, \mathbf{v}, \boldsymbol{\sigma})\pi(\boldsymbol{\beta}|\mathbf{s}, \rho^2)d\boldsymbol{\beta} \\
&= (2\pi)^{-n/2} \exp\left\{-\frac{1}{2}(\mathbf{y} - (1-2\tau)\mathbf{v})^T \mathbf{V}^{-1}(\mathbf{y} - (1-2\tau)\mathbf{v})\right\} \\
&\quad \times |\mathbf{V} + \rho^2 \mathbf{X} \boldsymbol{\Lambda} \mathbf{X}^T|^{-1/2}.
\end{aligned}$$

Next, we have

$$\begin{aligned}
& \int \int \int \int \int \pi(\mathbf{y}|\mathbf{X}, \boldsymbol{\beta}, \mathbf{v}, \boldsymbol{\sigma}) \pi(\boldsymbol{\beta}|\mathbf{s}, \rho^2) \pi(\mathbf{v}|\boldsymbol{\sigma}) \pi(\sigma|\rho^2) \pi(\rho^2) \pi(\mathbf{s}) d\boldsymbol{\beta} d\mathbf{v} d\boldsymbol{\sigma} ds d\rho^2 \\
&= \int \int \int \int (2\pi)^{-n/2} \exp \left\{ -\frac{1}{2} (\mathbf{y} - (1-2\tau)\mathbf{v})^T \mathbf{V}^{-1} (\mathbf{y} - (1-2\tau)\mathbf{v}) \right\} \\
&\quad \times |\mathbf{V} + \rho^2 \mathbf{X} \boldsymbol{\Lambda} \mathbf{X}^T|^{-1/2} \prod_{i=1}^n \frac{\tau(1-\tau)}{2\sigma_i} \exp \left\{ -\frac{\tau(1-\tau)v_i}{2\sigma_i} \right\} \pi(\sigma|\rho^2) \pi(\rho^2) \pi(\mathbf{s}) d\mathbf{v} d\boldsymbol{\sigma} ds d\rho^2 \\
&\leq \int \int \int \int (2\pi)^{-n/2} \exp \left\{ -\frac{1}{2} (\mathbf{y} - (1-2\tau)\mathbf{v})^T \mathbf{V}^{-1} (\mathbf{y} - (1-2\tau)\mathbf{v}) \right\} |\mathbf{V}|^{-1/2} \\
&\quad \times \prod_{i=1}^n \frac{\tau(1-\tau)}{2\sigma_i} \exp \left\{ -\frac{\tau(1-\tau)v_i}{2\sigma_i} \right\} \pi(\sigma|\rho^2) \pi(\rho^2) \pi(\mathbf{s}) d\mathbf{v} d\boldsymbol{\sigma} ds d\rho^2,
\end{aligned}$$

by using the fact that $|A+B| \geq |A|$ implies $|A+B|^{-1/2} \leq |A|^{-1/2}$ for a positive definite matrix A and a semi-positive definite matrix B .

Next, we consider the integral with respect to \mathbf{v} . First, we have

$$\begin{aligned}
& \int |\mathbf{V}|^{-1/2} \exp \left\{ -\frac{1}{2} (\mathbf{y} - (1-2\tau)\mathbf{v})^T \mathbf{V}^{-1} (\mathbf{y} - (1-2\tau)\mathbf{v}) \right\} \\
&\quad \times \prod_{i=1}^n \frac{\tau(1-\tau)}{2\sigma_i} \exp \left\{ -\frac{\tau(1-\tau)v_i}{2\sigma_i} \right\} d\mathbf{v} \\
&= \int \left(\frac{\tau(1-\tau)}{2} \right)^n 2^{-n} \left(\prod_{i=1}^n \sigma_i \right)^{-3/2} \left(\prod_{i=1}^n v_i \right)^{-1/2} \\
&\quad \times \prod_{i=1}^n \exp \left\{ -\frac{(y_i - (1-2\tau)v_i)^2}{8\sigma_i v_i} - \frac{\tau(1-\tau)v_i}{2\sigma_i} \right\} d\mathbf{v} \\
&= \left(\frac{\tau(1-\tau)}{4} \right)^n \left(\prod_{i=1}^n \sigma_i \right)^{-3/2} \\
&\quad \times \int \prod_{i=1}^n v_i^{-1/2} \exp \left\{ -\frac{(y_i - (1-2\tau)v_i)^2}{8\sigma_i v_i} - \frac{(1 - (1-2\tau)^2) v_i}{8\sigma_i} \right\} d\mathbf{v} \\
&= \left(\frac{\tau(1-\tau)}{4} \right)^n \left(\prod_{i=1}^n \sigma_i \right)^{-3/2} \\
&\quad \times \int \prod_{i=1}^n v_i^{-1/2} \exp \left\{ -\frac{y_i^2}{8\sigma_i v_i} - \frac{(1-2\tau)y_i}{4\sigma_i} - \frac{v_i}{8\sigma_i} \right\} d\mathbf{v} \\
&= \left(\frac{\tau(1-\tau)}{4} \right)^n \left(\prod_{i=1}^n \sigma_i \right)^{-3/2} \\
&\quad \times \int \prod_{i=1}^n v_i^{-1/2} \exp \left\{ -\frac{1}{2} \left(\frac{v_i}{4\sigma_i} + \frac{y_i^2}{4\sigma_i v_i} \right) \right\} \exp \left\{ -\frac{(1-2\tau)y_i}{4\sigma_i} \right\} d\mathbf{v}.
\end{aligned}$$

Letting $a^2 = \frac{1}{4\sigma_i}$ and $b^2 = \frac{y_i^2}{4\sigma_i}$ and using the equality (Equation (A.1)), we have

$$\begin{aligned}
& \int |\mathbf{V}|^{-1/2} \exp \left\{ -\frac{1}{2} (\mathbf{y} - (1-2\tau)\mathbf{v})^T \mathbf{V}^{-1} (\mathbf{y} - (1-2\tau)\mathbf{v}) \right\} \\
& \quad \times \prod_{i=1}^n \frac{\tau(1-\tau)}{2\sigma_i} \exp \left\{ -\frac{\tau(1-\tau)v_i}{2\sigma_i} \right\} d\mathbf{v} \\
& = \left(\frac{\tau(1-\tau)}{4} \right)^n \left(\prod_{i=1}^n \sigma_i \right)^{-3/2} \exp \left\{ -\frac{(1-2\tau)y_i}{4\sigma_i} \right\} \\
& \quad \times \int \prod_{i=1}^n v_i^{-1/2} \exp \left\{ -\frac{1}{2} (a^2 v_i + b^2 v_i^{-1}) \right\} d\mathbf{v} \\
& = \left(\frac{\tau(1-\tau)}{4} \right)^n \left(\prod_{i=1}^n \sigma_i \right)^{-3/2} \exp \left\{ -\frac{(1-2\tau)y_i}{4\sigma_i} \right\} \\
& \quad \times \prod_{i=1}^n (2\pi)^{1/2} (4\sigma_i)^{1/2} \exp \left\{ -\frac{|y_i|}{4\sigma_i} \right\} \\
& = (2\pi)^{n/2} \left(\frac{\tau(1-\tau)}{2} \right)^n \left(\prod_{i=1}^n \sigma_i \right)^{-1} \exp \left\{ -\frac{|y_i| + (1-2\tau)y_i}{4\sigma_i} \right\}.
\end{aligned}$$

Hence, we have

$$\begin{aligned}
& \iiint \pi(\mathbf{y}|\mathbf{X}, \boldsymbol{\beta}, \mathbf{v}, \boldsymbol{\sigma}) \pi(\boldsymbol{\beta}|\mathbf{s}, \rho^2) \pi(\mathbf{v}|\boldsymbol{\sigma}) \pi(\boldsymbol{\sigma}|\rho^2) \pi(\rho^2) \pi(\mathbf{s}) d\boldsymbol{\beta} d\mathbf{v} d\boldsymbol{\sigma} d\rho^2 \\
& \leq \iiint \left(\frac{\tau(1-\tau)}{2} \right)^n \left(\prod_{i=1}^n \sigma_i \right)^{-1} \exp \left\{ -\frac{|y_i| + (1-2\tau)y_i}{4\sigma_i} \right\} \\
& \quad \times \prod_{i=1}^n \frac{1}{2\rho^2 K_1(\eta)} \exp \left\{ -\frac{\eta}{2} \left(\frac{\sigma_i}{\rho^2} + \frac{\rho^2}{\sigma_i} \right) \right\} \pi(\rho^2) \pi(\mathbf{s}) d\boldsymbol{\sigma} d\rho^2 \\
& = \iiint \left(\frac{\tau(1-\tau)}{2} \right)^n \left(\frac{1}{2\rho^2 K_1(\eta)} \right)^n \\
& \quad \times \prod_{i=1}^n \sigma_i^{-1} \exp \left\{ -\frac{\eta}{2} \left(\frac{\sigma_i}{\rho^2} + \frac{\rho^2}{\sigma_i} \right) - \frac{|y_i| + (1-2\tau)y_i}{4\sigma_i} \right\} \pi(\rho^2) \pi(\mathbf{s}) d\boldsymbol{\sigma} d\rho^2.
\end{aligned}$$

Next, we consider the integral with respect to $\boldsymbol{\sigma}$. First, we have

$$\begin{aligned}
& \int \prod_{i=1}^n \sigma_i^{-1} \exp \left\{ -\frac{\eta}{2} \left(\frac{\sigma_i}{\rho^2} + \frac{\rho^2}{\sigma_i} \right) - \frac{|y_i| + (1-2\tau)y_i}{4\sigma_i} \right\} d\boldsymbol{\sigma} \\
& = \int \prod_{i=1}^n \sigma_i^{-1} \exp \left\{ -\frac{1}{2} \left(\frac{\eta\sigma_i}{\rho^2} + \left(\eta\rho^2 + \frac{|y_i| + (1-2\tau)y_i}{2} \right) \frac{1}{\sigma_i} \right) \right\} d\boldsymbol{\sigma}.
\end{aligned}$$

Letting $c^2 = \frac{\eta}{\rho^2}$ and $d^2 = \eta\rho^2 + \frac{|y_i| + (1-2\tau)y_i}{2}$ and using the fact that

$$K_\nu(cd) = \frac{1}{2} \left(\frac{c}{d} \right)^{-\nu} \int_0^\infty x^{\nu-1} \exp \left\{ -\frac{1}{2} \left(c^2 x + \frac{d^2}{x} \right) \right\} dx,$$

we have

$$\begin{aligned} & \int \prod_{i=1}^n \sigma_i^{-1} \exp \left\{ -\frac{\eta}{2} \left(\frac{\sigma_i}{\rho^2} + \frac{\rho^2}{\sigma_i} \right) - \frac{|y_i| + (1-2\tau)y_i}{4\sigma_i} \right\} d\boldsymbol{\sigma} \\ &= \prod_{i=1}^n 2K_0 \left(\sqrt{\frac{\eta}{\rho^2} \left(\eta\rho^2 + \frac{|y_i| + (1-2\tau)y_i}{2} \right)} \right), \end{aligned}$$

Hence, we have

$$\begin{aligned} & \iiint \pi(\mathbf{y}|\mathbf{X}, \boldsymbol{\beta}, \mathbf{v}, \boldsymbol{\sigma}) \pi(\boldsymbol{\beta}|\mathbf{s}, \rho^2) \pi(\mathbf{v}|\boldsymbol{\sigma}) \pi(\boldsymbol{\sigma}|\rho^2) \pi(\rho^2) \pi(\mathbf{s}) d\boldsymbol{\beta} d\mathbf{v} d\boldsymbol{\sigma} d\rho^2 \\ & \leq \iint \left(\frac{\tau(1-\tau)}{2} \right)^n \left(\frac{1}{2\rho^2 K_1(\eta)} \right)^n 2^n \prod_{i=1}^n K_0 \left(\sqrt{\frac{\eta}{\rho^2} \left(\eta\rho^2 + \frac{|y_i| + (1-2\tau)y_i}{2} \right)} \right) \\ & \quad \times \prod_{j=1}^k \frac{\lambda_1^2}{2} \exp \left\{ -\frac{\lambda_1^2 s_j}{2} \right\} \pi(\rho^2) d\mathbf{s} d\rho^2 \\ & = \int \left(\frac{\tau(1-\tau)}{2} \right)^n \left(\frac{1}{\rho^2 K_1(\eta)} \right)^n \prod_{i=1}^n K_0 \left(\sqrt{\frac{\eta}{\rho^2} \left(\eta\rho^2 + \frac{|y_i| + (1-2\tau)y_i}{2} \right)} \right) \frac{1}{\rho^2} d\rho^2 \\ & = \left(\frac{\tau(1-\tau)}{2K_1(\eta)} \right)^n \int (\rho^2)^{-(n+1)} \prod_{i=1}^n K_0 \left(\sqrt{\eta^2 + \eta \frac{|y_i| + (1-2\tau)y_i}{2\rho^2}} \right) d\rho^2. \end{aligned} \quad (\text{A.3})$$

In Equation (A.3), we note that the inequality

$$\sqrt{\eta^2 + \eta \frac{|y_i| + (1-2\tau)y_i}{2\rho^2}} \geq \sqrt{\frac{\eta}{\rho^2} \left(\frac{|y_i| + (1-2\tau)y_i}{2} \right)},$$

implies

$$K_0 \left(\sqrt{\eta^2 + \eta \frac{|y_i| + (1-2\tau)y_i}{2\rho^2}} \right) \leq K_0 \left(\sqrt{\frac{\eta}{\rho^2} \left(\frac{|y_i| + (1-2\tau)y_i}{2} \right)} \right),$$

for any $\eta > 0$ for $i = 1, \dots, n$. Hence, we have

$$\begin{aligned} & \iiint \pi(\mathbf{y}|\mathbf{X}, \boldsymbol{\beta}, \mathbf{v}, \boldsymbol{\sigma}) \pi(\boldsymbol{\beta}|\mathbf{s}, \rho^2) \pi(\mathbf{v}|\boldsymbol{\sigma}) \pi(\boldsymbol{\sigma}|\rho^2) \pi(\rho^2) \pi(\mathbf{s}) d\boldsymbol{\beta} d\mathbf{v} d\boldsymbol{\sigma} d\rho^2 \\ & \leq \left(\frac{\tau(1-\tau)}{2K_1(\eta)} \right)^n \int (\rho^2)^{-(n+1)} \prod_{i=1}^n K_0 \left(\sqrt{\eta \frac{|y_i| + (1-2\tau)y_i}{2\rho^2}} \right) d\rho^2. \end{aligned}$$

Using the fact that

$$K_0(x) < K_{1/2}(x) = \frac{\sqrt{\pi} e^{-x}}{\sqrt{2x}},$$

holds for all $x > 0$ (Yang and Chu (2017)), we obtain

$$\begin{aligned}
& \iiint \pi(\mathbf{y}|\mathbf{X}, \boldsymbol{\beta}, \mathbf{v}, \boldsymbol{\sigma}) \pi(\boldsymbol{\beta}|\mathbf{s}, \rho^2) \pi(\mathbf{v}|\boldsymbol{\sigma}) \pi(\boldsymbol{\sigma}|\rho^2) \pi(\rho^2) \pi(\mathbf{s}) d\boldsymbol{\beta} d\mathbf{v} d\boldsymbol{\sigma} d\rho^2 \\
& < \left(\frac{\tau(1-\tau)}{2K_1(\eta)} \right)^n \int (\rho^2)^{-(n+1)} \\
& \quad \times \prod_{i=1}^n \sqrt{\frac{\pi}{2}} \left(\eta \frac{|y_i| + (1-2\tau)y_i}{2\rho^2} \right)^{-1/4} \exp \left\{ -\sqrt{\eta \frac{|y_i| + (1-2\tau)y_i}{2\rho^2}} \right\} d\rho^2 \\
& = \left(\frac{\sqrt{\pi}\tau(1-\tau)}{2\sqrt{2}K_1(\eta)} \right)^n \left(\eta \frac{|y_i| + (1-2\tau)y_i}{2} \right)^{-1/4} \\
& \quad \times \int (\rho^2)^{-(3n/2+1)} \exp \left\{ -\frac{1}{\sqrt{\rho^2}} \sum_{i=1}^n \sqrt{\eta \frac{|y_i| + (1-2\tau)y_i}{2}} \right\} d\rho^2.
\end{aligned}$$

By using the transformation $\sqrt{\rho^2} = x$, we have

$$\begin{aligned}
& \int (\rho^2)^{-(3n/2+1)} \exp \left\{ -\frac{1}{\sqrt{\rho^2}} \sum_{i=1}^n \sqrt{\eta \frac{|y_i| + (1-2\tau)y_i}{2}} \right\} d\rho^2 \\
& = 2 \int x^{-3n/2-1} \exp \left\{ -\frac{1}{x} \sqrt{\frac{\eta}{2}} \sum_{i=1}^n \sqrt{|y_i| + (1-2\tau)y_i} \right\} dx. \tag{A.4}
\end{aligned}$$

Since the integrand is the kernel of $IG\left(\frac{3n}{2}, \sqrt{\frac{\eta}{2}} \sum_{i=1}^n \sqrt{|y_i| + (1-2\tau)y_i}\right)$ where $IG(\cdot)$ is the inverse Gamma distribution, the integral is finite for any n . Hence, the posterior distribution under the improper prior $\pi(\rho^2) \propto \frac{1}{\rho^2}$ is proper for any n .

A.4 Proposition 3.2

The joint posterior density of $(\boldsymbol{\beta}, \rho^2)$ is expressed by

$$\pi(\boldsymbol{\beta}, \rho^2|\mathbf{y}) = \iint \pi(\mathbf{y}|\mathbf{X}, \boldsymbol{\beta}, \boldsymbol{\sigma}, \mathbf{v}) \pi(\boldsymbol{\beta}|\rho^2) \pi(\mathbf{v}|\boldsymbol{\sigma}) \pi(\boldsymbol{\sigma}|\rho^2) \pi(\rho^2) d\mathbf{v} d\boldsymbol{\sigma}.$$

First, we consider the integral with respect to \mathbf{v} . We have

$$\begin{aligned}
& \int \pi(\mathbf{y}|\mathbf{X}, \boldsymbol{\beta}, \boldsymbol{\sigma}, \mathbf{v}) \pi(\mathbf{v}|\boldsymbol{\sigma}) d\mathbf{v} \\
& = \int \prod_{i=1}^n \frac{1}{\sqrt{8\pi\sigma_i v_i}} \exp \left\{ -\frac{(y_i - \mathbf{x}_i \boldsymbol{\beta} - (1-2\tau)v_i)^2}{8\sigma_i v_i} \right\} \\
& \quad \times \prod_{i=1}^n \frac{\tau(1-\tau)}{2\sigma_i} \exp \left\{ -\frac{\tau(1-\tau)v_i}{2\sigma_i} \right\} d\mathbf{v} \\
& = (8\pi)^{-n/2} \left(\frac{\tau(1-\tau)}{2} \right)^n \left(\prod_{i=1}^n \sigma_i \right)^{-3/2} \\
& \quad \times \int \prod_{i=1}^n v_i^{-1/2} \exp \left\{ -\frac{(y_i - \mathbf{x}_i \boldsymbol{\beta} - (1-2\tau)v_i)^2}{8\sigma_i v_i} - \frac{\tau(1-\tau)v_i}{2\sigma_i} \right\} d\mathbf{v} \\
& = \left(\frac{\tau(1-\tau)}{2} \right)^n \prod_{i=1}^n \sigma_i^{-1} \exp \left\{ -\frac{|y_i - \mathbf{x}_i \boldsymbol{\beta}| + (1-2\tau)(y_i - \mathbf{x}_i \boldsymbol{\beta})}{4\sigma_i} \right\}.
\end{aligned}$$

Hence, we have

$$\begin{aligned}
\pi(\boldsymbol{\beta}, \rho^2 | \mathbf{y}) &= \pi(\boldsymbol{\beta} | \rho^2) \pi(\rho^2) \int \left(\frac{\tau(1-\tau)}{2} \right)^n \prod_{i=1}^n \sigma_i^{-1} \exp \left\{ -\frac{|y_i - \mathbf{x}_i \boldsymbol{\beta}| + (1-2\tau)(y_i - \mathbf{x}_i \boldsymbol{\beta})}{4\sigma_i} \right\} \\
&\quad \times \prod_{i=1}^n \frac{1}{2\rho^2 K_1(\eta)} \exp \left\{ -\frac{\eta}{2} \left(\frac{\sigma_i}{\rho^2} + \frac{\rho^2}{\sigma_i} \right) \right\} d\boldsymbol{\sigma} \\
&= \pi(\boldsymbol{\beta} | \rho^2) \pi(\rho^2) (\rho^2)^{-n} \left(\frac{\tau(1-\tau)}{4K_1(\eta)} \right)^n \\
&\quad \times \int \prod_{i=1}^n \sigma_i^{-1} \exp \left\{ -\frac{1}{2} \left(\frac{\eta}{\rho^2 \sigma_i} + \left(\eta \rho^2 + \frac{|y_i - \mathbf{x}_i \boldsymbol{\beta}| + (1-2\tau)(y_i - \mathbf{x}_i \boldsymbol{\beta})}{2} \right) \frac{1}{\sigma_i} \right) \right\} d\boldsymbol{\sigma} \\
&= \pi(\boldsymbol{\beta} | \rho^2) \pi(\rho^2) (\rho^2)^{-n} \left(\frac{\tau(1-\tau)}{4K_1(\eta)} \right)^n \\
&\quad \times \prod_{i=1}^n 2K_0 \left(\sqrt{\frac{\eta}{\rho^2} \left(\frac{|y_i - \mathbf{x}_i \boldsymbol{\beta}| + (1-2\tau)(y_i - \mathbf{x}_i \boldsymbol{\beta})}{2} \right)} \right) \\
&\propto (\rho^2)^{-1} (\rho^2)^{-k/2} (\rho^2)^{-n} \prod_{j=1}^k \exp \left\{ -\frac{\lambda_1 |\beta_j|}{\sqrt{\rho^2}} \right\} \\
&\quad \times \prod_{i=1}^n K_0 \left(\sqrt{\frac{\eta}{\rho^2} \left(\frac{|y_i - \mathbf{x}_i \boldsymbol{\beta}| + (1-2\tau)(y_i - \mathbf{x}_i \boldsymbol{\beta})}{2} \right)} \right) \\
&= (\rho^2)^{-n-k/2-1} \exp \left\{ -\frac{\lambda_1}{\sqrt{\rho^2}} \sum_{j=1}^k |\beta_j| \right\} \\
&\quad \times \prod_{i=1}^n K_0 \left(\sqrt{\frac{\eta}{\rho^2} \left(\frac{|y_i - \mathbf{x}_i \boldsymbol{\beta}| + (1-2\tau)(y_i - \mathbf{x}_i \boldsymbol{\beta})}{2} \right)} \right).
\end{aligned}$$

Then the log posterior density is given by

$$\begin{aligned}
\log \pi(\boldsymbol{\beta}, \rho^2 | \mathbf{y}) &= - \left(n + \frac{k}{2} + 1 \right) \log \rho^2 - \frac{\lambda_1}{\sqrt{\rho^2}} \|\boldsymbol{\beta}\|_1 \\
&\quad + \sum_{i=1}^n \log \left[K_0 \left(\sqrt{\frac{\eta}{\rho^2} \left(\frac{|y_i - \mathbf{x}_i \boldsymbol{\beta}| + (1-2\tau)(y_i - \mathbf{x}_i \boldsymbol{\beta})}{2} \right)} \right) \right]. \tag{A.5}
\end{aligned}$$

Like Kawakami and Hashimoto (2023) and Cai and Sun (2021), we consider the coordinate transformation $\Phi \leftrightarrow \frac{\boldsymbol{\beta}}{\sqrt{\rho^2}}$, $\xi \leftrightarrow \frac{1}{\sqrt{\rho^2}}$. In the transformation coordinate, Equation (A.5) is given by

$$\begin{aligned}
&(2n + k - 2) \log \xi - \lambda_1 \|\Phi\|_1 \\
&\quad + \sum_{i=1}^n \log \left[K_0 \left(\sqrt{\eta^2 + \frac{\eta \xi}{2} (|\xi y_i - \mathbf{x}_i \Phi| + (1-2\tau)(\xi y_i - \mathbf{x}_i \Phi))} \right) \right]. \tag{A.6}
\end{aligned}$$

The first two terms in Equation (A.6) are concave. The last term is also concave, since the Theorem 2(b) of Baricz et al. (2011) is equivalent to log-convexity of K_ν for every ν . Therefore, the joint posterior $\pi(\boldsymbol{\beta}, \rho^2 | \mathbf{y})$ is unimodal. This completes the proof.

A.5 Proposition 3.3

Like the proof of Proposition 3.1, we follow in the similar manner. The overall posterior distribution is given by

$$\begin{aligned} & \pi(\boldsymbol{\beta}, \rho^2, \mathbf{v}, \boldsymbol{\sigma}, \mathbf{t} | \mathbf{y}) \\ &= \frac{\pi(\mathbf{y} | \mathbf{X}, \boldsymbol{\beta}, \mathbf{v}, \boldsymbol{\sigma}) \pi(\boldsymbol{\beta} | \mathbf{t}, \rho^2) \pi(\mathbf{v} | \boldsymbol{\sigma}) \pi(\boldsymbol{\sigma} | \rho^2) \pi(\rho^2) \pi(\mathbf{t})}{\iiint \pi(\mathbf{y} | \mathbf{X}, \boldsymbol{\beta}, \mathbf{v}, \boldsymbol{\sigma}) \pi(\boldsymbol{\beta} | \mathbf{t}, \rho^2) \pi(\mathbf{v} | \boldsymbol{\sigma}) \pi(\boldsymbol{\sigma} | \rho^2) \pi(\rho^2) \pi(\mathbf{t}) d\boldsymbol{\beta} d\mathbf{v} d\boldsymbol{\sigma} dt d\rho^2}. \end{aligned}$$

We show that the normalising constant of the posterior distribution is finite, that is,

$$\iiint \pi(\mathbf{y} | \mathbf{X}, \boldsymbol{\beta}, \mathbf{v}, \boldsymbol{\sigma}) \pi(\boldsymbol{\beta} | \mathbf{t}, \rho^2) \pi(\mathbf{v} | \boldsymbol{\sigma}) \pi(\boldsymbol{\sigma} | \rho^2) \pi(\rho^2) \pi(\mathbf{t}) d\boldsymbol{\beta} d\mathbf{v} d\boldsymbol{\sigma} dt d\rho^2 < \infty.$$

First, we consider the integral with respect to $\boldsymbol{\beta}$. We have

$$\begin{aligned} & \int \pi(\mathbf{y} | \mathbf{X}, \boldsymbol{\beta}, \mathbf{v}, \boldsymbol{\sigma}) \pi(\boldsymbol{\beta} | \mathbf{t}, \rho^2) d\boldsymbol{\beta} \\ &= \int (8\pi)^{-n/2} (\pi)^{-k/2} \lambda_4^{k/2} (\rho^2)^{-k/2} \left(\prod_{i=1}^n \sigma_i \right)^{-1/2} \left(\prod_{i=1}^n v_i \right)^{-1/2} \left(\prod_{j=1}^k \frac{t_j}{t_j - 1} \right)^{1/2} \\ & \quad \times \exp \left\{ -\frac{1}{2} (\mathbf{y} - \mathbf{X}\boldsymbol{\beta} - (1 - 2\tau)\mathbf{v})^T \mathbf{V}^{-1} (\mathbf{y} - \mathbf{X}\boldsymbol{\beta} - (1 - 2\tau)\mathbf{v}) \right\} \\ & \quad \times \exp \left\{ -\frac{\lambda_4}{\rho^2} \boldsymbol{\beta}^T \boldsymbol{\Lambda}_2^{-1} \boldsymbol{\beta} \right\} d\boldsymbol{\beta}, \end{aligned}$$

where $\mathbf{V} = \text{diag}(4\sigma_1 v_1, \dots, 4\sigma_n v_n)$ and $\boldsymbol{\Lambda}_2 = \text{diag}((t_1 - 1)t_1^{-1}, \dots, (t_n - 1)t_n^{-1})$. In particular, we have

$$\begin{aligned} & \int \exp \left\{ -\frac{1}{2} (\mathbf{y} - \mathbf{X}\boldsymbol{\beta} - (1 - 2\tau)\mathbf{v})^T \mathbf{V}^{-1} (\mathbf{y} - \mathbf{X}\boldsymbol{\beta} - (1 - 2\tau)\mathbf{v}) \right\} \times \exp \left\{ -\frac{\lambda_4}{\rho^2} \boldsymbol{\beta}^T \boldsymbol{\Lambda}_2^{-1} \boldsymbol{\beta} \right\} d\boldsymbol{\beta} \\ &= \exp \left\{ -\frac{1}{2} (\mathbf{y} - (1 - 2\tau)\mathbf{v})^T \mathbf{V}^{-1} (\mathbf{y} - (1 - 2\tau)\mathbf{v}) \right\} \\ & \quad \times (2\pi)^{k/2} \left| \left(\mathbf{X}^T \mathbf{V}^{-1} \mathbf{X} + \frac{2\lambda_4}{\rho^2} \boldsymbol{\Lambda}_2^{-1} \right)^{-1} \right|^{1/2} \\ &= \exp \left\{ -\frac{1}{2} (\mathbf{y} - (1 - 2\tau)\mathbf{v})^T \mathbf{V}^{-1} (\mathbf{y} - (1 - 2\tau)\mathbf{v}) \right\} \\ & \quad \times (2\pi)^{k/2} \left| \frac{2\lambda_4}{\rho^2} \boldsymbol{\Lambda}_2^{-1} \right|^{-1/2} |\mathbf{V}|^{1/2} \left| \mathbf{V} + \frac{\rho^2}{2\lambda_4} \mathbf{X} \boldsymbol{\Lambda}_2^{-1} \mathbf{X}^T \right|^{-1/2} \\ &= \exp \left\{ -\frac{1}{2} (\mathbf{y} - (1 - 2\tau)\mathbf{v})^T \mathbf{V}^{-1} (\mathbf{y} - (1 - 2\tau)\mathbf{v}) \right\} \\ & \quad \times (2\pi)^{k/2} 2^n 2^{k/2} (\rho^2)^{k/2} \lambda_4^{-k/2} \left(\prod_{j=1}^k \frac{t_j}{t_j - 1} \right)^{-1/2} \left(\prod_{i=1}^n \sigma_i \right)^{1/2} \left(\prod_{i=1}^n v_i \right)^{1/2} \\ & \quad \times \left| \mathbf{V} + \frac{\rho^2}{2\lambda_4} \mathbf{X} \boldsymbol{\Lambda}_2^{-1} \mathbf{X}^T \right|^{-1/2}. \end{aligned}$$

Hence, we have

$$\begin{aligned}
& \int \pi(\mathbf{y}|\mathbf{X}, \boldsymbol{\beta}, \mathbf{v}, \boldsymbol{\sigma}) \pi(\boldsymbol{\beta}|\mathbf{t}, \rho^2) d\boldsymbol{\beta} \\
&= (2\pi)^{n/2} \exp \left\{ -\frac{1}{2} (\mathbf{y} - (1-2\tau)\mathbf{v})^T \mathbf{V}^{-1} (\mathbf{y} - (1-2\tau)\mathbf{v}) \right\} \\
&\quad \times \left| \mathbf{V} + \frac{\rho^2}{2\lambda_4} \mathbf{X} \boldsymbol{\Lambda}_2^{-1} \mathbf{X}^T \right|^{-1/2}.
\end{aligned}$$

Next, we have

$$\begin{aligned}
& \iiint \pi(\mathbf{y}|\mathbf{X}, \boldsymbol{\beta}, \mathbf{v}, \boldsymbol{\sigma}) \pi(\boldsymbol{\beta}|\mathbf{t}, \rho^2) \pi(\mathbf{v}|\boldsymbol{\sigma}) \pi(\boldsymbol{\sigma}|\rho^2) \pi(\rho^2) \pi(\mathbf{t}) d\boldsymbol{\beta} d\mathbf{v} d\boldsymbol{\sigma} dt d\rho^2 \\
&= \iiint \int (2\pi)^{n/2} \exp \left\{ -\frac{1}{2} (\mathbf{y} - (1-2\tau)\mathbf{v})^T \mathbf{V}^{-1} (\mathbf{y} - (1-2\tau)\mathbf{v}) \right\} \\
&\quad \times \left| \mathbf{V} + \frac{\rho^2}{2\lambda_4} \mathbf{X} \boldsymbol{\Lambda}_2^{-1} \mathbf{X}^T \right|^{-1/2} \pi(\mathbf{v}|\boldsymbol{\sigma}) \pi(\boldsymbol{\sigma}|\rho^2) \pi(\rho^2) \pi(\mathbf{t}) d\mathbf{v} d\boldsymbol{\sigma} dt d\rho^2 \\
&\leq \iiint \int (2\pi)^{-n/2} \exp \left\{ -\frac{1}{2} (\mathbf{y} - (1-2\tau)\mathbf{v})^T \mathbf{V}^{-1} (\mathbf{y} - (1-2\tau)\mathbf{v}) \right\} |\mathbf{V}|^{-1/2} \\
&\quad \times \prod_{i=1}^n \frac{\tau(1-\tau)}{2\sigma_i} \exp \left\{ -\frac{\tau(1-\tau)v_i}{2\sigma_i} \right\} \pi(\boldsymbol{\sigma}|\rho^2) \pi(\rho^2) \pi(\mathbf{s}) d\mathbf{v} d\boldsymbol{\sigma} ds d\rho^2.
\end{aligned}$$

Next, we consider the integral with respect to \mathbf{v} . We have

$$\begin{aligned}
& \int |\mathbf{V}|^{-1/2} \exp \left\{ -\frac{1}{2} (\mathbf{y} - (1-2\tau)\mathbf{v})^T \mathbf{V}^{-1} (\mathbf{y} - (1-2\tau)\mathbf{v}) \right\} \\
&\quad \times \prod_{i=1}^n \frac{\tau(1-\tau)}{2\sigma_i} \exp \left\{ -\frac{\tau(1-\tau)v_i}{2\sigma_i} \right\} d\mathbf{v} \\
&= (2\pi)^{n/2} \left(\frac{\tau(1-\tau)}{2} \right)^n \left(\prod_{i=1}^n \sigma_i \right)^{-1} \exp \left\{ -\frac{|y_i| + (1-2\tau)y_i}{4\sigma_i} \right\}.
\end{aligned}$$

Hence, we have

$$\begin{aligned}
& \iiint \pi(\mathbf{y}|\mathbf{X}, \boldsymbol{\beta}, \mathbf{v}, \boldsymbol{\sigma}) \pi(\boldsymbol{\beta}|\mathbf{t}, \rho^2) \pi(\mathbf{v}|\boldsymbol{\sigma}) \pi(\boldsymbol{\sigma}|\rho^2) \pi(\rho^2) \pi(\mathbf{t}) d\boldsymbol{\beta} d\mathbf{v} d\boldsymbol{\sigma} dt d\rho^2 \\
& \leq \iiint \left(\frac{\tau(1-\tau)}{2} \right)^n \left(\prod_{i=1}^n \sigma_i \right)^{-1} \exp \left\{ -\frac{|y_i| + (1-2\tau)y_i}{4\sigma_i} \right\} \\
& \quad \times \prod_{i=1}^n \frac{1}{2\rho^2 K_1(\eta)} \exp \left\{ -\frac{\eta}{2} \left(\frac{\sigma_i}{\rho^2} + \frac{\rho^2}{\sigma_i} \right) \right\} \pi(\rho^2) \pi(\mathbf{t}) d\boldsymbol{\sigma} dt d\rho^2 \\
& = \iiint \left(\frac{\tau(1-\tau)}{4K_1(\eta)} \right)^n (\rho^2)^{-n} \\
& \quad \times \prod_{i=1}^n \sigma_i \exp \left\{ -\frac{1}{2} \left(\frac{\eta\sigma_i}{\rho^2} + \left(\eta\rho^2 + \frac{|y_i| + (1-2\tau)y_i}{2} \right) \frac{1}{\sigma_i} \right) \right\} \pi(\rho^2) \pi(\mathbf{t}) d\boldsymbol{\sigma} dt d\rho^2 \\
& = \iint \left(\frac{\tau(1-\tau)}{2K_1(\eta)} \right)^n (\rho^2)^{-n} \prod_{i=1}^n K_0 \left(\sqrt{\frac{\eta}{\rho^2} \left(\eta\rho^2 + \frac{|y_i| + (1-2\tau)y_i}{2} \right)} \right) \\
& \quad \times \prod_{j=1}^k \Gamma^{-1} \left(\frac{1}{2}, \tilde{\lambda}_3 \right) \sqrt{\frac{\tilde{\lambda}_3}{t_j}} \exp \left\{ -\tilde{\lambda}_3 t_j \right\} I(t_j > 1) \times \frac{1}{\rho^2} dt d\rho^2 \\
& = \left(\frac{\tau(1-\tau)}{2K_1(\eta)} \right)^n \tilde{\lambda}_3^{-k} \Gamma^{-k} \left(\frac{1}{2}, \tilde{\lambda}_3 \right) \Gamma^k \left(\frac{1}{2}, 1 \right) \\
& \quad \times \int (\rho^2)^{-n-1} \prod_{i=1}^n K_0 \left(\sqrt{\frac{\eta}{\rho^2} \left(\eta\rho^2 + \frac{|y_i| + (1-2\tau)y_i}{2} \right)} \right) d\rho^2 \\
& < \left(\frac{\tau(1-\tau)}{2K_1(\eta)} \right)^n \tilde{\lambda}_3^{-k} \Gamma^{-k} \left(\frac{1}{2}, \tilde{\lambda}_3 \right) \Gamma^k \left(\frac{1}{2}, 1 \right) \\
& \quad \times 2 \int x^{-3n/2-1} \exp \left\{ -\frac{1}{x} \sqrt{\frac{\eta}{2}} \sum_{i=1}^n \sqrt{|y_i| + (1-2\tau)y_i} \right\} dx.
\end{aligned}$$

As the integrand is same as that in (A.4), the integral is finite for any n . Hence, the posterior distribution under the improper prior $\pi(\rho^2) \propto \frac{1}{\rho^2}$ is proper for any n .

A.6 Proposition 3.4

Like the proof of Proposition 3.2, we follow in the similar manner. The joint posterior density of $(\boldsymbol{\beta}, \rho^2)$ is expressed by

$$\begin{aligned}
\pi(\boldsymbol{\beta}, \rho^2|\mathbf{y}) & = \iint \pi(\mathbf{y}|\mathbf{X}, \boldsymbol{\beta}, \boldsymbol{\sigma}, \mathbf{v}) \pi(\boldsymbol{\beta}|\rho^2) \pi(\mathbf{v}|\boldsymbol{\sigma}) \pi(\boldsymbol{\sigma}|\rho^2) \pi(\rho^2) d\mathbf{v} d\boldsymbol{\sigma} \\
& = \pi(\boldsymbol{\sigma}|\rho^2) \pi(\rho^2) \left(\frac{\tau(1-\tau)}{4K_1(\eta)} \right)^n (\rho^2)^{-n} \\
& \quad \times \prod_{i=1}^n K_0 \left(\sqrt{\frac{\eta}{\rho^2} \left(\frac{|y_i - \mathbf{x}_i \boldsymbol{\beta}| + (1-2\tau)(y_i - \mathbf{x}_i \boldsymbol{\beta})}{2} \right)} \right) \\
& \propto (\rho^2)^{-n-k/2-1} \exp \left\{ -\frac{\lambda_3}{\sqrt{\rho^2}} \sum_{j=1}^k |\beta_j| - \frac{\lambda_4}{\rho^2} \sum_{j=1}^k \beta_j^2 \right\} \\
& \quad \times \prod_{i=1}^n K_0 \left(\sqrt{\frac{\eta}{\rho^2} \left(\frac{|y_i - \mathbf{x}_i \boldsymbol{\beta}| + (1-2\tau)(y_i - \mathbf{x}_i \boldsymbol{\beta})}{2} \right)} \right).
\end{aligned}$$

Then the log posterior density is given by

$$\begin{aligned} \log \pi(\boldsymbol{\beta}, \rho^2 | \mathbf{y}) = & - \left(n + \frac{k}{2} + 1 \right) \log \rho^2 - \frac{\lambda_3}{\sqrt{\rho^2}} \|\boldsymbol{\beta}\|_1 - \frac{\lambda_4}{\rho^2} \|\boldsymbol{\beta}\|_2^2 \\ & + \sum_{i=1}^n \log \left[K_0 \left(\sqrt{\frac{\eta}{\rho^2} \left(\frac{|y_i - \mathbf{x}_i \boldsymbol{\beta}| + (1 - 2\tau)(y_i - \mathbf{x}_i \boldsymbol{\beta})}{2} \right)} \right) \right]. \end{aligned} \quad (\text{A.7})$$

We also consider the coordinate transformation $\Phi \leftrightarrow \frac{\boldsymbol{\beta}}{\sqrt{\rho^2}}$, $\xi \leftrightarrow \frac{1}{\sqrt{\rho^2}}$. In the transformation coordinate, Equation (A.7) is given by

$$\begin{aligned} & (2n + k + 2) \log \xi - \lambda_1 \|\Phi\|_1 - \lambda_4 \|\Phi\|_2^2 \\ & + \sum_{i=1}^n \log \left[K_0 \left(\sqrt{\eta^2 + \frac{\eta \xi}{2} (|\xi y_i - \mathbf{x}_i \Phi| + (1 - 2\tau)(\xi y_i - \mathbf{x}_i \Phi))} \right) \right]. \end{aligned}$$

Since the four terms are log-concave, the joint posterior of $\pi(\boldsymbol{\beta}, \rho^2 | \mathbf{y})$ is unimodal. This completes the proof.

B Details of Gibbs Sampling Algorithm

B.1 Bayesian Huberised Lasso Quantile Regression

The joint posterior distribution is as follows.

$$\begin{aligned} & \pi(\boldsymbol{\beta}, \rho^2, \mathbf{v}, \boldsymbol{\sigma}, \lambda_1, \mathbf{s} | \mathbf{y}) \\ & = \prod_{i=1}^n \frac{1}{\sqrt{8\pi\sigma_i v_i}} \exp \left\{ -\frac{(y_i - \mathbf{x}_i \boldsymbol{\beta} - (1 - 2\tau)v_i)^2}{8\sigma_i v_i} \right\} \\ & \quad \times \prod_{i=1}^n \frac{1}{2\rho^2 K_1(\eta)} \exp \left\{ -\frac{\eta}{2} \left(\frac{\sigma_i}{\rho^2} + \frac{\rho^2}{\sigma_i} \right) \right\} \\ & \quad \times \prod_{i=1}^n \frac{\tau(1 - \tau)}{2\sigma_i} \exp \left\{ -\frac{\tau(1 - \tau)v_i}{2\sigma_i} \right\} \\ & \quad \times \prod_{j=1}^k \frac{1}{\sqrt{2\pi\rho^2 s_j}} \exp \left\{ -\frac{\beta_j^2}{2\rho^2 s_j} \right\} \\ & \quad \times \prod_{j=1}^k \frac{\lambda_1^2}{2} \exp \left\{ -\frac{\lambda_1^2 s_j}{2} \right\} \\ & \quad \times \frac{b^a}{\Gamma(a)} (\lambda_1^2)^{a-1} \exp \{-b\lambda_1^2\} \\ & \quad \times \frac{d^c}{\Gamma(c)} \eta^{c-1} \exp \{-d\eta\} \\ & \quad \times \frac{1}{\rho^2}. \end{aligned}$$

The full conditional posterior distribution of $\boldsymbol{\beta}$ is given by

$$\begin{aligned}
\pi(\boldsymbol{\beta}|\mathbf{y}, \rho^2, \mathbf{v}, \boldsymbol{\sigma}, \lambda_1, \mathbf{s}) & \\
& \propto \prod_{i=1}^n \frac{1}{\sqrt{8\pi\sigma_i v_i}} \exp\left\{-\frac{(y_i - \mathbf{x}_i \boldsymbol{\beta} - (1-2\tau)v_i)^2}{8\sigma_i v_i}\right\} \\
& \quad \times \prod_{j=1}^k \frac{1}{\sqrt{2\pi\rho^2 s_j}} \exp\left\{-\frac{\beta_j^2}{2\rho^2 s_j}\right\} \\
& \propto \exp\left\{-\frac{1}{2}(\mathbf{y} - \mathbf{X}\boldsymbol{\beta} - (1-2\tau)\mathbf{v})^T \mathbf{V}^{-1}(\mathbf{y} - \mathbf{X}\boldsymbol{\beta} - (1-2\tau)\mathbf{v})\right\} \\
& \quad \times \exp\left\{-\frac{1}{2\rho^2} \boldsymbol{\beta}^T \boldsymbol{\Lambda}^{-1} \boldsymbol{\beta}\right\} \\
& \propto \exp\left\{-\frac{1}{2} \left(\boldsymbol{\beta}^T \left(\mathbf{X}^T \mathbf{V}^{-1} \mathbf{X} + \frac{1}{\rho^2} \boldsymbol{\Lambda}^{-1}\right) \boldsymbol{\beta} - 2\boldsymbol{\beta}^T \mathbf{X}^T \mathbf{V}^{-1}(\mathbf{y} - (1-2\tau)\mathbf{v})\right)\right\} \\
& \propto N(\boldsymbol{\mu}_\beta, \boldsymbol{\Sigma}_\beta),
\end{aligned}$$

where $\mathbf{V} = \text{diag}(4\sigma_1 v_1, \dots, 4\sigma_n v_n)$, $\boldsymbol{\Lambda} = \text{diag}(s_1, \dots, s_k)$, $\boldsymbol{\Sigma}_\beta = \left(\mathbf{X}^T \mathbf{V}^{-1} \mathbf{X} + \frac{1}{\rho^2} \boldsymbol{\Lambda}^{-1}\right)^{-1}$ and $\boldsymbol{\mu}_\beta = \boldsymbol{\Sigma}_\beta \mathbf{X}^T \mathbf{V}^{-1}(\mathbf{y} - (1-2\tau)\mathbf{v})$.

The full conditional posterior distribution of σ_i , $i = 1, \dots, n$, is given by

$$\begin{aligned}
\pi(\sigma_i|\mathbf{y}, \boldsymbol{\beta}, \rho^2, \mathbf{v}, \lambda_1, \mathbf{s}) & \\
& \propto \prod_{i=1}^n \frac{1}{\sqrt{8\pi\sigma_i v_i}} \exp\left\{-\frac{(y_i - \mathbf{x}_i \boldsymbol{\beta} - (1-2\tau)v_i)^2}{8\sigma_i v_i}\right\} \\
& \quad \times \prod_{i=1}^n \frac{1}{2\rho^2 K_1(\eta)} \exp\left\{-\frac{\eta}{2} \left(\frac{\sigma_i}{\rho^2} + \frac{\rho^2}{\sigma_i}\right)\right\} \\
& \quad \times \prod_{i=1}^n \frac{\tau(1-\tau)}{2\sigma_i} \exp\left\{-\frac{\tau(1-\tau)v_i}{2\sigma_i}\right\} \\
& \propto \sigma_i^{-3/2} \exp\left\{-\frac{1}{2} \left(\frac{\eta}{\rho^2} \sigma_i + \left(\frac{(y_i - \mathbf{x}_i \boldsymbol{\beta} - (1-2\tau)v_i)^2}{4v_i} + \tau(1-\tau)v_i + \eta\rho^2\right) \frac{1}{\sigma_i}\right)\right\} \\
& \propto GIG\left(-\frac{1}{2}, \frac{\eta}{\rho^2}, \frac{(y_i - \mathbf{x}_i \boldsymbol{\beta} - (1-2\tau)v_i)^2}{4v_i} + \tau(1-\tau)v_i + \eta\rho^2\right).
\end{aligned}$$

The full conditional posterior distribution of v_i , $i = 1, \dots, n$, is given by

$$\begin{aligned}
\pi(v_i|\mathbf{y}, \boldsymbol{\beta}, \rho^2, \boldsymbol{\sigma}, \lambda_1, \mathbf{s}) & \\
& \propto \prod_{i=1}^n \frac{1}{\sqrt{8\pi\sigma_i v_i}} \exp\left\{-\frac{(y_i - \mathbf{x}_i \boldsymbol{\beta} - (1-2\tau)v_i)^2}{8\sigma_i v_i}\right\} \\
& \quad \times \prod_{i=1}^n \frac{\tau(1-\tau)}{2\sigma_i} \exp\left\{-\frac{\tau(1-\tau)v_i}{2\sigma_i}\right\} \\
& \propto v_i^{-1/2} \exp\left\{-\frac{1}{2} \left(\frac{(y_i - \mathbf{x}_i \boldsymbol{\beta} - (1-2\tau)v_i)^2}{4\sigma_i v_i} + \frac{\tau(1-\tau)v_i}{\sigma_i}\right)\right\} \\
& \propto v_i^{-1/2} \exp\left\{-\frac{1}{2} \left(\frac{(y_i - \mathbf{x}_i \boldsymbol{\beta})^2}{4\sigma_i} \frac{1}{v_i} + \left(\frac{(1-2\tau)^2}{4\sigma_i} + \frac{\tau(1-\tau)}{\sigma_i}\right) v_i\right)\right\} \\
& \propto GIG\left(\frac{1}{2}, \frac{(1-2\tau)^2}{4\sigma_i} + \frac{\tau(1-\tau)}{\sigma_i}, \frac{(y_i - \mathbf{x}_i \boldsymbol{\beta})^2}{4\sigma_i}\right).
\end{aligned}$$

The full conditional posterior distribution of ρ^2 is given by

$$\begin{aligned}
\pi(\rho^2|\mathbf{y}, \boldsymbol{\beta}, \mathbf{v}, \boldsymbol{\sigma}, \lambda_1, \mathbf{s}) & \\
& \propto \prod_{i=1}^n \frac{1}{2\rho^2 K_1(\eta)} \exp\left\{-\frac{\eta}{2}\left(\frac{\sigma_i}{\rho^2} + \frac{\rho^2}{\sigma_i}\right)\right\} \\
& \quad \times \prod_{j=1}^k \frac{1}{\sqrt{2\pi\rho^2 s_j}} \exp\left\{-\frac{\beta_j^2}{2\rho^2 s_j}\right\} \\
& \quad \times \frac{1}{\rho^2} \\
& \propto (\rho^2)^{-n-\frac{k}{2}-1} \exp\left\{\frac{1}{2}\left(\sum_{i=1}^n \frac{\eta}{\sigma_i} \rho^2 + \left(\sum_{i=1}^n \eta\sigma_i + \sum_{j=1}^k \frac{\beta_j^2}{s_j}\right) \frac{1}{\rho^2}\right)\right\} \\
& \propto GIG\left(-n - \frac{k}{2}, \sum_{i=1}^n \frac{\eta}{\sigma_i}, \sum_{i=1}^n \eta\sigma_i + \sum_{j=1}^k \frac{\beta_j^2}{s_j}\right).
\end{aligned}$$

The full conditional posterior distribution of s_j , $j = 1, \dots, k$, is given by

$$\begin{aligned}
\pi(s_j|\mathbf{y}, \boldsymbol{\beta}, \rho^2, \mathbf{v}, \boldsymbol{\sigma}, \lambda_1) & \\
& \propto \frac{1}{\sqrt{2\pi\rho^2 s_j}} \exp\left\{-\frac{\beta_j^2}{2\rho^2 s_j}\right\} \times \frac{\lambda_1^2}{2} \exp\left\{-\frac{\lambda_1^2 s_j}{2}\right\} \\
& \propto s_j^{-1/2} \exp\left\{-\frac{1}{2}\left(\frac{\beta_j^2}{\rho^2} \frac{1}{s_j} + \lambda_1^2 s_j\right)\right\} \\
& \propto GIG\left(\frac{1}{2}, \lambda_1^2, \frac{\beta_j^2}{\rho^2}\right).
\end{aligned}$$

The full conditional posterior distribution of λ_1 is given by

$$\begin{aligned}
\pi(\lambda_1|\mathbf{y}, \boldsymbol{\beta}, \rho^2, \mathbf{v}, \boldsymbol{\sigma}, \mathbf{s}) & \\
& \propto \prod_{j=1}^k \frac{\lambda_1^2}{2} \exp\left\{-\frac{\lambda_1^2 s_j}{2}\right\} \\
& \quad \times \frac{b^a}{\Gamma(a)} (\lambda_1^2)^{a-1} \exp\{-b\lambda_1^2\} \\
& \propto (\lambda_1^2)^{a+k-1} \exp\left\{-\left(b + \sum_{j=1}^k \frac{s_j}{2}\right) \lambda_1^2\right\} \\
& \propto \text{Gamma}\left(a + k, b + \sum_{j=1}^k \frac{s_j}{2}\right).
\end{aligned}$$

B.2 Bayesian Huberised Elastic Net Quantile regression

The joint posterior distribution is as follows.

$$\begin{aligned}
& \pi(\boldsymbol{\beta}, \rho^2, \mathbf{v}, \boldsymbol{\sigma}, \mathbf{t}, \lambda_3, \lambda_4 | \mathbf{y}) \\
&= \prod_{i=1}^n \frac{1}{\sqrt{8\pi\sigma_i v_i}} \exp \left\{ -\frac{(y_i - \mathbf{x}_i \boldsymbol{\beta} - (1 - 2\tau)v_i)^2}{8\sigma_i v_i} \right\} \\
&\quad \times \prod_{i=1}^n \frac{1}{2\rho^2 K_1(\eta)} \exp \left\{ -\frac{\eta}{2} \left(\frac{\sigma_i}{\rho^2} + \frac{\rho^2}{\sigma_i} \right) \right\} \\
&\quad \times \prod_{i=1}^n \frac{\tau(1-\tau)}{2\sigma_i} \exp \left\{ -\frac{\tau(1-\tau)v_i}{2\sigma_i} \right\} \\
&\quad \times \prod_{j=1}^k \sqrt{\frac{\lambda_4 t_j}{\pi \rho^2 (t_j - 1)}} \exp \left\{ -\frac{\lambda_4 t_j \beta_j^2}{\rho^2 (t_j - 1)} \right\} \\
&\quad \times \prod_{j=1}^k \Gamma^{-1} \left(\frac{1}{2}, \tilde{\lambda}_3 \right) \sqrt{\frac{\tilde{\lambda}_3}{t_j}} \exp \left\{ -\tilde{\lambda}_3 t_j \right\} I(t_j > 1) \\
&\quad \times \frac{b_1^{a_1}}{\Gamma(a_1)} (\tilde{\lambda}_3)^{a_1-1} \exp \left\{ -b_1 \tilde{\lambda}_3 \right\} \\
&\quad \times \frac{b_2^{a_2}}{\Gamma(a_2)} \lambda_2^{a_2-1} \exp \left\{ -b_2 \lambda_4 \right\} \\
&\quad \times \frac{b_3^{a_3}}{\Gamma(a_3)} \eta^{a_3-1} \exp \left\{ -b_3 \eta \right\} \\
&\quad \times \frac{1}{\rho^2}.
\end{aligned}$$

Clearly, it is obvious to see that the full conditional posterior distributions of σ_i and v_i , $i = 1, \dots, n$ are the same in the Bayesian Huberised lasso quantile regression.

The full conditional posterior distribution of $\boldsymbol{\beta}$ is given by

$$\begin{aligned}
& \pi(\boldsymbol{\beta} | \mathbf{y}, \rho^2, \mathbf{v}, \boldsymbol{\sigma}, \mathbf{t}, \lambda_3, \lambda_4) \\
&= \prod_{i=1}^n \frac{1}{\sqrt{8\pi\sigma_i v_i}} \exp \left\{ -\frac{(y_i - \mathbf{x}_i \boldsymbol{\beta} - (1 - 2\tau)v_i)^2}{8\sigma_i v_i} \right\} \\
&\quad \times \prod_{j=1}^k \sqrt{\frac{\lambda_4 t_j}{\pi \rho^2 (t_j - 1)}} \exp \left\{ -\frac{\lambda_4 t_j \beta_j^2}{\rho^2 (t_j - 1)} \right\} \\
&\propto \exp \left\{ -\frac{1}{2} (\mathbf{y} - \mathbf{X}\boldsymbol{\beta} - (1 - 2\tau)\mathbf{v})^T \mathbf{V}^{-1} (\mathbf{y} - \mathbf{X}\boldsymbol{\beta} - (1 - 2\tau)\mathbf{v}) \right\} \\
&\quad \times \exp \left\{ -\frac{\lambda_4}{\rho^2} \boldsymbol{\beta}^T \mathbf{T}^{-1} \boldsymbol{\beta} \right\} \\
&\propto \exp \left\{ -\frac{1}{2} \left(\boldsymbol{\beta}^T \left(\mathbf{X}\mathbf{V}^{-1}\mathbf{X} + \frac{2\lambda_4}{\rho^2} \mathbf{T}^{-1} \right) \boldsymbol{\beta} - 2\boldsymbol{\beta}^T \mathbf{X}^T \mathbf{V}^{-1} (\mathbf{y} - (1 - 2\tau)\mathbf{v}) \right) \right\} \\
&\propto N(\boldsymbol{\mu}_\beta, \boldsymbol{\Sigma}_\beta),
\end{aligned}$$

where $\mathbf{V} = \text{diag}(4\sigma_1 v_1, \dots, 4\sigma_n v_n)$, $\mathbf{T} = \text{diag}((t_1 - 1)t_1^{-1}, \dots, (t_n - 1)t_n^{-1})$, $\boldsymbol{\Sigma}_\beta = \left(\mathbf{X}\mathbf{V}^{-1}\mathbf{X} + \frac{2\lambda_4}{\rho^2} \mathbf{T}^{-1} \right)^{-1}$ and $\boldsymbol{\mu} = \boldsymbol{\Sigma}_\beta \mathbf{X}^T \mathbf{V}^{-1} (\mathbf{y} - (1 - 2\tau)\mathbf{v})$.

The full conditional posterior distribution of ρ^2 is given by

$$\begin{aligned}
& \pi(\rho^2 | \mathbf{y}, \boldsymbol{\beta}, \mathbf{v}, \boldsymbol{\sigma}, \mathbf{t}, \lambda_3, \lambda_4) \\
& \propto \prod_{i=1}^n \frac{1}{2\rho^2 K_1(\eta)} \exp \left\{ -\frac{\eta}{2} \left(\frac{\sigma_i}{\rho^2} + \frac{\rho^2}{\sigma_i} \right) \right\} \\
& \quad \times \prod_{j=1}^k \sqrt{\frac{\lambda_4 t_j}{\pi \rho^2 (t_j - 1)}} \exp \left\{ -\frac{\lambda_4 t_j \beta_j^2}{\rho^2 (t_j - 1)} \right\} \\
& \quad \times \frac{1}{\rho^2} \\
& \propto (\rho^2)^{-n - \frac{k}{2} - 1} \exp \left\{ \frac{1}{2} \left(\sum_{i=1}^n \frac{\eta}{\sigma_i} \rho^2 + \left(\sum_{i=1}^n \eta \sigma_i + \sum_{j=1}^k \frac{2\lambda_4 t_j \beta_j^2}{t_j - 1} \right) \frac{1}{\rho^2} \right) \right\} \\
& \propto GIG \left(-n - \frac{k}{2}, \sum_{i=1}^n \frac{\eta}{\sigma_i}, \sum_{i=1}^n \eta \sigma_i + \sum_{j=1}^k \frac{2t_j \lambda_4 \beta_j^2}{t_j - 1} \right).
\end{aligned}$$

The full conditional posterior distribution of $t_j - 1$ is given by

$$\begin{aligned}
& \pi(t_j - 1 | \mathbf{y}, \boldsymbol{\beta}, \rho^2, \mathbf{v}, \boldsymbol{\sigma}, \lambda_3, \lambda_4) \\
& \propto \sqrt{\frac{\lambda_4 t_j}{\pi \rho^2 (t_j - 1)}} \exp \left\{ -\frac{\lambda_4 t_j \beta_j^2}{\rho^2 (t_j - 1)} \right\} \\
& \quad \times \Gamma^{-1} \left(\frac{1}{2}, \tilde{\lambda}_3 \right) \sqrt{\frac{\tilde{\lambda}_3}{t_j}} \exp \left\{ -\tilde{\lambda}_3 t_j \right\} I(t_j > 1) \\
& \propto (t_j - 1)^{-1/2} \exp \left\{ -\frac{\lambda_4 t_j \beta_j^2}{\rho^2 (t_j - 1)} - \tilde{\lambda}_3 t_j \right\} I(t_j > 1) \\
& \propto (t_j - 1)^{-1/2} \exp \left\{ -\frac{1}{2} \left(\frac{2\lambda_4 \beta_j^2}{\rho^2} \frac{1}{t_j - 1} + 2\tilde{\lambda}_3 (t_j - 1) \right) \right\} I(t_j - 1 > 0) \\
& \propto GIG \left(\frac{1}{2}, 2\tilde{\lambda}_3, \frac{2\lambda_4 \beta_j^2}{\rho^2} \right) I(t_j - 1 > 0).
\end{aligned}$$

The full conditional posterior distribution of $\tilde{\lambda}_3$ is given by

$$\begin{aligned}
& \pi(\tilde{\lambda}_3 | \mathbf{y}, \boldsymbol{\beta}, \rho^2, \mathbf{v}, \boldsymbol{\sigma}, \mathbf{t}, \lambda_3, \lambda_4) \\
& \propto \prod_{j=1}^k \Gamma^{-1} \left(\frac{1}{2}, \tilde{\lambda}_3 \right) \sqrt{\frac{\tilde{\lambda}_3}{t_j}} \exp \left\{ -\tilde{\lambda}_3 t_j \right\} I(t_j > 1) \\
& \quad \times \frac{b_1^{a_1}}{\Gamma(a_1)} (\tilde{\lambda}_3)^{a_1 - 1} \exp \left\{ -b_1 \tilde{\lambda}_3 \right\} \\
& \propto \Gamma^{-k} \left(\frac{1}{2}, \tilde{\lambda}_3 \right) (\tilde{\lambda}_3)^{\frac{k}{2} + a_1 - 1} \exp \left\{ -\left(\sum_{j=1}^k t_j + b_1 \right) \tilde{\lambda}_3 \right\}.
\end{aligned}$$

As it is infeasible to directly sample from $\pi(\tilde{\lambda}_3 | \mathbf{y}, \boldsymbol{\beta}, \rho^2, \mathbf{v}, \boldsymbol{\sigma}, \mathbf{t}, \lambda_3, \lambda_4)$, the one-step Metropolis-Hastings algorithm is employed. Following Li et al. (2010), the proposal distribution is

$q(\tilde{\lambda}_3|\mathbf{t}) \sim \text{Gamma}\left(k + a_1, b_1 + \sum_{j=1}^k (t_j - 1)\right)$. They showed that

$$\lim_{\tilde{\lambda}_3 \rightarrow \infty} \frac{\sqrt{\tilde{\lambda}_3} \exp(\tilde{\lambda}_3)}{\Gamma^{-1}\left(\frac{1}{2}, \tilde{\lambda}_3\right)} = 1,$$

implies that

$$\lim_{\tilde{\lambda}_3 \rightarrow \infty} \frac{\pi(\tilde{\lambda}_3|\mathbf{y}, \boldsymbol{\beta}, \rho^2, \mathbf{v}, \boldsymbol{\sigma}, \mathbf{t}, \lambda_3, \lambda_4)}{q(\tilde{\lambda}_3|\mathbf{t})},$$

exists and equals to some positive constant. Hence, the tail behaviours of $q(\tilde{\lambda}_3|\mathbf{t})$ and $\pi(\tilde{\lambda}_3|\mathbf{y}, \boldsymbol{\beta}, \rho^2, \mathbf{v}, \boldsymbol{\sigma}, \mathbf{t}, \lambda_3, \lambda_4)$ are similar.

The full conditional posterior distribution of λ_4 is given by

$$\begin{aligned} & \pi(\lambda_4|\mathbf{y}, \boldsymbol{\beta}, \rho^2, \mathbf{v}, \boldsymbol{\sigma}, \mathbf{t}, \lambda_3) \\ & \propto \prod_{j=1}^k \sqrt{\frac{\lambda_4 t_j}{\pi \rho^2 (t_j - 1)}} \exp\left\{-\frac{\lambda_4 t_j \beta_j^2}{\rho^2 (t_j - 1)}\right\} \\ & \quad \times \frac{b_2^{a_2}}{\Gamma(a_2)} \lambda_4^{a_2-1} \exp\{-b_2 \lambda_4\} \\ & \propto \lambda_4^{\frac{k}{2} + a_2 - 1} \exp\left\{-\left(\sum_{j=1}^k \frac{t_j \beta_j^2}{\rho^2 (t_j - 1)} + b_2\right) \lambda_4\right\} \\ & \propto \text{Gamma}\left(\frac{k}{2} + a_2, \sum_{j=1}^k \frac{t_j \beta_j^2}{\rho^2 (t_j - 1)} + b_2\right). \end{aligned}$$

C Results for Simulation Studies and Real Data Examples

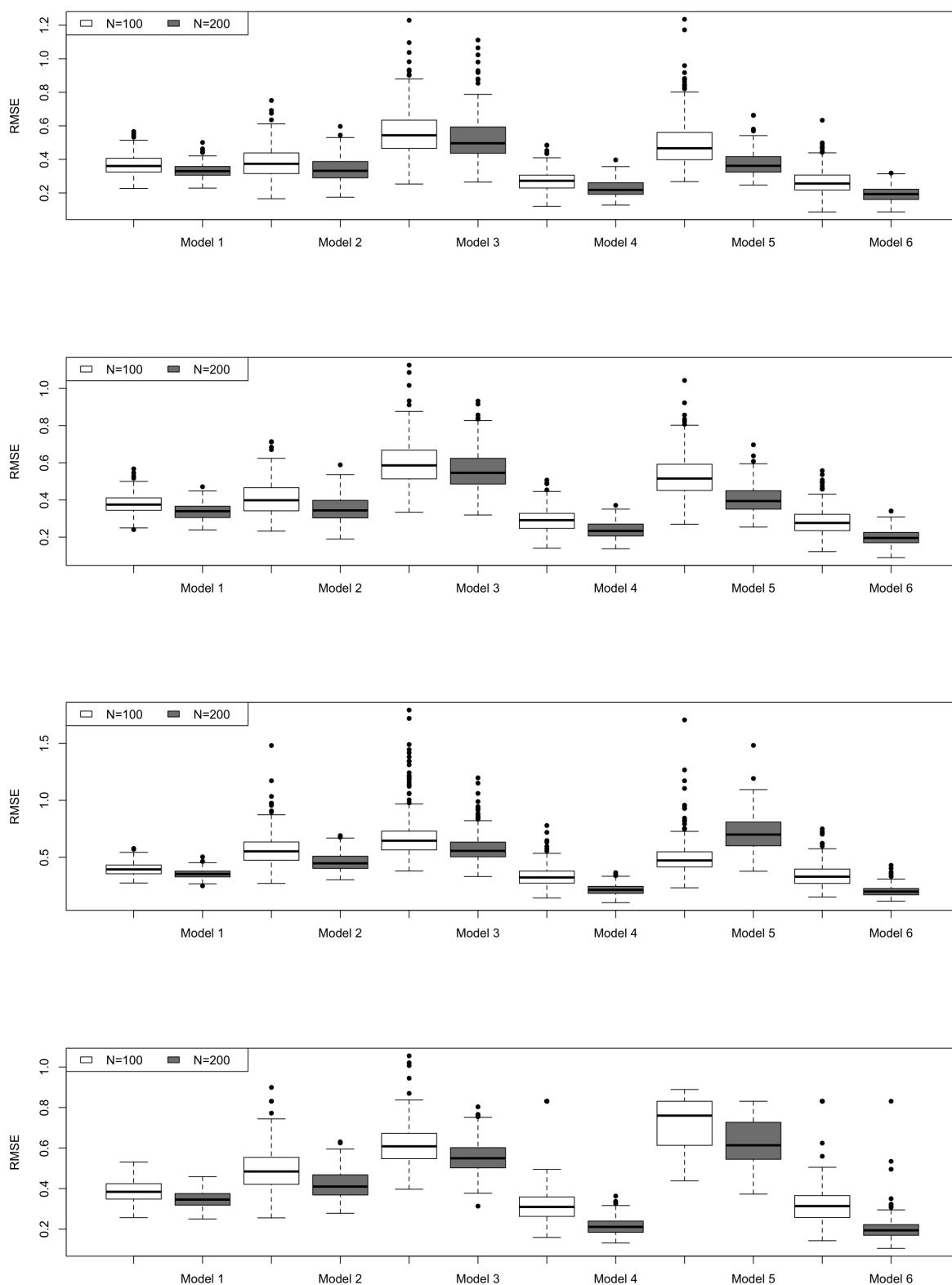


Figure 11: Boxplots of RMSE based on 300 replications in six simulation scenarios for HBQR-BL, HBQR-EN, BQR-BL and BQR-EN in this order ($\tau = 0.25$).

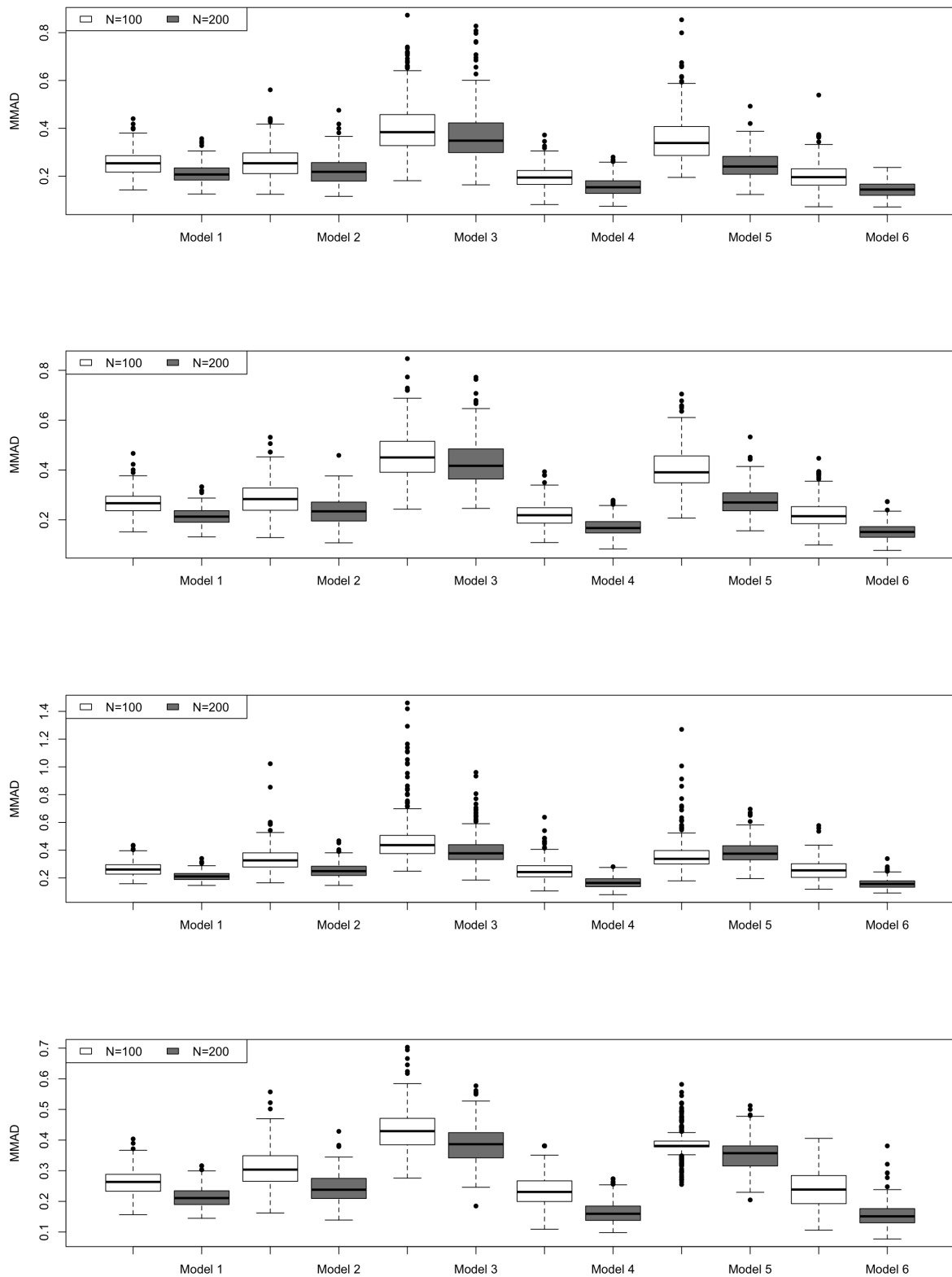


Figure 12: Boxplots of MMAD based on 300 replications in six simulation scenarios for HBQR-BL, HBQR-EN, BQR-BL and BQR-EN in this order ($\tau = 0.25$).

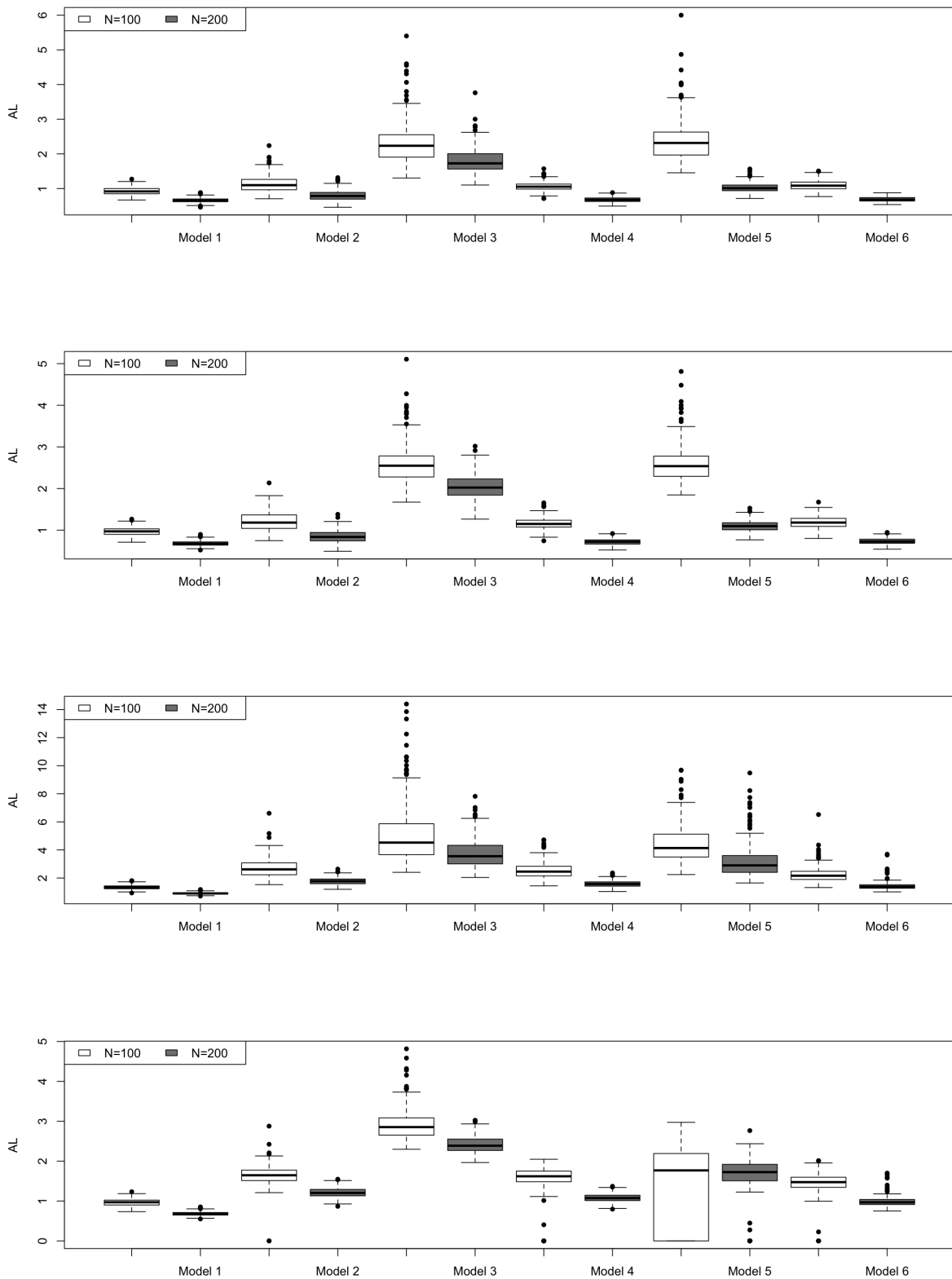


Figure 13: Boxplots of AL based on 300 replications in six simulation scenarios for HBQR-BL, HBQR-EN, BQR-BL and BQR-EN in this order ($\tau = 0.25$).

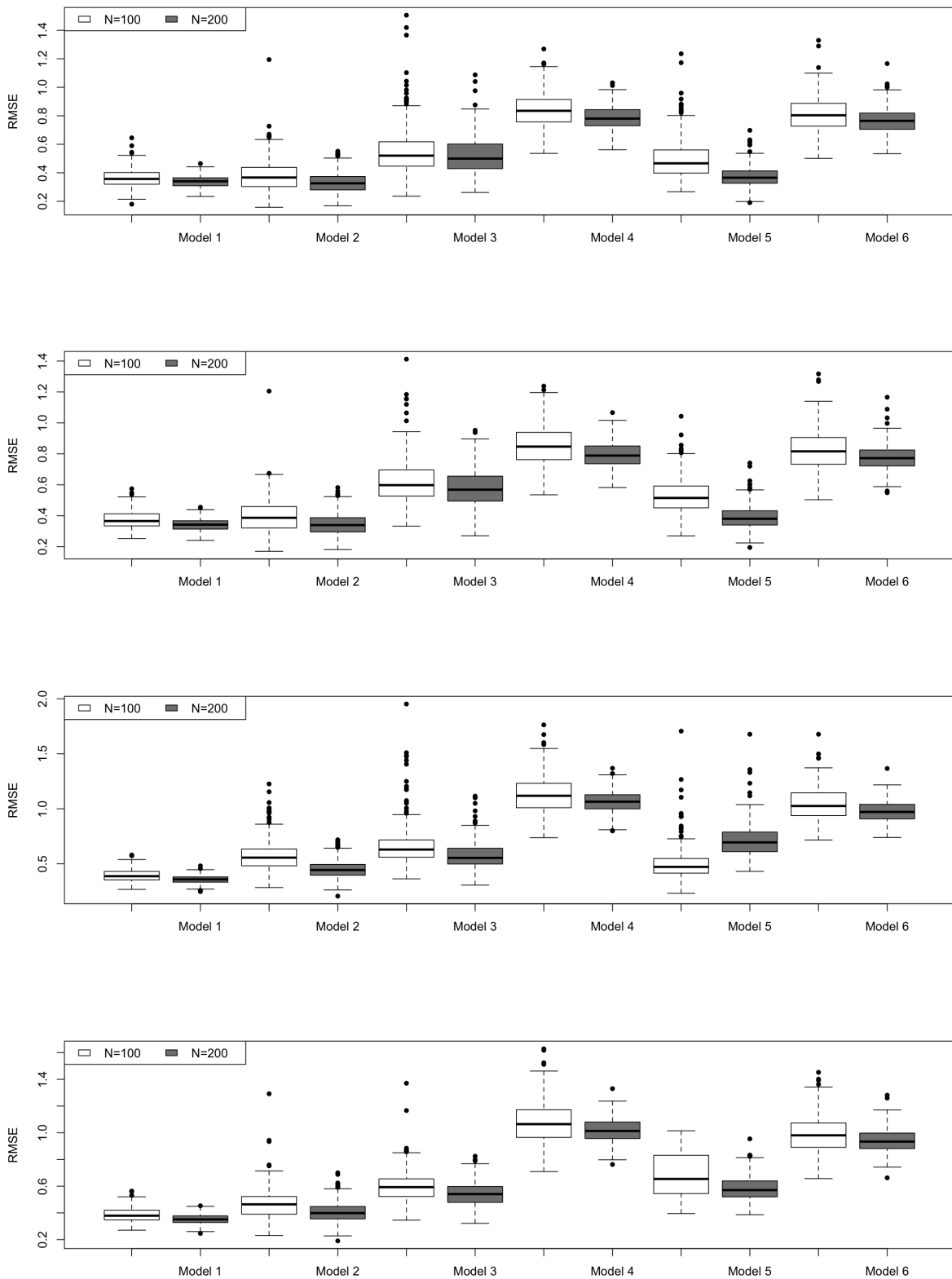


Figure 14: Boxplots of RMSE based on 300 replications in six simulation scenarios for HBQR-BL, HBQR-EN, BQR-BL and BQR-EN in this order ($\tau = 0.75$).

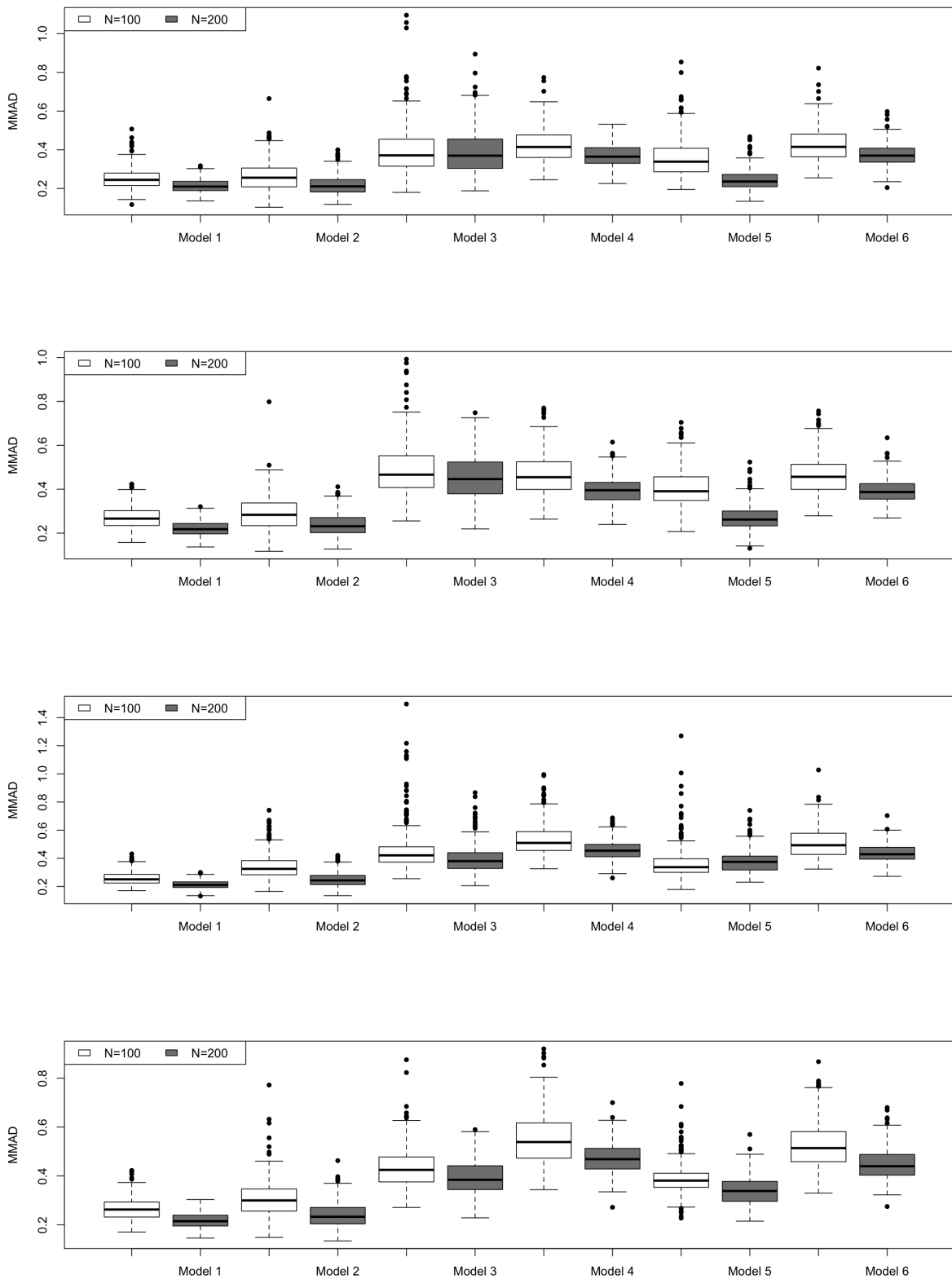


Figure 15: Boxplots of MMAD based on 300 replications in six simulation scenarios for HBQR-BL, HBQR-EN, BQR-BL and BQR-EN in this order ($\tau = 0.75$).

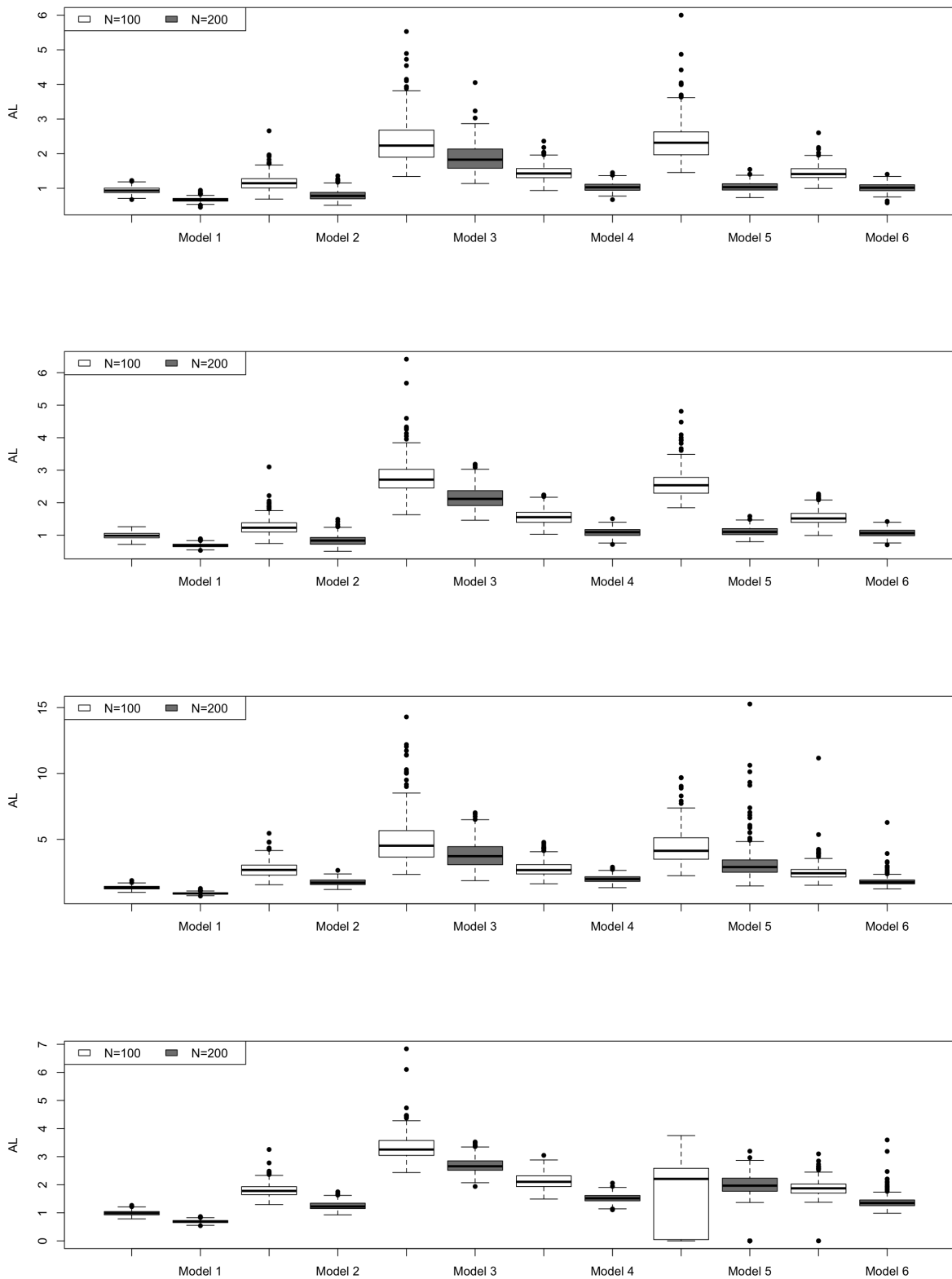


Figure 16: Boxplots of AL based on 300 replications in six simulation scenarios for HBQR-BL, HBQR-EN, BQR-BL and BQR-EN in this order ($\tau = 0.75$).

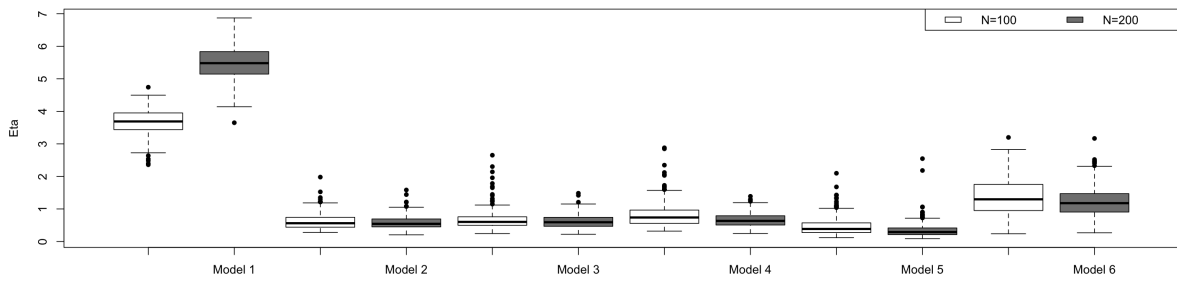
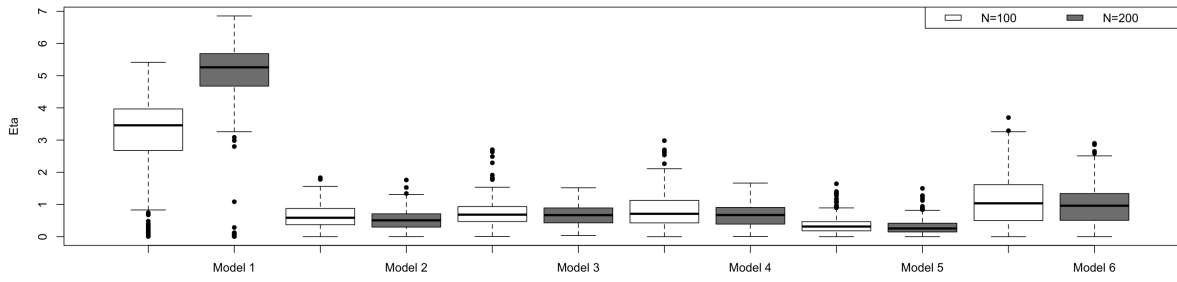


Figure 17: Boxplots of posterior median of η based on 300 replications in six simulation scenarios for HBQR-BL (top) and HBQR-EN (bottom) ($\tau = 0.25$).

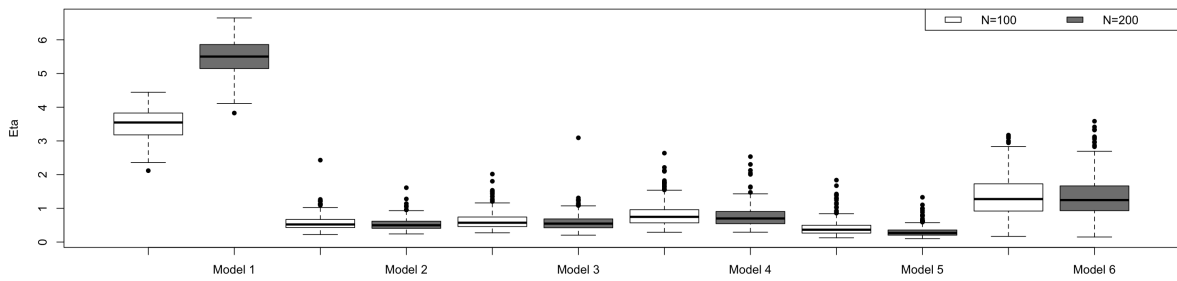
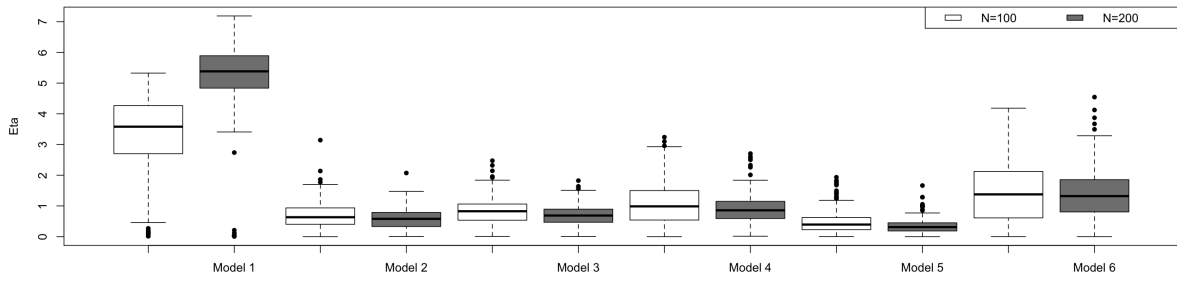


Figure 18: Boxplots of posterior median of η based on 300 replications in six simulation scenarios for HBQR-BL (top) and HBQR-EN (bottom) ($\tau = 0.75$).

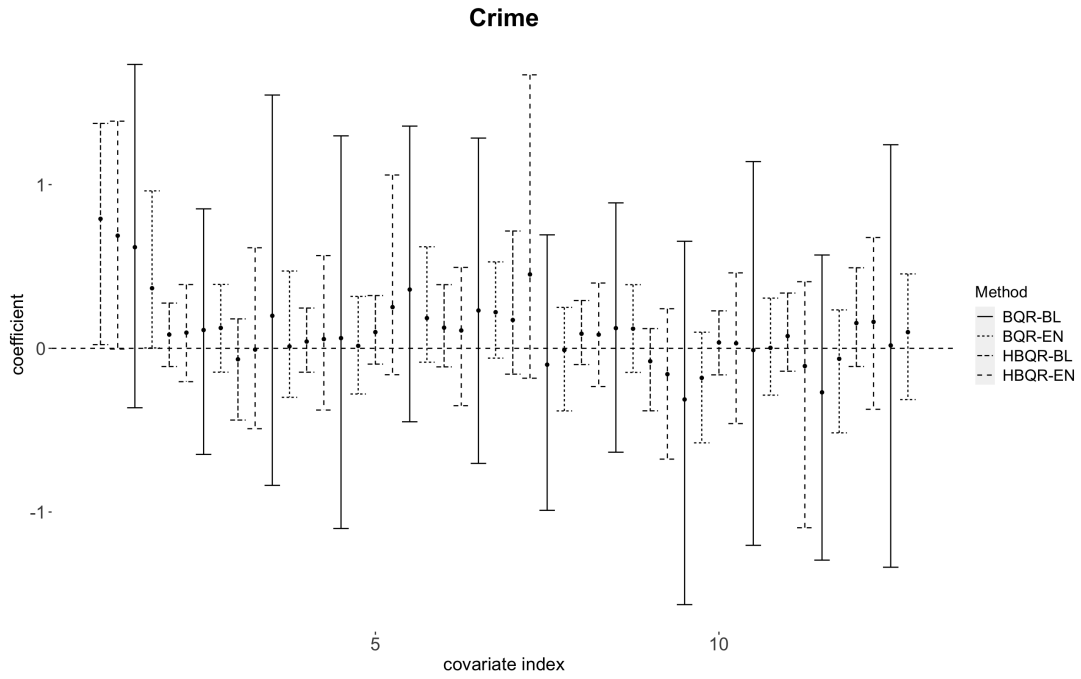


Figure 19: Posterior medians and 95% credible intervals of the regression coefficients at $\tau = 0.1$ in the Bayesian quantile regression with Bayesian lasso (BQR-BL), Bayesian quantile regression with elastic net (BQR-EN) and the proposed Bayesian quantile regression with Bayesian lasso (HBQR-BL) and elastic net (HBQR-EN), applied to the Crime data.

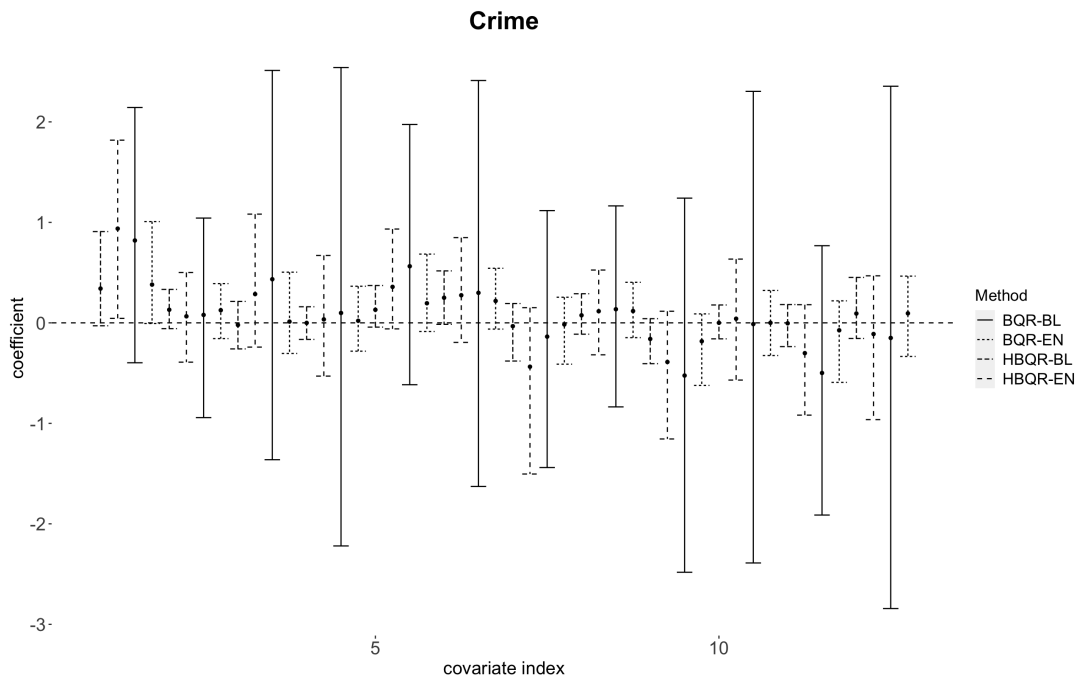


Figure 20: Posterior medians and 95% credible intervals of the regression coefficients at $\tau = 0.9$ in the Bayesian quantile regression with Bayesian lasso (BQR-BL), Bayesian quantile regression with elastic net (BQR-EN) and the proposed Bayesian quantile regression with Bayesian lasso (HBQR-BL) and elastic net (HBQR-EN), applied to the Crime data.

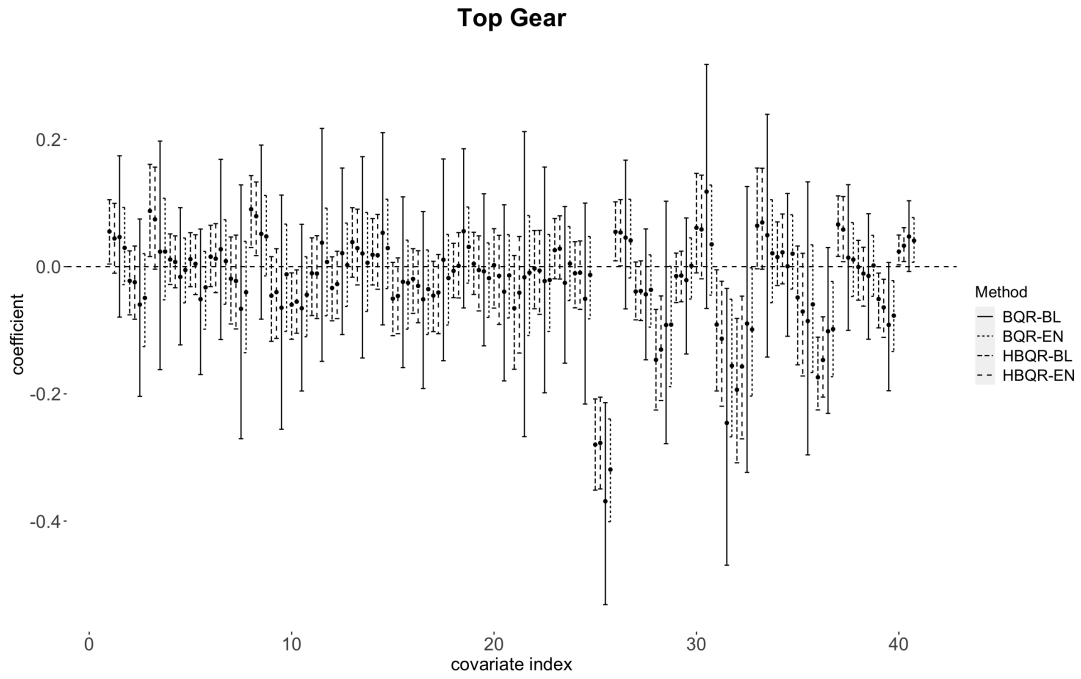


Figure 21: Posterior medians and 95% credible intervals of the regression coefficients at $\tau = 0.1$ in the Bayesian quantile regression with Bayesian lasso (BQR-BL), Bayesian quantile regression with elastic net (BQR-EN) and the proposed Bayesian quantile regression with Bayesian lasso (HBQR-BL) and elastic net (HBQR-EN), applied to the Top Gear data.

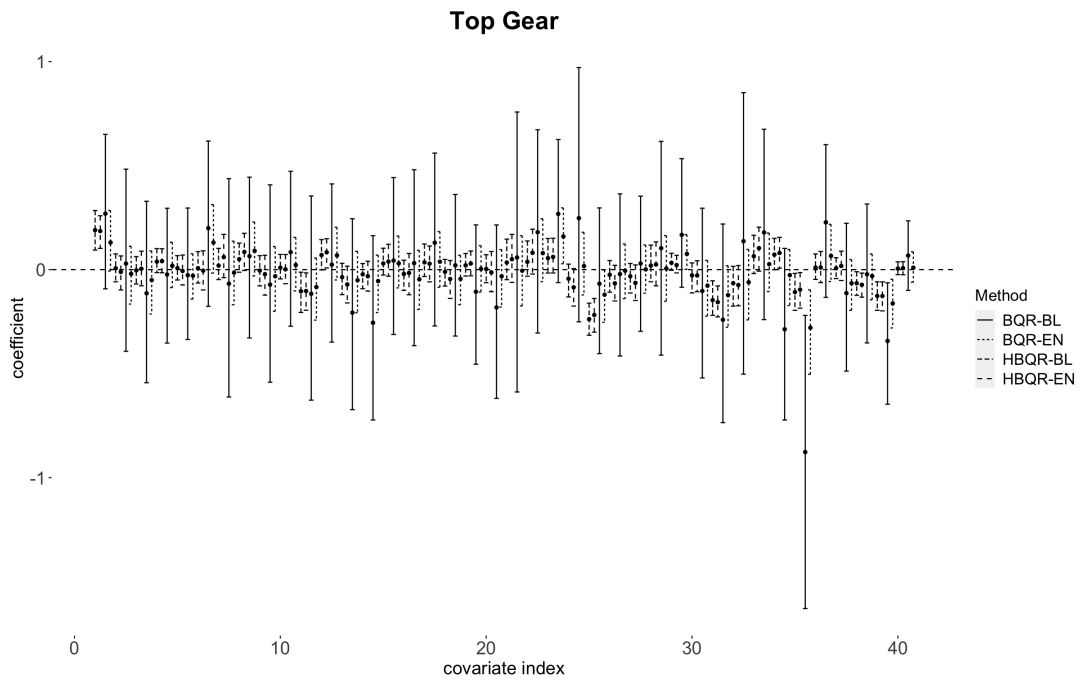


Figure 22: Posterior medians and 95% credible intervals of the regression coefficients at $\tau = 0.9$ in the Bayesian quantile regression with Bayesian lasso (BQR-BL), Bayesian quantile regression with elastic net (BQR-EN) and the proposed Bayesian quantile regression with Bayesian lasso (HBQR-BL) and elastic net (HBQR-EN), applied to the Top Gear data.